IMPROVEMENT AND VALIDATION OF OSCAR-3 USAGE IN SAFARI-1 CORE MODELLING

Focus on Cross Section Library Creation and Target Plate Irradiation Rigs Modelling

by

Lesego Ernest Moloko

Submitted in partial fulfilment of the requirements for the degree of Master of Science in Applied Radiation Science and Technology (MARST), in the Faculty of Agriculture, Science and Technology

at the

NORTHWEST UNIVERSITY

Supervisor:

Dr. A. L. Graham
Radiation and Reactor Theory Group
Necsa
Pelindaba
South Africa

ACKNOWLEDGEMENTS

I would like to give my sincere thanks to my supervisor, Dr. Andy Graham. Without his guidance and open mindedness, I might not have been able to complete this work.

Mr. Frederik Reitsma and Mr Rian Prinsloo, also has my complete gratitude. Their experience and previous work played a very important role in enabling me to complete my thesis.

I also extend my thanks to Mr Alan D'Arcy of the SAFARI-1 Reactor for all the time he has devoted to providing me with information.

My sincerest appreciation goes to Hantie Labuschagne, for dedicating her time to my thesis by ensuring consistency in its layout and format. I also extend my sincere thanks to all my postgraduate and RRT colleagues for their help and support.

A special note of thanks goes to Necsa and the Northwest University for their financial support and permission to publish this work.

At last, I want to devote this thesis to my Lord. Thank Him for giving me good friends, family, colleagues and my supervisor Dr. Andy Graham and Mr. Rian Prinsloo. It would not have been possible to complete this master's program without His grace.

ABSTRACT

The SAFARI-1 nuclear reactor, an acronym for South African Fundamental Atomic Reactor Installation-1, is a 20 MW tank in pool Oak Ridge type Material Testing Reactor at Pelindaba near Pretoria in South Africa. SAFARI-1 is a research reactor built primarily to supply neutrons for basic research and radioisotope production. Various calculational tools and computer codes are essential for the estimation of safety parameters, core reload planning, and effective fuel and product utilisation support.

The ever increasing demand for isotope production, specifically Mo-99 fission product, produced by in-core irradiation of target plates, has led to the development of various methodologies of including target plate irradiation models in SAFARI-1 calculations. These studies are essential for optimisation of isotope production yields, while ensuring that safety limits are met.

The methods under consideration for modelling the on-power loading and unloading of the target plates use the core calculational code system, OSCAR-3. Results are evaluated based on comparison to plant data, results from existing methodologies, and past experience of reload planning operation.

Effects on the reactivity, flux and power distributions, fuel economy and safety, as a result of target plate irradiations were quantified for each of the various modelling methods using core cycle calculations. The inclusion of target plates in reload calculations, showed a significant increase in predicted reactivity of up to 2000pcm. A core-wide power redistribution and tilt of up to 2% along with much improved cycle length prediction was found.

It is concluded that all considered methods of including target plates will find application, some important for safety, others for planning and core-follow calculations. Independent of which methods will eventually be applied, it is clear that the inclusion of target plates is essential for accurate reload planning and should be applied in future.

TABLE OF CONTENTS

LIST OF TABLES

LIST OF FIGURES

1. GENERAL REACTOR THEORY AND BACKGROUND

1.1. INTRODUCTION

A Nuclear Reactor is a very efficient source of energy, which is produced by controlled nuclear fission chain reactions and it has evolved from an embryonic research tool into the mammoth electrical generating units that drive hundreds of central-station power plants around the world today. Recently the shortage of fossil fuels has made it difficult for such plants to be run and it is apparent that nuclear fission reactors will play a dominant role in meeting man's energy requirement for decades to come.

All reactors consist of some essential elements such as, **fuel or fissile material**, a **moderator** (to thermalise neutrons, may not be present for fast reactors) and **reflectors** surrounding the **core** (fuel elements plus moderator) to reduce neutron leakage and thereby reduce the critical size of a reactor. It also consists of a **containment vessel** to prevent the escape of radioactive fission products, **shielding** to prevent neutrons and gammas from causing biological harm to the operating personnel and **coolant** to remove heat from the core. Lastly, it needs a **control system** to allow the operator to control the power level and to keep it constant during normal operation and various **emergency systems** designed to prevent runaway operations in the event of a failure of the control or coolant [4].

1.1.1. T ypes of Reactors

The most basic classification describes the use for which the reactor is intended and can be defined in three categories, which are;

i. Power generating reactors (e.g. Koeberg)
ii. Research reactors (e.g. SAFARI-1)
iii. Converters (Breeder reactors)

The power reactors extract the kinetic energy of the fission fragments as heat and convert the heat energy to electrical energy while the research reactors are designed to produce neutrons for research in areas such as nuclear or solid state physics and they operate at a low power level (1-100MW). Converters are reactors designed to have high efficiency for converting materials that are not fissionable with thermal neutrons to materials that are fissionable with neutrons of these energies. The specific conversions that are generally used are U-238 to Pu-239 and Th-232 to U-233 [2], [3].

These reactors can be designed to operate with either thermal (0-1eV), intermediate (eV-keV), or fast neutrons (keV-MeV). The intermediate-energy (eV-keV) reactors require considerably less volume than the thermal reactors and because of lower cross sections for fast neutrons, fast neutron reactors require of the order of 10-100 times the fuel of thermal reactors providing the same power. However, because of the lack of moderator, the core of a fast reactor occupies a smaller volume than the core of a thermal reactor [3], [4].

1.1.2. Types of Nuclear Fuels

The most commonly used fuels are natural uranium (0.72% U-235), enriched uranium (>0.72% U-235), Pu-239 and U-233. The latter two are obtained from chemical processing of fertile material from converter or breeder reactors. These are the only three nuclides that have stability to permit storage for a long time and can sustain the fission chain reaction. Enriched uranium, which is the most commonly used fuel in power reactors, is produced in quantity at great expense from processes sensitive to the small mass difference between U-235 and U-238. Highly enriched U-235 and Pu-239 are bomb grade fissile materials, while the uranium at 2-5% enrichment as used in certain types of reactors, is not [3].

Uranium enrichment is defined as the process whereby uranium in which the isotope U-235 has a concentration greater that its natural value and depleted

uranium is defined as uranium in which the isotope U-235 has a concentration of less than its natural value. Although depleted uranium is referred to as a by-product of the enrichment process, it does have uses in the nuclear field and in commercial and defence industries.

Now that we have a basic idea of what a reactor is, that is, their types, fuel used and fuel types, and essentially, the components making up the whole reactor structure, we will look at what happens in the reactor, and the conditions required for good and safe operation, in the next few chapters. It is also important to bear in mind that there are an enormous number of neutrons ($\approx 10^{18}$ cm^{-3}) and even larger numbers of nuclei ($\approx 10^{22}$ cm^{-3}) in the reactor core [3]. Hence, we will concern ourselves with the average behaviour of the neutrons in some statistical sense only and we wish to calculate the probabilities at which the various neutron-nuclear interactions will occur. The SAFARI-1 reactor will be used as an example for the purpose of this study and is described in the section that follows.

1.2. BACKGROUND TO THE STUDY

1.2.1. SAFARI-1 Reactor

SAFARI-1, an acronym for the South African Fundamental Atomic Reactor Installation One, was commissioned in 1965 by Necsa and is of the MTR type, that is, material testing reactor (of Oak Ridge Research Reactor design). It is a 20MW tank in pool type reactor; the coolant and moderator is light water and cooling occurs via the primary and secondary heat exchange system. The SAFARI-1 reactor core layout is shown in Figure1-1 below.

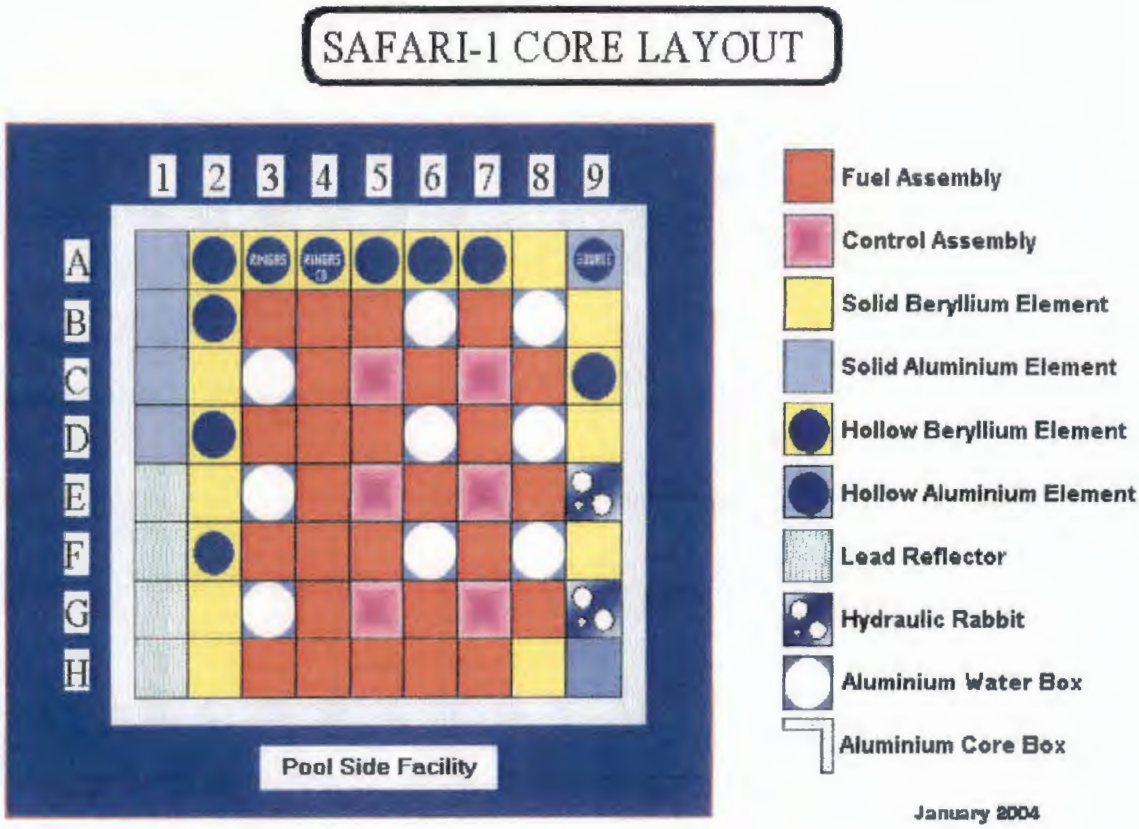

Figure 1-1: SAFARI-1 Core Layout [12], [17]

It has an 8 x 9 core lattice, which houses 26 MTR-type fuel elements, 5 control rods, 1 regulating rod, in-core irradiation facilities and reflector elements. The core is fuelled with MTR-type fuel elements with 19 plates. The reactor vessel is cylindrical in shape except for one flattened side, which is also the wall of the rectangular core box adjacent to the poolside facility. The large ex-core poolside facility allows irradiations to be performed in relatively high neutron fluxes since it is directly adjacent to the fuel elements. The reactor is also equipped with a number of beam tubes, which are used for the neutron radiography, neutron scattering, and prompt gamma neutron activation facilities, while hydraulic and pneumatic rabbit facilities provide for the irradiation of various samples [12], [17], [19].

The locally produced fuel elements are manufactured from ~ 90 wt% enriched uranium-aluminium alloy (HEU). It is planned to convert to LEU fuel in the

NWU LIBRARY

near future [20]. The effective control of the reactor is established using fuel-follower type cadmium control rods.

One of the most important irradiation activities is that of the target plates for Mo-99 production, the target plate irradiation rig is briefly described below.

Figure 1-2 shows the target plates usually irradiated in positions C3, E3, G3, B8, D8 and F8 of Figure 1-1 for Mo-99 fission product production.

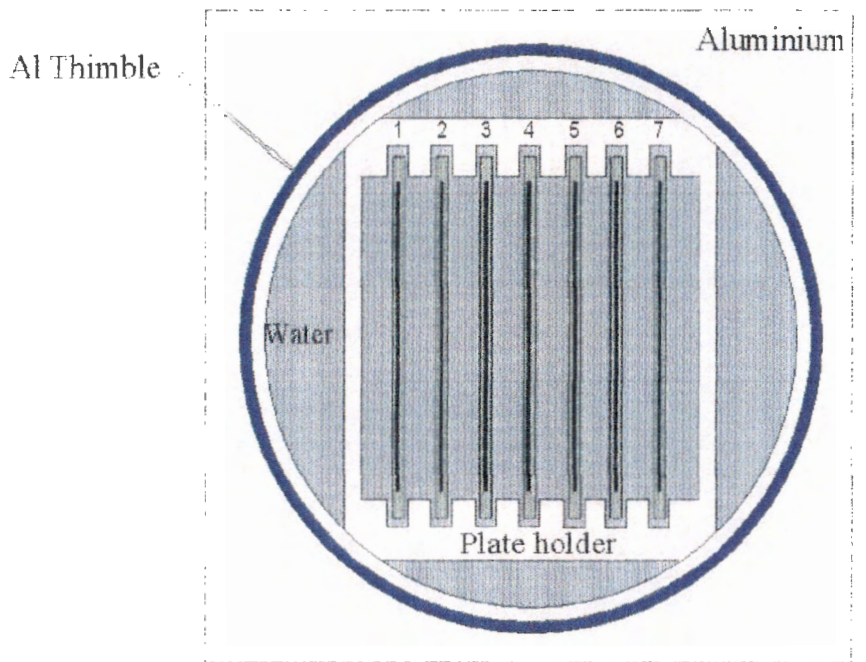

Figure 1-2: Target Plate Irradiation Rig [12]

The locally produced Mo-99, a strategic radiochemical that is the cornerstone of nuclear medicine, is produced by irradiation of 45% enriched U-235 target plates. The fission yield is about 6.1% of Mo-99. The rig or plate holder can hold or load a maximum of seven plates. Depending on the Mo-99 production required, a different number of plates can be loaded. When a position is not loaded, an aluminium dummy plate is inserted. The target plates irradiation rigs are loaded at the core centreline, on the axial flux peak [8], [9] [12].

This radioisotope has a relatively short half-life of 66.7 hours, thus a continuous and constant supply is important. The isotope business at Necsa

is currently fourth in the world and Necsa has a market share of about 15% in reactor produced medical isotopes [8]. Therefore modelling of the effects introduced by these irradiations positions (in six positions at present) is essential.

The target plates are loaded in rigs (see Figure 1.2) and are irradiated per schedule, which may vary from cycle to cycle. The number of target plates loaded or irradiated, depend on the Mo-99 fission product demand. At the start of cycle, all positions are loaded. The irradiations can be judged to follow a cycle of 7 days at a time with deviation only in the last production run due to the shutdown time. There is a two hour change from irradiated to fresh target plates, during which time the core position is empty.

The on-power loading of these target plate irradiation rigs can perturb the reactor power, flux distribution and hence the effective utilization of the SAFARI-1 reactor. It is thus important to be able to predict the reactor's behaviour or response as a result of the introduction of these rigs, using available calculational methods.

The SAFARI-1 reactor is supported by an advanced on-site infrastructure consisting, amongst others, a MTR fuel fabrication plant, hot cell facilities, an isotope production centre, a pipe storage facility for interim dry storage of spent fuel and a disposal site for low and intermediate radioactive waste. There are also support personnel consisting of theoretical and experimental reactor physics, radiochemistry and radio-analysis groups [8], [12] [19].

1.2.2. Research Problem

Core analysis calculations have been performed for many years for the SAFARI-1 research reactor using versions 1, 2 and 3 of the OSCAR system. OSCAR-3, the latest multi-group analytic nodal code system has been used as a core planning and core follow tool. It plays a critical role in estimation of

safety parameters, core reload planning and effective fuel and product utilization, and is increasingly being used by other international research reactors [1].

The code system requires a quality assured cross section data library to perform core analysis calculations, that is, explicit modelling of all the reactor materials having influence on neutron economy (in-core and ex-core materials) to create the required cross section library.

However, the present OSCAR-3 calculations are done without detailed and explicit modelling of some of the SAFARI-1 reactor materials (e.g. target plate irradiation rigs), and the irradiation position material, that is, the target plate irradiation rigs cross sections are not included in the cross section library used at present. The on-power loading and unloading of irradiation target plate rigs can have large effects, both local and global, on the flux and power distributions, control rod worth and shutdown margins and ultimately, safety and fuel economy of the SAFARI-1 core, and these effects have not been modelled in OSCAR-3 system up to now.

This study aims at improving the OSCAR-3 cross section library, and to create an improved set for use in core planning and core follow calculations of the SAFARI-1 reactor.

The library will be regenerated using accurate engineering data and existing materials. Secondly, after regeneration of the cross section library including target plate irradiation rig cross sections, a suitable method of including the target plates in the OSCAR-3 calculational system will be devised. Thus, a method or methods will be adopted after quantifying the explicitly modelled effects caused by the on-power loading and unloading of these target plate irradiation rigs. Since numerous rig types and materials are involved, specific focus will be placed on the target plate irradiation rigs shown in Figure 1-2.

In this way, valuable information, important not only for the OSCAR-3 core-follow calculations, but also for utilization will be derived from the newly

improved OSCAR-3 core calculations. For example, the yield of Mo-99 fission product can be approximated and this can help in improving the planning of the production runs of this isotope for reasons already mentioned. The fact that the library will be improved will further contribute to the optimum operating conditions for the SAFARI-1 reactor.

1.2.3. Research Objective

The SAFARI-1 reactor engineering data and material drawings were used to obtain the information needed for the regeneration of existing materials within the cross-section library [7], [8]. A single cycle, taken from the previous core calculations will be chosen as a reference for this study in order to examine the effects that might be introduced by the presence of the target plates (some of the possible effects are already mentioned in the previous section).

The library regeneration will include redesigning of the fuel model for 200g and 300g fuel elements and the 200g control elements. As mentioned before, core elements that influence the neutronics will be considered for modelling; these include:

- The in-core reflector and filler elements such as the solid aluminium and beryllium elements, hollow aluminium and hollow beryllium elements, hydraulic rabbits, target plate irradiation rigs and any other elements that may influence the operation thus affecting the core neutronics.

For data analysis using the new library a variation in k-effective due to the on-power loading and un-loading of the target plates will be investigated based on the comparison of several methods (discussed later) to include the target plates in our core model.

The relative (local and global) effects on the core neutronics due to the introduction of the target plates are investigated. This includes the flux and

power profiles, core reactivity, fuel burnup and cycle length. This important information will be used to evaluate and choose a suitable method of including the target plate irradiation rigs in the OSCAR-3 core calculations.

2. LITERATURE SURVEY

The fundamental concepts involved in predicting the distribution of neutrons in a nuclear reactor core in order to understand and design a fission chain reaction system are considered in this chapter and two different subjects need to be considered;

i. The determination of the probabilities of occurrence of various neutron-nuclear reactions, and
ii. The derivation and solution of an equation that uses these probabilities to determine the neutron density and fission rate in a nuclear reactor core.

The equation that expresses the motion of neutrons based on the subjects mentioned above, and the fact that the neutron motion can be approximated as a diffusion process, will be briefly discussed here. It will then be used in the SAFARI-1 reactor core calculational system (OSCAR-3), which will be discussed later in this section.

2.1. CROSS SECTIONS FOR NEUTRON REACTIONS

A measure of likelihood of a particular interaction, that is, neutron-nuclear reaction occurring, is characterized by a quantity called the nuclear cross section [3].

If a given material is exposed to the action of neutrons, the rate at which any particular nuclear reaction occurs depends on the number of neutrons, their speed, and the number and nature of nuclei in the specific material. Therefore, in summary, the concept of the cross section of a target nucleus for any given reaction, is a measure of the probability of a particular neutron-nucleus interaction and is a property of a nucleus and of the energy of the

incident neutron. There are different types of interactions and they are discussed in the following sections [2], [3], [5].

2.1.1. Microscopic Cross Section

We consider a mono-energetic neutron beam incident upon a sufficiently thin target (no nuclei in the target will be shielded by other nuclei from the incident neutron beam). The rate at which reactions occur per unit area on the target can be written as,

$$\text{Rate} \equiv R = \sigma I N_A \qquad (2.1.1)$$

In this case, the rate of neutron-nuclear reactions in the target will be proportional to both the incident neutron beam intensity I ($cm^{-2}.sec^{-1}$), and the number of target atoms per unit area N_A (cm^{-2}) and σ is the proportionality constant called the microscopic cross-section. These cross sections are usually measured in units of 10^{-24} cm^2 called barns (b), that is, 10^{-24} cm^2 = 1 barn (b). Therefore the nuclear cross section, σ for a specified reaction (at a given neutron energy) is then defined as the average number of individual processes occurring per target nucleus per incident neutron in the beam, thus,

$$\sigma = \frac{R}{N_A I} \qquad (2.1.2)$$

Each of the processes described by which neutrons interact with nuclei is denoted by a characteristic cross-section. Thus, elastic scattering is described by the elastic scattering cross-section σ_e, inelastic scattering cross-section by σ_{in}, radiative capture cross-section by σ_γ, fission cross-section by σ_f, scattering cross section by σ_s, etc. The total cross-section is thus given by the sum of the cross-sections for all possible interactions, that is

$$\sigma_t = \sigma_s + \sigma_a = \sigma_e + \sigma_{in} + \sigma_f + \sigma_\gamma + ... + ... \qquad (2.1.3)$$

The total cross-section measures the probability that an interaction of any type will occur when neutrons strike a target. The cross-section σ_a, is known as an absorption cross-section. Thus

$$\sigma_a = \sigma_p + \sigma_\alpha + \sigma_f + \sigma_\gamma + ... + ... \qquad (2.1.4)$$

where, σ_p and σ_α are cross-sections for the (n, p) and (n, α) reactions. Fission therefore is an absorption process.

2.1.2. Macroscopic Cross Section

So far, we have looked at a neutron beam incident upon a very thin target. What about the thicker target? The nuclei deeper within the target would tend to be shielded from the incident beam by the nuclei nearer the surface since interactions remove neutrons from the beam.

We now consider a neutron beam incident upon a target of arbitrary thickness [3]. Consider a differential thickness of target between x and $x + dx$, and dx is infinitesimally thin, thus we can use the result from our study of thin targets to calculate the rate at which neutrons suffer interactions in dx per cm^2.

Reaction rate = decrease in beam intensity between x and $x + dx$, that is,

$$-\frac{dI}{I} = N\sigma_t dx$$

and integration over material thickness x of the material gives

$$I_x = I_0 e^{-N\sigma_t x} \qquad (2.1.5)$$

Where I_0 is the number of incident neutrons falling on a particular area, and I_x is the number, which succeeds in passing through x cm of the material over the same area.

In nuclear reactor studies the product $N\sigma_t$, atomic number density and microscopic cross-section, appears frequently and it has become customary to denote it by a special symbol,

$$\Sigma_t = N\sigma_t = [\#/cm^3][cm^2] = [cm^{-1}] \qquad (2.1.6)$$

Σ_t, is referred to as total macroscopic cross-section or the probability per unit path length that a neutron will undergo some sort of a collision as it moves about in a medium. The ratio, $\frac{I_x}{I_0} = e^{-\Sigma x}$, is the probability that a neutron can move through distance x without having a collision. The average distance that a neutron moves between collisions is called mean free path and is given by;

$$\lambda = \frac{1}{\Sigma_t} \qquad (2.1.7)$$

The definition of macroscopic cross-sections applies to all reactions, that is

$$\Sigma_f = N\sigma_f,\ \Sigma_a = N\sigma_a,\ \Sigma_s = N\sigma_s$$

thus, $\Sigma_t = \Sigma_s + \Sigma_a$.

However, macroscopic cross-sections can depend on additional variables such as number density dependence on the position $\underline{r}$ in the sample, and hence macroscopic cross-sections themselves will be space-dependent. A number density might depend on time, e.g. the nuclide of interest was unstable such that its number density was decaying as a function of time. Therefore, in the most general case we would write;

$$\Sigma(\underline{r}, E, t) = N(\underline{r}, t)\sigma(E) \qquad (2.1.8)$$

describing explicit dependence of macroscopic cross-section on neutron energy E, position $\underline{r}$, and time t.

Nuclear cross-sections can be used to characterize the probability of various types of neutron-nuclear reactions occurring, and they play a vital role in the study of fission chain reactions.

The general concepts of neutron cross-sections take into account the fact that the incident neutron usually experiences a change in both direction of motion and energy in the scattering events. The microscopic scattering cross-section will only describe the probability of the reaction occurring but not give information about the change in the neutron direction or energy that occurs in such a collision.

The latter information is very important in certain types of reactor studies. This information is characterized by what is called differential scattering cross sections.

Such differential cross-sections are important in nuclear reactor analysis since they determine the manner in which neutrons move about in the reactor core, as well as the rate at which they leak out of the reactor.

2.2. CROSS-SECTION GENERATION

The neutron cross-section of a material has four fairly distinct energy regions that have to be considered. The first is the *thermal region* (low neutron energy, 0-0.1eV) where the probability of interaction is characterized by a smooth relationship as a function of neutron energy.

Following this region is the *resonance region*, usually for neutrons with energies of roughly 0.1-1000eV. This region is characterized by the occurrence of peaks where the absorption cross-section rises sharply to high

values for certain neutron energies and then falls again. The large peaks are because of neutron energies corresponding to transitions between pairs of nuclear energy levels.

Immediately beyond the region of well-defined *resonances*, the minor or *unresolved resonance* peaks may occur and the nuclear cross-section decreases steadily with increasing neutron energy. At energies in excess of about 10keV, there is what is called the *fast neutron region*.

Thermal neutrons are important in this study since the probability of interaction is determined by the time the neutron spends in the vicinity of the nucleus (i.e. cross section for slow neutrons are inversely proportional to the neutron's velocity, 1/v law). Therefore, this kind of neutron will cause most fission reactions in a nuclear reactor [3].

2.2.1. The Doppler Effect

Although cross sections are commonly associated with neutron energy as discussed above, they actually depend on the relative energy of the interacting neutron and nucleus. If the nuclei were at rest, the relative energy would be identical to the neutron energy. In practice, however, the nuclei in a solid are vibrating about fixed points in the crystal lattice and the energy of vibration increases with temperature.

Furthermore, even at a given temperature, vibrational energies will tend to have a Maxwellian distribution over a wide range of energies. Thus, even for an incident beam of mono-energetic neutrons, the energies, relative to the target nuclei, will vary over a range extending both below and above the single measured neutron energy. This phenomenon is referred to as the *Doppler effect* because of its similarity to the changes in wavelength observed with a moving source of light or sound of apparently fixed frequency [2], [3].

It should be noted that as temperature increases, the range of neutron-nucleus relative energies also increases. Hence, as a result of the *Doppler effect,* the width of a resonance peak is increased as the temperature is raised; this phenomenon is called *Doppler broadening* [2], [3].

2.2.2. Cross Section for Reactor Calculations

For use in nuclear reactor calculations, experimental values or data of the cross-sections and resonance parameters are collected and stored. The data are then evaluated and adjusted, taking into account probable experimental errors, theoretical calculations based on various models, and actual measurements with reactor mockups [2], [3].

A complete set of selected evaluated data suitable for calculating various reactor characteristics are stored electronically in for example the ENDF system [2], [3].

Cross-sections for specified energy ranges, such as are used in various multi-group calculations, are determined by appropriate methods and are available in "libraries" for neutrons with energies above and below 1eV, respectively. An evaluated data set is intended to be independent of the reactor composition, geometries, energy group structure and spectra [3].

2.3. NUCLEAR FISSION

Fission processes occur as a result of a heavy nucleus being unstable thus splitting into more tightly bound lighter nuclei (more stable) thereby giving-off energy. The heavier more unstable nuclei might fission spontaneously, without external intervention (happens rarely).

The fact that the binding energy per nucleon decreases with increasing mass number (A) explains the fission process more clearly; that is, a more stable

configuration of nucleons is obtained whenever a heavy nucleus splits into two parts (fission). The stability displayed by heavy nuclei is due to very strong short range (~10^{-15} m) forces within the nucleus, giving rise to a potential energy barrier (size of this fission barrier is about 6-9 MeV in most heavy nuclei of interest) that must be overcome before the nucleus undergoes fission.

The barrier can be overcome by slamming an energetic particle (with kinetic energy greater than the fission barrier) into the nucleus. An example would be a high-energy gamma striking a heavy nucleus, thereby inducing fission. An alternative would be to let the heavy nucleus capture a neutron with sufficient binding energy to overcome the fission barrier and induce fission.

Heavy nuclei such as ^{233}U, ^{235}U, ^{239}Pu and ^{241}Pu can be induced to fission with neutrons of essentially zero kinetic energy. Such nuclides are referred to as *fissile nuclides* and they can sustain fission chain reactions due to their large fission cross-sections. Nuclides that can be fissioned with only fast neutrons (high-energy neutrons) are referred to as *fissionable*. Examples are ^{232}Th, ^{238}U, and ^{240}Pu as well as fissile nuclei ^{235}U. Fissionable nuclides unlike the fissile ones cannot sustain stable fission chain reactions by themselves due to small fission cross-sections and a rapid decrease in neutron energy to below the threshold value because of inelastic scattering. Hence, they must always be used in combination with fissile nuclides as nuclear fuels [3], [6].

2.3.1. Nuclear Fission Reactions

The nuclear fission reaction produces a number of reaction products, that is fissioned nuclei or fission products, several neutrons as well as gammas, betas and neutrinos. One of the most important fission products for this study is Mo-99 as discussed before. A typical nuclear reaction is [3],

$$^{1}n + {}^{235}U \rightarrow (^{236}U^{*}) \rightarrow fission\ reaction\ products$$

A considerable amount of energy is released in such a reaction, that is, energy in the order of 200MeV. The process is shown schematically below,

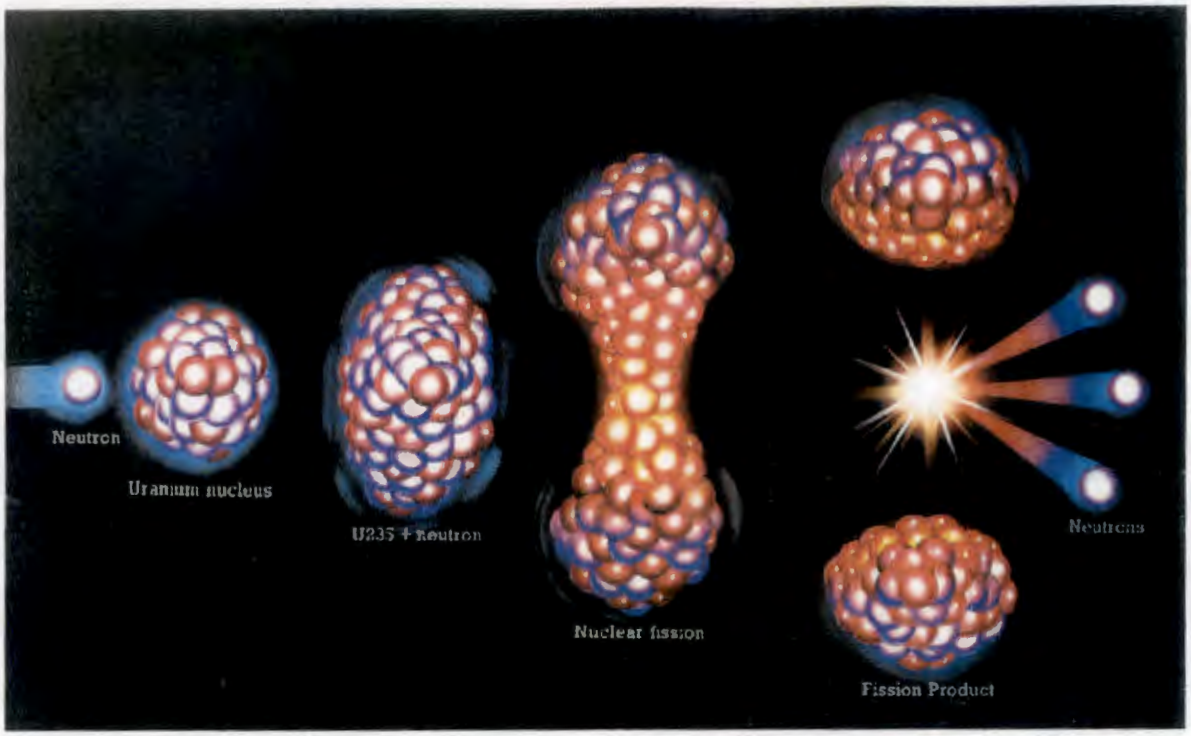

Figure 2-1: Fission Process [8]

This figure shows a neutron incident on a uranium nucleus, to be specific U-235, and upon absorption, it induces fission. A release of fission fragments, and some neutrons that might induce other fissions or interact in different ways, accompanies the reaction.

Most of the neutrons released in fission (usually more than 99%) are emitted essentially instantaneously (within 10^{-14}s of the fission event). These neutrons are referred to as **prompt** (we also have prompt γ-rays). The so-called **delayed** neutrons appear within an appreciable time delay from a subsequent decay of radioactive fission products (a very small fraction < 1%). This small fraction of neutrons plays a vital role in the effective control of the fission chain reaction. The total number of neutrons (both prompt and delayed) released per fission will vary; therefore the average number of neutrons released per fission ν is introduced. As the energy of the incident neutron is increased, ν

NWU LIBRARY

increases slowly. One additional neutron is emitted for every 6-7MeV increase in neutron energy [2], [3], [5].

The distribution of energies due to fission will depend on the nuclear isotope involved and to a lesser extent on the incident neutron energy, and will differ for prompt and delayed neutrons. To characterize this variation in fission neutron energy, we define the fission neutron energy spectrum (fission spectrum) $\chi(E)$ defined as,

$\chi(E)dE \equiv$ average number of fission neutrons emitted with energy E in the interval E to $E+dE$ per fission neutron.

The prompt fission neutrons are emitted as a continuous energy spectrum, with the most probable energy corresponding to the peak of the $\chi(E)$ curve at 0.73MeV.

The delayed neutrons originate in the decay neutron emission of nuclei produced in the β-decay of certain fission products. This is illustrated by a typical fission product decay scheme leading to the emission of these neutrons (delayed neutrons).

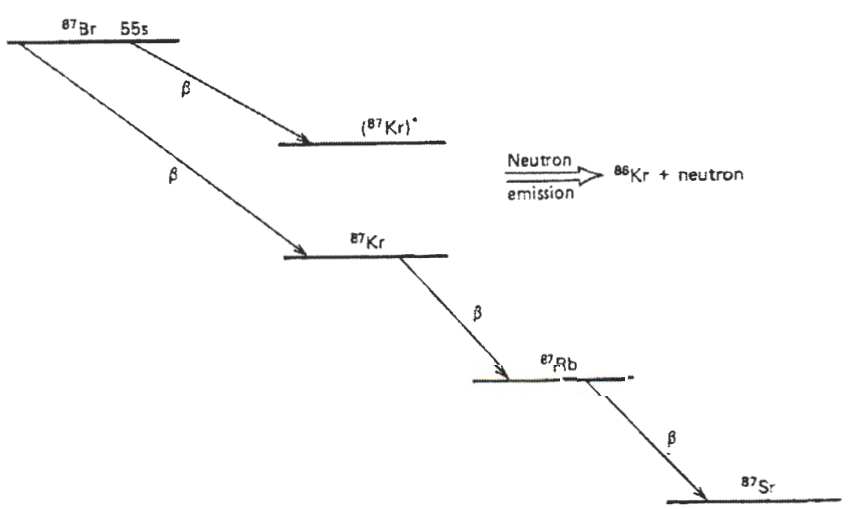

Decay of the ^{87}Br delayed neutron precursor.

Figure 2-2: Decay of the ^{87}Br Delayed Neutron Precursor [3]

Nuclei such as ^{87}Br are called delayed neutron precursors (fission fragments resulting in delayed neutrons emission). These precursors are grouped into classes characterized by approximate half-lives of 55, 22, 6, 0.5, and 0.2 sec. Each precursor group will contain a number of different isotopes. For example, ^{87}Br belongs to the 55s precursor group which is almost entirely due to it. The major contributors to the 22s group are ^{88}Br and ^{137}I. The parameters used in this reaction are defined as,

λ_i = decay constant (β-decay) of I^{th} precursor group

β_i = fraction of all fission neutron (both prompt and delayed) emitted per fission that appear from I^{th} precursor group.

$\beta = \Sigma_i \beta_i$ = the total fraction neutrons which are delayed.

The experimental value of β for U-235 is 0.0065 while for Pu-239 it is 0.0021. It should be clear that the value of β in a reactor would be dependent on the source of fission. For a thermal reactor loaded with fresh enriched U-235 fuel the initial β will be dominated by U-235, while towards the end of cycle (or with burned fuel) the buildup and consequent fission of Pu-239 may contribute up to 40% of the power.

More advanced methods are generally used to calculate β_{eff} in practice. It is an important parameter in safety and transient studies. This parameter expresses the fraction of all neutrons that cause fission that were born delayed.

2.3.2. The Fission Products

Thermal induced U-235 fission has been shown to result in the compound nucleus to split up in more than 40 ways yielding over 80 primary fission products. The fission yield is defined as the proportion (or percentage) of the

total nuclear fissions that form products of a given mass number. The fission yield range from 10^{-5} to over 6% and it should be noted that since two fragments are formed the yield add up to 200% [3], [6].

2.3.3. Amounts and Activities of Fission Products

The amounts and activities of individual fission products and of the total fission-product inventory in the reactor fuel during operation as well as after shutdown are important from several standpoints. These quantities are used for several purposes.

The rate at which the nuclear concentration, say N_i, the number of nuclei per unit volume, of a given fission product nuclei i changes with time, both during and after reactor operation, may be expressed in the general form [2],

$$\frac{dN_i}{dt} = formation\ rate - destruction\ rate - decay\ rate. \qquad (2.3.1)$$

Under certain conditions equation (2.3.1) reduces to

$$\frac{dN_i}{dt} \approx \gamma_i \Sigma_f \phi - \lambda_i N_i . \qquad (2.3.2)$$

Manipulating and integrating this result when irradiation is started ($t = 0$) gives

$$A_i(t) \approx \gamma_i \Sigma_f \phi (1 - e^{-\lambda_i t}), \qquad (2.3.3)$$

where t is the time of irradiation, $A_i(t)$ is the activity (or rate of particle emission), γ_i is the fission yield of the nuclide i expressed as a fraction of the total number of fissions in which i is produced directly, λ_i is the decay constant of i, Σ_f is the average macroscopic fission cross section and ϕ is

the average neutron flux. The quantity $1-e^{-\lambda_i t} \to 1$ when $t \to \infty$, hence after sufficient time, the activity of a species will approach a limiting value given by

$$A_i(saturation) \approx \gamma_i \Sigma_f \phi . \qquad (2.3.4)$$

This quantity is called saturation activity and is equal to the rate of disintegrations.

2.3.4. The Energy Released in Fission

The energy release in a nuclear fission reaction is distributed among a variety of reaction products. It is important to distinguish between the total energy released in the process and the energy that can be recovered in the reactor and is therefore available for the production of heat. Most of the energy released in fission appears as the kinetic energy of the fission fragments. These fission fragments come to rest within 0.001-0.01cm of the fission site so that all their energy is converted into heat [3].

The energies of the fission product, β-rays and γ-rays, the prompt and the delayed neutrons, and the prompt γ-rays are also recoverable since almost none of this radiation ever escapes from the nuclear power system. This energy will be distributed over the core of the reactor and adjacent material such as shielding, etc.

The recoverable energy per fission is approximately 200MeV, and in the absence of more accurate data, this value is normally used, at least in preliminary calculations.

2.3.5. Fission Fuels

It has been noted that the principle nuclides of concern in nuclear reactor applications are *fissile nuclides* and those susceptible to fast neutron fission, *fissionable nuclides* [2], [3]. The low concentration of ^{235}U is increased above its natural value (enriched) for most present day reactor types (e.g. SAFARI-1, 90% enrichment ^{235}U and 45% for the target plate irradiation rig).

Fertile isotopes play an important role via a process called transmutation, which takes place in present day reactors. The key parameter in these processes is the number of neutrons produced in each fission reaction per neutron absorbed in the fuel.

$$\eta \equiv Average\ number\ of\ neutrons\ produced\ per\ neutron\ absorbed\ in\ fuel$$

$$\eta = \nu \frac{\Sigma_f}{\Sigma_a} \qquad (2.3.5)$$

where, Σ_f is the macroscopic fission cross section of fissile nuclides and Σ_a is the total absorption cross section. For a single material, $\frac{\Sigma_f}{\Sigma_a}$ may be replaced by $\frac{\sigma_f}{\sigma_a}$.

At low energy neutrons, $\eta(E)$ is of the order of two but increases with energy above 0.1MeV as the capture-to-fission ratio $\frac{\sigma_\gamma}{\sigma_f}$ decreases.

2.4. FISSION CHAIN REACTION AND NUCLEAR REACTORS

Now that we have discussed how fission occurs, we need to apply these fission reactions to the practical utilization of nuclear energy. Essential conditions are required to maintain a self-sustained fission chain reaction. In

other words, the rate of neutron absorption and leakage are balanced by the rate of fission neutron production.

Since at least two neutrons are released in every fission event and these neutrons are capable of inducing fission of the other nuclei, and so on, it would appear that the conditions of a self-sustaining fission chain reaction would be met. However, it must be taken into account that the neutrons produced in the fission process can take part in other (non-fission) reactions. In addition to this competition for neutrons, there is the inevitable loss of neutrons from the system by leakage [3].

The minimum condition for a chain reaction to be maintained is that for each nucleus capturing a neutron and undergoing fission there shall be produced, on average, at least one neutron that causes the fission of another nucleus.

This minimum condition can conveniently be expressed in terms of a multiplication factor or reproduction factor [2], [3], defined as;

$$k = \frac{number\ of\ \ fissions\ in\ one\ generation}{number\ of\ \ fissions\ in\ \ preceding\ \ generation}.$$

2.4.1. Reactor Criticality

If k is exactly equal to, or slightly greater than unity, a chain reaction will be possible. However, if k is less than unity, even by a very small amount, the chain cannot be maintained. In summary we have;

$$k < 1 \Rightarrow sub - critical$$
$$k = 1 \Rightarrow critical$$
$$k > 1 \Rightarrow \sup er - critical$$

In the first case, the number of fission neutrons will decrease with time and hence the chain reaction dies out. For the second case the chain reaction will

proceed at a constant rate, is time-independent and energy is released at a steady level. Finally, for the last case where the number of neutrons increases from generation to generation, energy will increase with time.

A practical definition of the multiplication factor k can be given by;

$$k = \frac{rate\ of\ neutron\ production\ in\ reactor}{rate\ of\ neutron\ loss\ (leakage + absorption)\ in\ reactor}$$

$$k \equiv \frac{P(t)}{L(t)} \qquad (2.4.1)$$

It has also been noted that the production and loss rate may change with time (e.g. due to fuel consumption).

Since one neutron per fission is required to maintain the chain reaction, the number of neutrons will increase by $k-1$ in one generation. Thus, if there are N_0 neutrons present initially, the rate of increase will be $N_0(k-1)$ per generation. If l is the average neutron lifetime between successive neutron generations in the system under consideration, then

$$\frac{dN}{dt} = \frac{N_0(k-1)}{l} \qquad (2.4.2)$$

where $\frac{dN}{dt} \equiv$ Production rate - Loss rate = $P(t) - L(t)$ and $l = \frac{N(t)}{L(t)}$

Upon integration we have;

$$N = N_0 e^{(k-1)t/l} \qquad (2.4.3)$$

This model shows us that the growth or decay of the neutron population in a reactor obeys an exponential growth law. As long as the multiplication factor

is less than unity, no matter by how small a margin, the number of neutrons must inevitably decrease with time, and a self-sustaining reaction is impossible.

We can also regard the time behaviour of the reactor power level as being exponential with a time constant or reactor period T given by,

$$T = \frac{l}{(k-1)} \qquad (2.4.4)$$

$k \to 1 \Rightarrow T \to \infty$ this corresponds to a time independent neutron population or reactor power level.

Suppose we change a critical reactor so that k = 1.001. Since the neutron lifetime in a typical LWR reactor is about 10^{-4}sec, the reactor period is 0.1sec. Hence in one second, the power will increase by a factor $e^{10} \cong$ 22,000! Reactor control would be very difficult if a fission chain could only be maintained by means of the prompt neutrons [3].

In this model, we have neglected the effect of delayed neutrons, which significantly slow down the reactor time response.

By defining an effective lifetime as a properly weighted average of the prompt and delayed lifetimes, delayed neutrons can be included:

$$l = 10^{-4}\,\text{sec}$$

$$l_{eff} = 10^{-1}\,\text{sec}$$

$$T = 100\,\text{sec}$$

2.4.2. The Formal Calculation of k for Thermal Reactors

Suppose that we want to calculate k for a pile of uranium that we wish to turn into a nuclear reactor, and that the material composition is assumed to be homogeneously mixed, that is, a uniform reactor composition.

Since, for the present purpose, the multiplication factor may be defined as the ratio of the total number of thermal neutrons absorbed, on average, in one generation to the number of thermal neutrons absorbed in the preceding generation, on average, in an infinite medium, it follows that

$$k_{\infty} = \eta \varepsilon p f \qquad (2.4.5)$$

where, η is the average number of fast fission neutrons emitted as a result of the capture of one thermal neutron in fuel material (i.e. both ^{235}U and ^{238}U). ε is the ratio of the total number of fission neutrons to the number from thermal fission p is the resonance escape probability, which is the fraction of the fast fission neutrons that escapes capture while being slowed down, f the thermal utilization, is the fraction of the thermal neutrons absorbed in fuel to the total thermal neutrons absorbed.

This result is referred to as the *four-factor formula*. Therefore, for a self-sustaining chain reaction in a system of infinite size, the multiplication factor should be unity; the criterion for natural uranium system is therefore $\eta \varepsilon p f = 1$.

Now, lets consider a system where there is leakage, in a reactor of a finite size. The energy distribution will not be the same everywhere in the system, as is true for an infinite (homogenous) system, but will depend on the position in the reactor. For a reactor of finite size, the condition that the multiplication factor should be unity is no longer adequate for a self-sustaining chain reaction. It is required that, for every thermal neutron absorbed in fuel there shall be produced, on average, one thermal neutron in addition to the loss by leakage from the reactor.

Then, our new definition for the multiplication factor is

$$k = \eta \varepsilon p f P_{FNL} P_{TNL} \qquad (2.4.6)$$

where, P_{FNL} is the probability that fast neutrons will not leak out (fast non-leakage), and P_{TNL} is the probability that thermal neutron will not leak out (thermal non-leakage).

This is known as the six-factor formula [3] and k is referred to as effective multiplication factor, given by,

$$k_{eff} = k_{\infty} P_{FNL} P_{TNL}. \qquad (2.4.7)$$

2.4.3. Critical Size of the Reactor

The escape of neutrons occurs at the exterior, but absorption, leading to fission and neutron production, occurs throughout the whole of the interior of the reactor. The number of neutrons lost by escape thus depends on the external surface area, while the volume determines the number formed. To minimize the loss of neutrons and thereby increase the non-leakage probability, it is necessary to decrease the ratio of area to volume; increasing the size of the reactor can do this. The critical size is that for which the non-leakage probability $P_{NL} = P_{FNL} P_{TNL}$, is such that $k_{\infty} P_{NL}$ is just equal to unity [2], [3].

Since the area-to-volume ratio depends on the geometrical shape, the shape of the reactor will determine the non-leakage probability.

NWU LIBRARY

2.4.4. Reactivity

The *reactivity*, ρ, is the fractional departure of a system from criticality, and is defined by [2],

$$\rho = \frac{k_i - k_f}{k_i}, \qquad (2.4.8)$$

where, k_i is the initial multiplication factor and k_f the final multiplication factor. *Reactivity* is measured in the units of 'pcm'. 1 pcm is equivalent to a reactivity of 10^{-5}. Equation 2.4.8 is a general expression, which applies for all the values of k, that is, for values of k less than one, greater than one or equal to one.

2.4.5. Reactor Control

Practically, a reactor must be constructed so that it is actually appreciably greater than critical size for operational purposes. The reason for this is to achieve a critical chain reaction using a minimum mass of fissile material called the critical mass (mass required to make a reactor critical). The multiplication factor will exceed unity, therefore producing the only feasible means of increasing the number of neutrons, and hence the fission rate up to a point where the required power level is attained. Once this has been reached it is necessary to decrease the effective multiplication factor to unity, and then the reactor will remain in a steady state, that is neutrons produced as fast as they are used up by leakage and capture.

The extra multiplication is normally required for [3];

i. Cycle burn-up: to operate at a power level for a period of time one must provide enough excess fuel to compensate for those fuel nuclei destroyed in fission reactions during the power distribution.

ii. Negative temperature coefficient: ambient-operational temperature, increases with a decrease in multiplication of the reactor.

iii. Power level change: to be able to adjust between super-critical and sub-critical.

Some control mechanism should be provided to suppress the effect of this excess multiplication if not used to achieve criticality. Such control is usually achieved by introducing into the reactor core materials characterized by large absorption cross-sections. They will then serve to absorb the excess neutrons provided in the chain reaction.

The reactor control mechanisms required are [3];

i. Shim control: control absorbers are used to hold down the excess multiplication introduced to compensate for fuel burn-up.

ii. Scram control: to force the reactor to sub-critical in the case of an emergency.

iii. Manoeuvring control: to regulate the power level of the reactor.

2.4.6. Control Rod Worth

The total worth of the control rods is clearly an important reactor design parameter. The most important criterion of a control rod is its effect on the criticality value of the core. Control rod effectiveness is therefore measured in terms of its reactivity effect on the core.

A commonly used unit for the effectiveness of the control rods is the control rod worth, measured in dollars ($). It represents the negative reactivity introduced by the control rod, divided by the effective delayed neutron fraction lifetime (β_{eff}) of the core [2], [3].

$$\textit{Reactivity in dollars} \equiv \frac{\rho}{\beta_{eff}} \qquad (2.4.9)$$

When prompt critical, a reactor has a reactivity of exactly one dollar. For a thermal reactor using U-235 as the fissile material, for example, a reactivity of \$1.50 would imply a value of 1.50 x 0.0065, i.e., 0.0097, and an effective multiplication factor of about 1.0098 [3].

2.5. COMPUTER CODES AND THE TRANSPORT THEORY

2.5.1. Introduction

The reactor core design requires powerful computers and extensive, versatile software packages to meet the need for sophisticated mathematical modelling of neutron behaviour and distribution in the core (neutronic calculations). After the software has been developed, it is necessary to maintain it in operational conditions during its period of use, which may extend over some years.

Such codes are available for different applications, for example, shielding, thermal-hydraulics, structural analysis, etc. The OSCAR-3 code package for nuclear reactor core analysis is an example of such a code.

To apply the OSCAR-3 code system one should be familiar with the neutronic theory, which describes the behaviour and distribution of neutrons in a nuclear reactor. The theory is briefly discussed in the following section.

2.5.2. Neutron Transport Theory

The behaviour of neutrons in a nuclear reactor is governed by the distribution in space, energy, and time of these neutrons in a system. One of the central problems of reactor theory is to predict this distribution and behaviour; once

this is done, we will be able to infer stability of the fission chain reaction. This behaviour is investigated by considering the process of neutron transport, which is the motion of neutrons as they stream about the reactor core. The neutron motion can also be approximated as a diffusion process where neutrons "diffuse" from a region of high neutron concentration to a region of low concentration [2], [3], [5].

The fundamental equation expressing the principle of conservation of neutrons is called the BOLTZMANN TRANSPORT EQUATION. In a linear form suitable for describing our neutron "gas" the expression is called the NEUTRON TRANSPORT EQUATION. The expression is given by [3],

$$\frac{1}{v}\frac{\partial\Psi(\underline{r},E,\hat{\Omega},t)}{\partial t}+\hat{\Omega}\nabla\Psi+\sum(\underline{r},E)\Psi(\underline{r},E,\hat{\Omega},t)=$$
$$\int_{4\pi} d\hat{\Omega}'\int_{0}^{\infty} dE'\sum_{S}(\underline{r},E'\rightarrow E,\hat{\Omega}'\rightarrow\hat{\Omega})\Psi(\underline{r},E',\hat{\Omega}',t)+S(\underline{r},E,\hat{\Omega},t) \qquad (2.5.1)$$

where $S(\underline{r}, E, \hat{\Omega}, t)$ is the neutron source term, with the initial conditions,

$$\Psi(\underline{r},E,0) = \Psi_0(\underline{r},E,\hat{\Omega}) \qquad (2.5.2)$$

and for example, the black boundary condition is one possibility

$$\Psi(\underline{r}_S, E, \hat{\Omega}, t) = 0 \text{ if } \hat{\Omega}.\hat{e}_S < 0, \textit{ for all } \underline{r}_S \textit{ on } S \qquad (2.5.3)$$

$\Psi(\underline{r}, E, \hat{\Omega}, t)$ is the angular neutron flux distribution with units *neutrons.cm*$^{-2}$*s*$^{-1}$, and is defined as,

$$\Psi(\underline{r}, E, \hat{\Omega}, t) = vn(\underline{r}, E, \hat{\Omega}, t) \qquad (2.5.4)$$

The derivation of this equation is based on several assumptions and that the neutrons are conserved in the system.

In this expression the dependent variable is the angular distribution of neutron velocity vectors, $n(\underline{r},v,\hat{\Omega})$, which is defined as the number of neutrons at $\underline{r}$ per unit volume that are travelling with speed v per unit velocity in the direction $\hat{\Omega}$ per unit solid angle.

It should be noted that the transport equation is linear in the unknown dependent variables $n(\underline{r},v,\hat{\Omega},t)$ with seven independent variables and it is an "integro-differential" equation. The presence of derivatives suggests the use of initial and boundary conditions for the angular density as stated before.

The result is the neutron transport equation, which expresses the distribution of neutrons in space, energy, and time in a straightforward manner. If the conditions are such that the neutron density does not change with time, the equation then refers to a system in steady state. Typical neutron energies range from 20MeV down to 0MeV and the time in a typical reactor cycle can be weeks or several months.

Direct analytical solutions are only possible for the simplest of problems. Instead, various other methods have to be devised to obtain a solution of the equation.

For many reactor calculations, the detail of the angular dependence of the neutron flux is not necessary. Integrating the neutron transport equation over all angles and defining the neutron flux $\underline{\phi}(\underline{r},E,t)$ as,

$$\underline{\phi}(\underline{r},E,t) \equiv \int_{4\pi} d\hat{\Omega}\Psi(\underline{r},E,\hat{\Omega},t) \qquad (2.5.5)$$

yields the neutron continuity equation,

$$\frac{1}{\underline{v}}\frac{\partial \underline{\phi}(\underline{r},E,t)}{\partial t} + \underline{\nabla} \bullet \underline{J}(\underline{r},E,t) + \Sigma_t(\underline{r},E)\underline{\phi}(\underline{r},E,t) =$$

$$\int_0^\infty dE' \Sigma_s(\underline{r},E' \rightarrow E)\underline{\phi}(\underline{r},E',t) + S(\underline{r},E,t) \qquad (2.5.6)$$

where $S(\underline{r}, E, t)$ is the angular integrated source term and $\underline{J}$ is the neutron current density defined by,

$$\underline{J}(\underline{r},E,t) \equiv \int_{4\pi} d\hat{\Omega}\hat{\Omega}\Psi(\underline{r},E,\hat{\Omega},t) \qquad (2.5.7)$$

An additional unknown is introduced by the removal of the angular dependence, which make it impossible for the equation to be solved.

2.5.2.1. Numerical solutions to the neutron transport equation

There are various numerical solution methods for the neutron transport equation, all of which discretise the system under consideration in one way or another. These include [1], [3];

i. Discrete Ordinate (S_N) methods

ii. Collision Probability methods, and

iii. Method of Characteristics

The first simplification that is made in all neutron transport and indeed all neutron diffusion calculations is the discretisation of energy into distinct energy regions or bins. Many of the methods apply to 1-D or 2-D geometries.

The neutron distribution problem could be solved by inserting a complete set of appropriate cross-sections into the transport equation, which represents the neutron interaction probabilities, together with the geometrical arrangement of the materials in the system. In practice, however this proves not to be possible due to the following reasons [1], [3];

i. The cross-sections and their variation with neutron energy are very complicated and not completely known,

ii. The geometrical arrangement of the materials in a reactor is generally so complex that the solution of the transport equation in its original form is difficult to solve, and requires a great deal of computing time.

2.5.3. The Diffusion Theory Approximation

As stated before, neutrons will move from the region of higher neutron density to the region of lower neutron density (or flux). According to Fick's law of diffusion, the net rate of neutron flow in a given direction is proportional to the (negative) spatial gradient of the neutron flux [2], [3], [6].

$$\underline{J}(\underline{r},t) = -D(\underline{r})\nabla\underline{\phi}(\underline{r},t) \qquad (2.5.8)$$

where,

$$D(\underline{r}) \cong [3\Sigma_{tr}(\underline{r})]^{-1} = [3(\Sigma_t(\underline{r}) - \overline{\mu_o}\Sigma_s(\underline{r}))]^{-1} \qquad (2.5.9)$$

and is called the neutron *diffusion coefficient*.

The macroscopic transport cross section Σ_{tr} is given by,

$$\Sigma_{tr} = \Sigma_t(\underline{r}) - \overline{\mu}_0\Sigma_s(\underline{r}) \qquad (2.5.10)$$

and $\bar{\mu}_0$ is the average scattering angle cosine.

Introducing this law to our angular independent neutron transport equation 2.5.6 we get the following time dependent diffusion approximation results, after rearrangement and simplification,

$$\frac{1}{v}\frac{\partial \phi(\underline{r},t)}{\partial t} - \underline{\nabla} \bullet D(\underline{r})\underline{\nabla}\phi(\underline{r},t) + \Sigma_a(\underline{r})\phi(\underline{r},t) = s(\underline{r},t) \qquad (2.5.11)$$

where,

$$\Sigma_a(\underline{r}) = \Sigma_t(\underline{r}) - \Sigma_s(\underline{r}) \qquad (2.5.12)$$

Equation 2.5.11 is usually referred to as the *diffusion equation*. For a system in the steady state, the first term falls off, and then we have the steady state *diffusion equation* for one-speed neutrons as follows [3];

$$-\underline{\nabla} \bullet D(\underline{r})\underline{\nabla}\phi(\underline{r},t) + \Sigma_a(\underline{r})\phi(\underline{r},t) = S(\underline{r},t) \qquad (2.5.13)$$

This equation is useful since it is amenable to simple mathematical treatment, and it provides insight into the characteristics of both non-multiplying and multiplying systems. It allows us to study many of the more important concepts arising in nuclear reactor analysis.

The following assumptions [3] had to be made to obtain the one speed diffusion approximation or single energy group (all the terms evaluated at the same energy),

i. Angular flux is linearly anisotropic (expand to first order) - weak angular dependence.

ii. The one-speed approximation – single neutron energy group

NW LIBRARY

iii. Isotropic neutron source – higher source moments vanishes

iv. The neutron current density changes slowly on a time scale compared to the mean collision time.

Although this approximation is valid for most cases, the assumption of weak angular dependence is violated in the following cases [3];

i. Near boundaries or where the material properties change dramatically from point to point over distances comparable to the mean free path.

ii. Near localized sources, and

iii. In strongly absorbing media

This implies that strong angular dependence can be associated with neutron fluxes having a strong spatial variation. The diffusion approximation is normally valid if flux is slowly varying in space [3]. Various methods have been employed to improve the model for regions where the diffusion theory is not applicable. This is mostly done by including transport results in the diffusion calculation by some means (e.g. applying equivalence theory).

2.5.3.1. Numerical solution of the neutron diffusion equation

The most common method of numerical solution of the diffusion equation is the *finite difference* method, in which the spatial region is divided into small intervals. Differentials in the equation are represented as differences between these regions. The problem with this approach is that it results in a very large number of spatial meshes, which makes the solution matrix large and the solution time relatively long [1].

An alternative method to finite difference is the **Nodal method**, described below. This is the method employed in MGRAC, the neutronics code that forms the basis of OSCAR-3 [1], [3].

i. **Nodal Method**

This is an alternative method, which allows larger spatial homogenized volumes or nodes to be considered. For example, a nodal volume might be the same size as a SAFARI-1 reactor fuel assembly. This method permits the determination of average power per node and multiplication factor of the reactor without lengthy calculations.

Several nodal methods exist, each differing in the in-node flux approximation and the solution technique applied to solve auxiliary 1-D equations. Most widely used are analytic and polynomial approaches, with OSCAR-3 using the analytic approach. In the analytical nodal method, the auxiliary 1-D equation in a given direction is solved using analytic methods. The only approximation that this introduces is the one that has to be assumed for the transverse leakage shape.

2.5.4. Reactor Calculation System

Code systems used for nuclear reactor calculations can be placed in some broad, sometimes overlapping categories. The one with which we will concern ourselves is the Steady State Reactor Physics category. Steady State is the most frequently performed reactor calculation, which starts with a nuclear data library together with engineering specifications and results in the neutron flux distribution in space, energy and time (treated quasi-statically). From this distribution, design quantities such as a multiplication factor, power distribution, reactivity effects and reaction rates are determined [1].

This category is usually divided into cell, lattice and core physics. OSCAR-3 falls into this category.

2.5.5. Core Calculation Path

The direct solution of the transport equation for the entire reactor core is not feasible; hence, the calculation proceeds in stages. A small system, with detailed representation of energy and spatial dependence of the neutron flux is required at the start. The size is increased at each succeeding stage of the system, while the detail of energy and space representation is reduced. After each stage, equivalent cross-sections are produced for use in the next stage. This is achieved by a procedure known as group condensation and homogenization [1], [3].

A typical reactor calculation would start with the calculation of a single pin cell, followed by a fuel assembly and ending with the entire reactor core. A modern approach is to combine the first two steps into a single calculation.

2.6. THE OSCAR CALCULATIONAL SYSTEM

2.6.1. The OSCAR-3 System

OSCAR, an acronym for "Overall System for the Calculation of Reactors" is an integrated code package for nuclear reactor core analysis for PWR and MTR type reactors. It offers capabilities such as a 3-D full core multi-cycle core analysis (i.e. 3-D, multi-group, advanced nodal diffusion code, full cross section feedback and depletion capabilities) and graphical result outputs. The other versions of OSCAR, that is OSCAR-1 (early 80's) and OSCAR-2 (late 80's) were based on finite difference neutronic methods and consisted of several codes which were difficult to use and impractical for routine reactor core analyses [1].

The aim in developing or designing the OSCAR-3 system (developed since 1991), was to provide a user friendly, quality assured, high accuracy, and fast

system for core-follow calculations. This has been achieved using advanced calculational methods and an integrated code development platform.

This code is divided into several sub-systems, namely MAESTRO, CROGEN, CROLIN and CORANA. The interrelation of the systems is depicted in Figure 2-3 below. Although the MAESTRO sub-system is still under development, it is the module that controls the system integration (communication) and execution. It constitutes the interface between the user and the system. CROGEN, CROLIN, and CORANA are available for limited but practical applications to MTRs and PWRs [1].

In these sub-systems the component codes currently communicate via well-defined interface files and codes and are run in stand-alone mode. The sub-systems are discussed in more detail in the sections to follow.

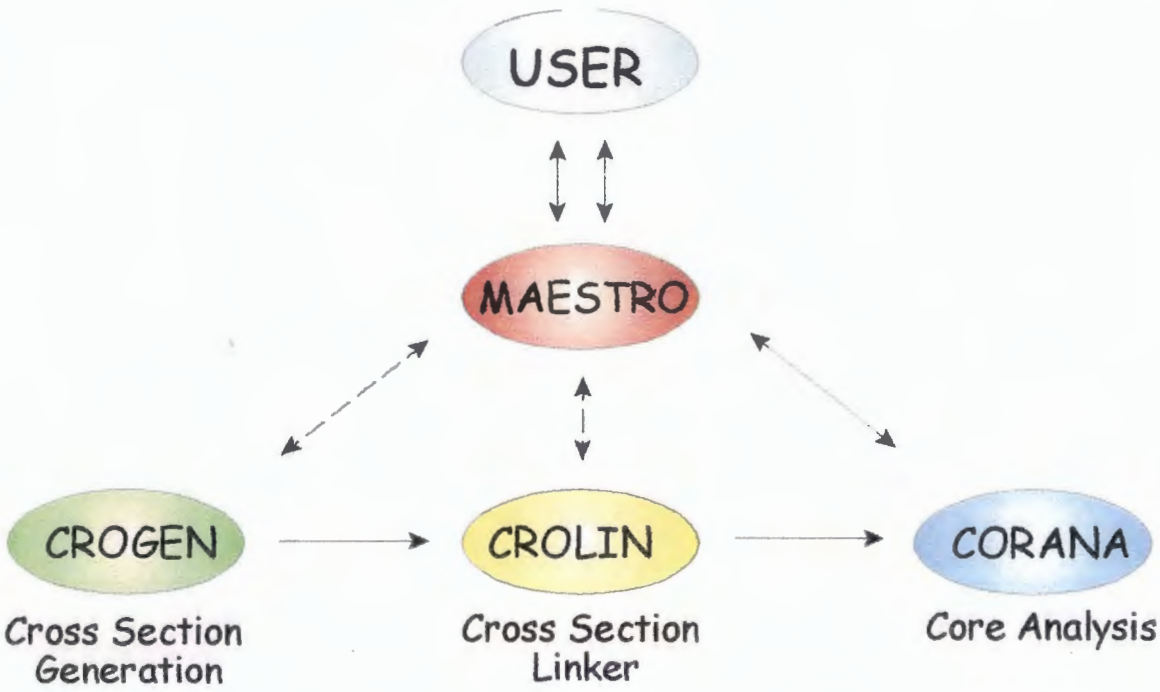

Figure 2-3: Sub-Systems in OSCAR-3 [1], [14], [15]

i. **MAESTRO**

This is a graphical interface for the OSCAR-3 system. It is intended to control all the sub-systems, but is currently only associated with CORANA [1], [15]. The programs available here are: *config editor*, *exposure editor*, *shuffle*, *mgrac*, *results viewer* and *report generator*.

The main function of this sub-system is information management to ensure the quality control of calculations and results. The other main function is to enhance the reliability of core analyses and the efficiency of core performance analysts who perform a great variety of complex calculational sequences.

ii. **CROGEN**

CROGEN is the acronym for "CROss section GENeration"; the package encompasses a whole range of codes used in the production of few-group cross section libraries [1], [15]. The sub-system is responsible for generating a cross section via two paths; for fuel assembly cross sections and for reflector cross sections. The main code in this sub-system is HEADE.

HEADE is the acronym for "HEterogeneous Assembly DEpletion". It is a modern two-dimensional code which incorporates all the functions required for generating few-group homogenized assembly cross sections, flux or power form functions and interface flux discontinuity factors as functions of exposure, water density, water temperature, fuel temperature, control rod status, etc. The homogenized assembly cross-sections and other data can be written to a so-called HEADE file.

Another path of cross section generation is by STYX, which is a two-dimensional collision probability code used for special purpose calculations. These include the determination of few-group cross sections for irradiation rigs and the control portion of the SAFARI-1 control

element, which consists of an upper control section and a bottom fuel follower section. It also plays an important role in determining the heterogeneous flux form functions for irradiation rigs, which are used in conjunction with nodal reactor calculation results to estimate specific reaction rates.

iii. **CROLIN**

CROLIN, the acronym for "CROss section LINker", consists of the POLX and the LINX codes (see Appendix E). It takes files from the CROGEN calculation and converts them into a common file format that can be used in core calculations [1], [15].

POLX reads a single file (e.g. HEADE) containing few-group cross sections and other data tabulated as a function of several state parameters to perform a least-squares quadratic polynomial fit on data for a given assembly (e.g. fuel assembly or reflector assembly). The polynomial coefficients as well as burnup chain data are written to an assembly specific POLX file and stored for repeated use later.

LINX is used to merge several POLX files into a single run-time library (LINX file) for direct use by the MGRAC nodal code.

iv. **CORANA**

CORANA is an acronym for the CORe ANAlysis module. It has two main codes, the MGRAC nodal depletion code and the fuel shuffling code, SHUFFLE. The main interface between these two codes is the EXPOSURE file, which contains core loading information, nodal exposures and isotopic number densities. MGRAC utilizes at most two such files, namely an input EXPOSURE file and an output EXPOSURE file [1], [15].

MGRAC, is an acronym for the "Multi-Group Reactor Analysis Code". It solves the static neutron diffusion equation in an arbitrary number of energy groups using either a standard mesh-centred finite difference or an advanced multi-group analytic nodal method.

MGRAC allows calculations to be run in one, two or three dimensions in conjunction with a range of symmetry options (whole, half, quarter or eighth core) and boundary conditions (zero-flux, vacuum, reflective or albedo). It uses a quasi-static approach to model the long-term depletion behaviour of a reactor core; static diffusion theory calculation at selected time points determine the flux or power levels used for the solution of time-dependent isotopic depletion equations (i.e. a microscopic depletion model) over broad time steps (burnup steps). The depletion equations are solved analytically, subject to the assumption that the flux spectrum and flux or power levels remain constant during a burnup sub-step. For the static neutronic calculations, a sophisticated cross section feedback model utilizing a quadratic polynomial library (a LINX file) is incorporated to cater for power and burnup-dependent feedback.

Any new reactor cycle can be modelled by reading an input EXPOSURE file containing the number densities and exposures at the beginning of cycle (BOC). At the end of a cycle calculation, MGRAC writes the end of cycle (EOC) exposure and isotopic data to an output EXPOSURE file for later use by the SHUFFLE code.

SHUFFLE allows for the fuel reload of the reactor for the next cycle by providing an easy data management system. Its primary function is to create the MGRAC input EXPOSURE file and a run-time polynomial cross section (LINX) file for each new reactor cycle to be analyzed with MGRAC. In order to do this, SHUFFLE makes use of several pairs of files, each defining a particular facility's (reactor core or storage pool) geometric configuration (a CONFIGURATION file) and its current loading status (an EXPOSURE file). For the core to be loaded, the EXPOSURE

file will only contain the current loading status after the SHUFFLE execution.

The actual loading instructions are given in the 'LOADING" file (the SHUFFLE input data deck) and these instructions are always referred to actual physical positions in the facility using frames of reference contained in the CONFIGURATION files. SHUFFLE also performs many consistency checks, one of which is to determine if the destination core has indeed been loaded according to user-specified symmetry.

3. RESEARCH DESIGN

3.1. INTRODUCTION

The Reactor and Radiation Theory Group (RRT) of Necsa provides a comprehensive theoretical and calculational support to the SAFARI-1 reactor. The calculational support is based on various modern methods and uses computer codes developed both locally and internationally. At present OSCAR-3 is used for core planning and core follow calculation without the inclusion of the target plates in the irradiation positions. In this study the OSCAR-3 code will be used to create a quality assured cross section library and devise a method to include the target plates in irradiation positions and ultimately in the core planning and core follow calculations.

3.2. RESEARCH METHODOLOGY

3.2.1. Quality Cross Section Generation

A few-group homogenized cross section library was generated using the OSCAR-3 two-dimensional sub-codes, HEADE and STYX (i.e. CROGEN subsystem) [1], [15].

For this purpose the SAFARI-1 material information was gathered, that is engineering drawings with precise dimensions, material composition, etc. This was done for the ex- and in-core SAFARI-1 assembly elements, including reflector elements (i.e. aluminium, beryllium, lead), hydraulic rabbits, control elements, in-core irradiation facilities (e.g. target plate irradiation rig), fuel element, aluminium core box, aluminium water-box, etc [7], [8].

The material compositions, such as U-235 enrichment in the case of fuel elements and any other assemblies with fuel and number densities of

materials were considered. Information on reactor operation conditions was obtained in order to determine the depletion and off-base calculations that should be performed [8].

The information mentioned above together with the sample (e.g. fuel, reflector assemblies, etc.) will play an important part when setting up HEADE or STYX input [1]. In addition, environment surrounding a particular assembly of interest will be considered. As an example a fuel assembly 2-D geometry sample is shown in Figure 3-1 below,

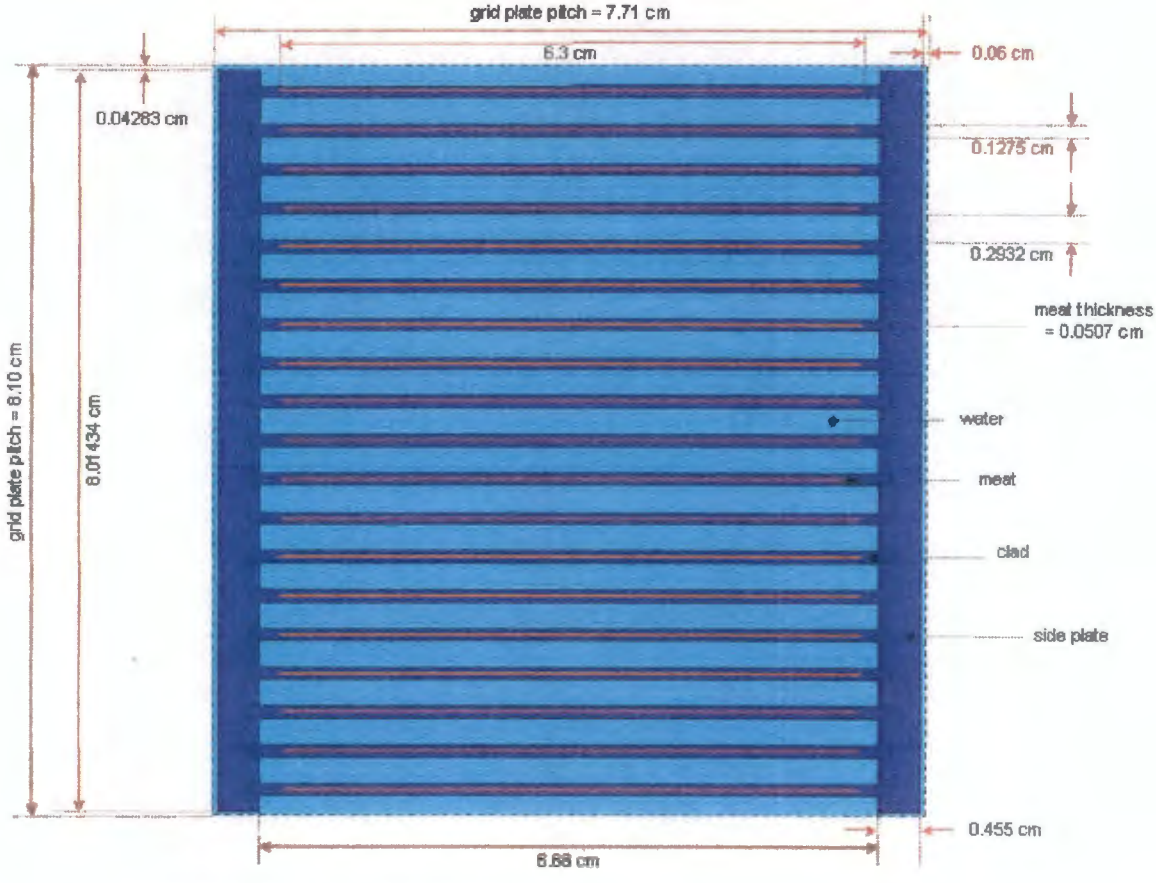

Figure 3-1: Fuel Assembly Geometry

This is an MTR (SAFARI-1) fuel assembly consisting of 19 fuel plates being held in place by an aluminium support structure with water as the moderator. The 200g and 300g fuel assemblies were considered, as these are the assemblies being used in SAFARI-1.

3.2.1.1. Sampling of SAFARI-1 assemblies

A suitable way of sub-dividing the assembly in Figure 3-1 into regions of equal composition was implemented. The selected sub-division is shown in Figure 3-2 below. Sub-dividing an assembly element is important because HEADE or STYX need the assembly problem described in terms of rectangular nodes (cells), which can contain either cylindrical pins or plates and it also simplifies the input since one can treat cells with equal composition the same [1].

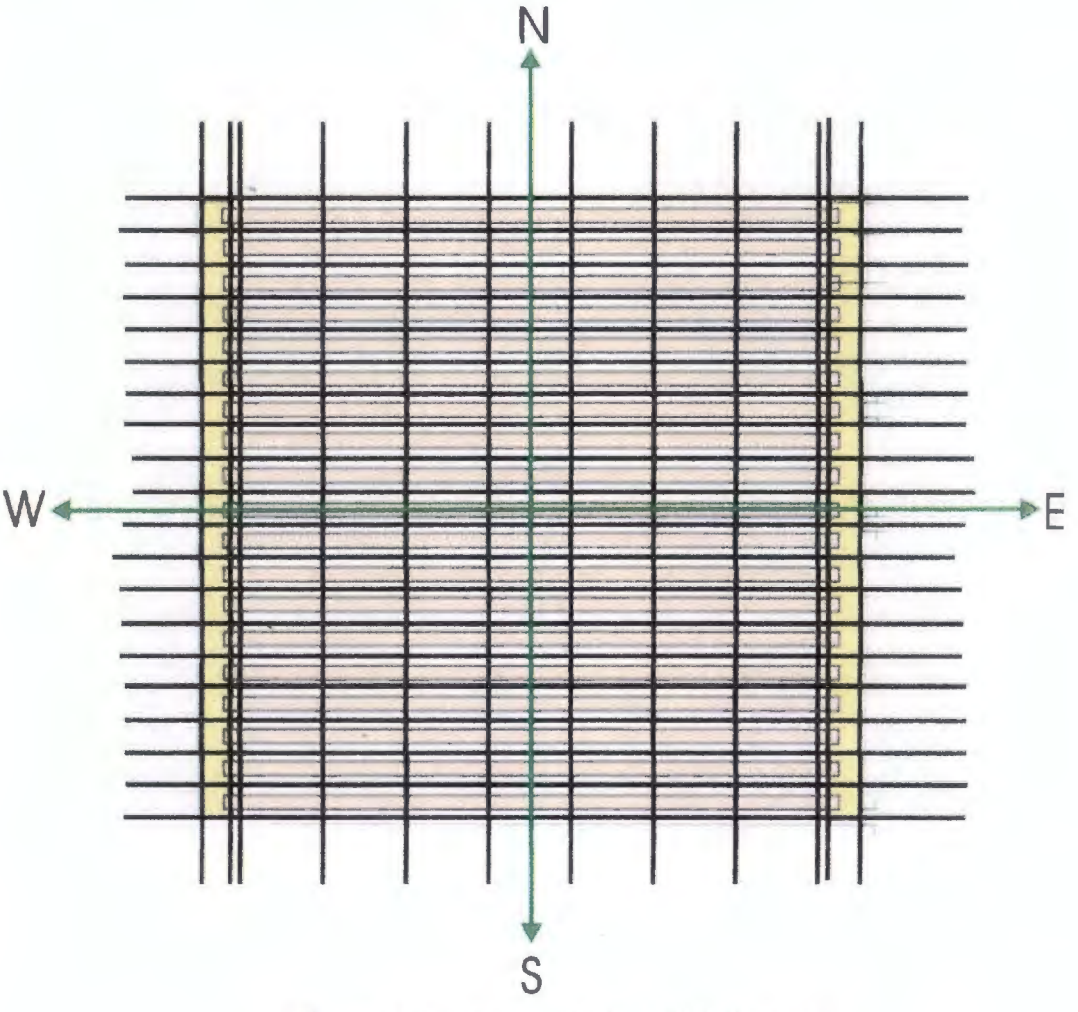

Figure 3-2: Assembly Subdivisions [1]

Each fuel plate was divided into nine cells in the east-west direction, with the outer two cells representing the area containing aluminium side plates. The rest of the fuel plate was then subdivided into seven regions of equal

NWU LIBRARY

composition. For each of the fuel plate cells some of the surrounding water was taken into account. The supporting structure (side plates) forms one cell and for simplicity of the model, the fuel plates protruding into the structure were treated as part of the supporting structure (no fuel protruding into the support structure, only the clad, i.e. Al). Some water is also added into this cell to account for the water surrounding the assembly.

HEADE provides symmetry segments, which can be used to reduce the size of the problem under consideration. The symmetries range from no symmetry to a $1/8^{th}$ symmetry. When choosing symmetry for a specific assembly, one must be careful because there are a number of factors that CORANA might require, for example one can only place assemblies with the same symmetry above each other in a single channel of the core. In the case of a fuel assembly and its top and bottom reflector full symmetry was chosen since they will form a single channel in CORANA.

Simplified models of all the assembly elements were setup in the same way and defined in HEADE, which applies straightforward flux-volume weighting in order to get homogenized multi-group cross sections.

3.2.1.2. Plan for cross section data processing and analysis

After data collection and sampling, the HEADE or STYX input file was prepared for each assembly considered for modelling. The manuals clearly explain and specify how and where to use the data collected and sample prepared. The input is organized into cards, each having a particular function.

The sample for HEADE fuel assembly input files is attached in Appendix B with the HEADE DATA FLOW in Appendix C. To run the OSCAR-3 code (i.e. HEADE or STYX input files) a Linux machine was used, and the entire path environment was well specified.

A STYX (DATA FLOW in Appendix D) input file, which is similar to a HEADE input file in the sense that it has cards each specifying certain data, was used for the control rod assembly which is made up of the absorber section (i.e. cadmium) and the fuel region at the bottom (known as fuel follower). HEADE was used to perform assembly calculations for the fuel part and not for the absorber part. The reason for this is that the large neutron absorber in the control will introduce steep flux gradients that may exceed the HEADE method's capability; hence STYX was applied here [1], [15].

On the other hand, control off-base calculations are required to handle the difference between having fuel in a certain volume and having the absorber inserted into the volume. STYX makes use of HEADE cross sections created from a simplified model not considering the assembly's exact geometry. Fine group cross sections (typically 24 energy groups) are edited from the HEADE calculation and are used as input to the STYX calculation. The STYX model has a detailed geometry description and solves the neutron distribution for the model to edit the few group homogenized cross sections for the absorber section. This data is written to a STYX file.

The STYX output file for the absorber section and the HEADE output file for the fuel follower were then combined using DUCO, a code in OSCAR-3, to create a HEADE output file that contains the required off-bases.

When running the problem is completed without errors, that is, the HEADE output file is created; information on cross section data and other information such as the number densities, the fluxes, etc. are examined (written in HEADE output file or the HED file).

Other parameters that were looked at were, the k-infinity values considered for the following off-base cases;

i. Effects of exposure on assembly
ii. Changing moderator temperature, fuel temperature, moderator density

The U-235 masses were also looked at. After examining all the necessary parameters in the output file results, the cross-section library created was used in subsequent codes in the CROLIN sub-system to create the final library for core calculations. A detailed description is given in the OSCAR-3 manual.

In CROLIN, with sub-codes POLX and LINX, the inputs were created using the HEADE output files (i.e. for POLX input). An important POLX output, is the accuracy of the polynomial fit to cross section data. The POLX output were then combined using LINX to create the output called the LINX cross section library. The library contains all the assembly types that will be needed during the reactor operation lifetime.

The cross section library created can only be validated when performing core calculations. One of the reasons is that in core calculations, a direct comparison of the code's results to plant data or past OSCAR-3 core calculations can be evaluated and hence the quality of the cross section library can be assessed.

3.2.2. C ore Analyses Calculational Methods for a Single Cycle

At this stage, the library was used in CORANA for core calculations. The graphical user interface, MAESTRO, was used to do the following [1];

a) Designing a reactor core and other facilities, for example;
   - SAFARI-1 core
   - Vault (for introducing new assemblies into our core)
   - Pool (intermediate and burned assemblies stored here), etc.

b) Creating new assemblies for our vault

c) Performing core reload (loading required assemblies in the new BOC core)

d) Defining a cycle calculation and executing the run

e) Analysing the results

Creation of new assemblies is dependent on the assembly type and geometry, but the model has a restriction of 17-layered meshes in which one can pack mixtures of choice with pre-determined cross sections. This is explained in more detail in the following section.

3.2.2.1. Creating new assemblies

In the MGRAC model, the core is divided into 17 axial meshes in which different mixtures with cross sections created in HEADE can be packed to make an assembly of choice (e.g. fuel, reflector assembly, etc.). The active core height (59.37 cm) is made up of 13 meshes and 15 cm of the 2 top and bottom meshes for reflector regions [1].

The target plate irradiation rigs are loaded in only four meshes, two of heights 4.625 cm from the core centre line to the top and two of heights 2.700 cm and 5.900 cm from the core centre line to the bottom, totalling to the plate dimension of 17.85 cm. The other meshes were packed with water with some traces of U-235. The reason for this is that MGRAC needs an active SAFARI-1 assembly height of 59.37 cm as defined in the CONFIGURATION file, that is, an assembly can be defined as fuel or non-fuel for this height, and therefore it needs fuel in the entire height. Similarly, the fuel assembly takes the total height of about 59.37 cm (i.e. total core active height).

3.2.2.2. Plan for core analyses calculational methods data processing

For our calculations, we chose cycle 0405 (i.e. cycle 4 of 2005) from the previous OSCAR-3 calculations. This cycle was chosen because it was originally calculated by the current calculational method to be two days shorter than the eventual plant cycle length. Note that in the current cycle calculations target plates were not included in the irradiation positions (per

OSCAR-3 calculations), unlike in the plant where they are included. The two days short cycle length, through experience, might be covered by the introduction of the target plates in the plant. This effect is because of the excess reactivity added by the target plates since they are fuel.

This choice was made because we have to have a calculational approximation or method, which is as close as possible to reality (SAFARI-1 reactor data) as far as loading target plates is concerned.

To set up the input for calculational methods, MAESTRO, the graphical user interface was used together with the MGRAC input for cycle 0405. The cross section library created and any necessary changes were incorporated into this input [1]. Depending on how the target plate irradiation rigs are loaded, four methods for MGRAC inputs were defined as follow;

- *The Reference Method*

  This method represents MGRAC input for C0405 without the target plate irradiation rigs in all six SAFARI-1 reactor irradiation positions. It resembles the current OSCAR-3 calculational method; thus it will be used as a reference (hence termed ***The Reference Method***) throughout this discussions.

- *Target plates in* method

  The MGRAC input for *The Reference Method* will now be modified to include the target plate irradiation rigs in all six irradiation positions, and the target plate will be in place for the entire cycle (i.e. they will not be removed at any time while running this input). Hence termed "***Target plates in* method**".

- *Target plates without shuffles* method

  This method will follow the irradiation schedule except that the burned target plate will be replaced by itself at the beginning of an irradiation period, i.e. target plate are removed at the end of irradiation and inserted again at the beginning of irradiation period, there is no shuffle procedure to introduce fresh target plates. Therefore the method will be called "***Target plates without shuffles***".

- *Target plates shuffling* method

  The last method for target plates irradiation resembles reality. In this method, the target plates will be *shuffled* as per schedule. This implies that at the end of every irradiation period for a specific rig (with seven plates), new target plates will replace the irradiated target plates. This is an ideal method, but is more cumbersome to implement on a regular basis since it includes creating a number of MGRAC inputs unlike in the previous methods where we had only one MGRAC input.

  Multiple MGRAC input in this method is a result of *shuffling*, since MGRAC does not have *shuffling* capabilities, SHUFFLE is run independently (with new or fresh target plates replacing the removed irradiated ones) and then the output EXPOSURE is used for a MGRAC run. Thus, before every MGRAC run, we have to SHUFFLE first except for the first MGRAC input, in which fresh target plates are specified in all irradiation positions. This method will be termed ***Target plates shuffling***.

In the latter two methods, the irradiation rigs were simulated in OSCAR-3 using a pseudo control rod model. This entails defining the Mo-99 irradiation rigs positions as control rod positions in OSCAR-3 model, i.e. allowing either full insertion (rigs without target plates) or full extraction (rigs with target plates) as operational options (see Appendix G).

Our choice of a suitable approximate method out of the three will be based on the evaluation of the following parameters:

a) Cycle length prediction and other core planning calculations (e.g. flux and power profiles)
b) Safety parameter calculations
c) Core follow calculations

We will examine the results of these parameters using "*The Reference Method*" results as a reference to the three methods discussed above, and a feasible solution will be suggested for each parameter if possible and the method of use.

MGRAC inputs were prepared for each method (see for example Appendix G, MGRAC input for *target plates without shuffles*), and the vault was created for the *target plate shuffling* method. In the vault, the new (fresh) target plate assemblies were created for use when performing *shuffles* and together with that, a SHUFFLE input created.

The last task is now to run the MGRAC cycle for all the methods. The code simulates two or three weeks of reactor operation in about 5 minutes. Note that SHUFFLE runs were performed after the first MGRAC run and after each MGRAC run for the *target plates shuffling* method until end of cycle (EOC). The summarised version of the core follow calculational path or data flow is attached in Appendix F.

There is huge volume of the results data generated from MGRAC runs; thus only information important for our study is investigated for the four methods. That is, the reactivity effects, mass burnup, cycle length, power and flux profiles and effects on the full core mass at EOC will be quantified for all the methods. After examining the effects, a suitable method or methods for including target plates will be chosen.

4. ANALYSIS AND INTERPRETATION OF RESULTS

4.1. INTRODUCTION

The results from the cross section generation sub-section will only be quantified when using the generated cross section library in the core calculation module, that is, MGRAC. CORANA uses this cross section library for calculations and some of the results can be examined to see if they reasonably approximate the plant data. This will also give an idea of how efficient our library is for use in core calculations.

The following chapter will examine effects on factors or parameters indicated in Section 3.2.2.2 using the cross section library generated and the cycle of choice (i.e. Cycle 0405). The effects will be investigated and quantified for each of the three anticipated methods of including the target plates relative to *The Reference Method*.

The aim of the study is to have a cross section library that can be used in day-to-day OSCAR-3 core calculations, with the most feasible method of including target plates in cycle calculations.

4.2. SINGLE CYCLE CALCULATIONS

The single cycle analyses were conducted for each of the above methods and reactivity effects were investigated, as it is important for reactor safety [11], [13]. The results of the calculation for each method are summarized in Sub-section 4.2.1 below.

4.2.1. Reactivity Comparison

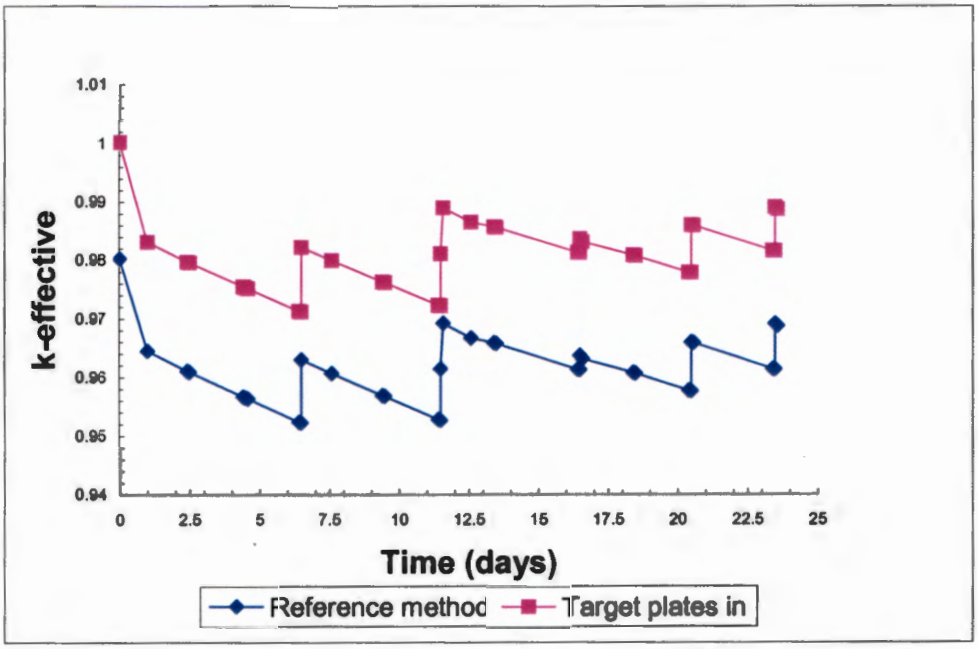

Figure 4-1: Reactivity Comparisons for *Target Plates in* and *The Reference Method*

The *Target plates in method* shows a marked effect on core reactivity in comparison with *The Reference method*. The reactivity effects or relative change in k-effective of about 2000pcm (relative Δk-eff x 10^5) were observed between the two methods.

The fact that *target plates in* have higher reactivity as compared to *The Reference Method* already gives us an idea of how reactivity effects will vary due to the introduction of target plates in the other two methods (i.e. *target plates without shuffles* and *target plates shuffling*). To quantify reactivity effects, all three methods were examined. Starting with the comparison of the two methods, *target plates without shuffles* and *target plates shuffling*, the differences shown in Figure 4-2 were observed.

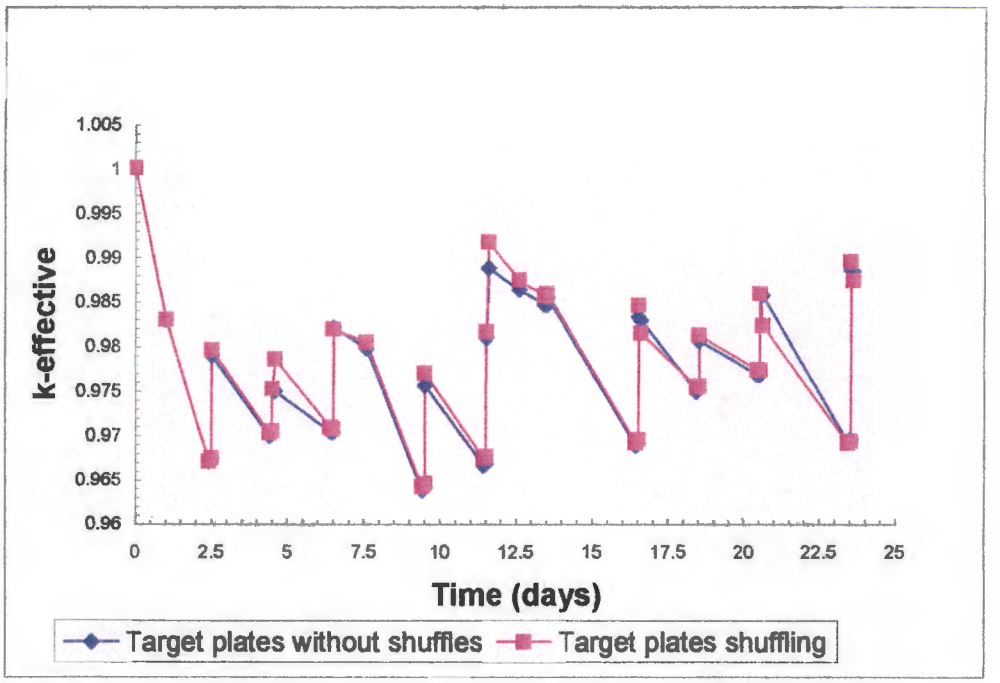

Figure 4-2: Reactivity Comparison for *Target Plates Without Shuffles* and *Target Plates Shuffling* Methods

The k-effective plots are the same for *target plates shuffling* and *target plates without shuffles* at the beginning of the cycle to just before 2.5 days, where the *shuffling* is performed for the *target plates shuffling* method (some irradiated target plates replaced with fresh target plate) versus *target plates without shuffles* (burned plate replaced by itself after two hours).

Figure 4-2 clearly shows the effect of loading fresh target plates (*shuffling*) as compared to the one *without shuffles*. There is an increase in reactivity for the shuffling methods as expected. The increase is also dependent on the number of target plates loaded or withdrawn per schedule. That is, k-effective will be higher in the case of three sets of fresh target plates as compared to two or one set of fresh target plates loaded. A reactivity effect of about 41.4pcm was observed between *target plates shuffling* and *target plates without shuffles*.

The reactivity effects are summarised in Figure 4-3 and Table 4-1 below for all three methods and *The Reference Method*.

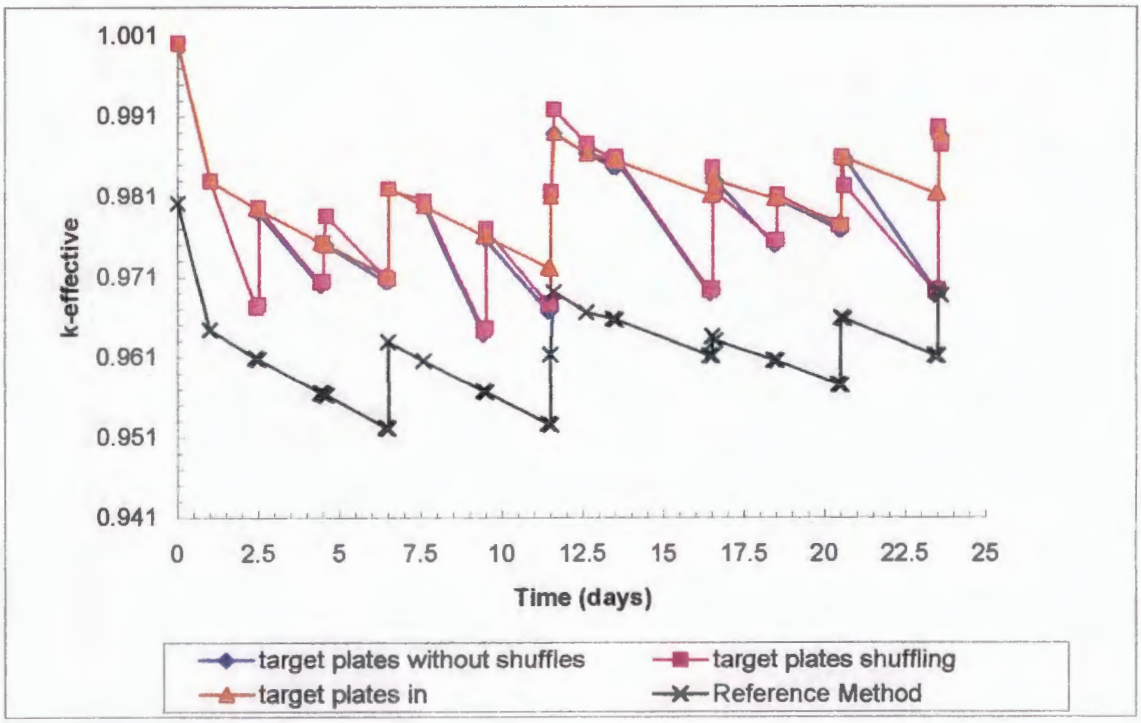

Figure 4-3: Summary of the Reactivity Effects for the Reference Method and Three Proposed Methods of Including or Modelling the Target Plates

The effect of some target plates in or out is clearly marked in the two graphs of *target plates shuffling* and *target plates without shuffles* methods. Firstly, for a step from 2.417 days to 2.5 days, where three rigs are removed resulted in the first sharp drop in k-effective observed for both methods. Note that the continuous drop from 1-2.417 days for *target plates shuffling* and *target plates without shuffle* is as result of the graph resolution (i.e. effects between small time-steps not visible on the scale of the graph), otherwise the two methods follow the *target plates in* curve till a point where plates are removed.

The plates (fresh or burned) are again in at 2.5 days, hence the rise in k-effective. The trend remains throughout the calculation depending on the number of rigs removed or loaded as per irradiation schedule. The graphs for the two methods also show a larger drop in k-effective with three rigs out (i.e. at 2.417-2.5 days) than with two rigs out (i.e. at 4.417-4.5 days) or one rig out (i.e. at 6.417-6.5 days).

The rise in k-effective after every two hour step depicted by the graphs for all methods is also because of the pure flux calculations performed immediately after every two hour step, power and control rod adjustment.

At many times the reactivity changes for the *target plates without shuffles* and *target plates shuffling* methods are lower compared to the *target plates in*. This noticeable difference is as a result of the big drop in reactivity when the target plates are removed in both *target plates without shuffles* and *target plates shuffling* methods, this is shown in the table below. *The Reference Method* is lower than all the cases, as expected.

Table 4-1: Reactivity Comparisons of the Three Modelling Methods to *The Reference Method* (averaged values)

Methods	**Average k-effective**	**Reactivity**
The Reference Method	0.961255	-
Target plates in	0.980871	2000pcm
Target plates without Shuffles	0.977410	1653pcm
Target plates Shuffling	0.977815	1694pcm

For *target plates shuffling* compared to *The Reference Method* we have reactivity change of about 1694pcm, and 1653pcm for *target plates without shuffles*. This resulted in a difference of about 41pcm observed before for these two methods.

Reactivity changes of about –353pcm and –312pcm for *target plates without shuffles* and *target plates shuffling* against *target plate in* were observed respectively.

The three methods have clearly displayed the reactivity effects as a result of introducing the target plates using different methods, as well as the effects of introducing a certain number of target plates as per irradiation schedule, either fresh or burned, (introducing excess reactivity) throughout the reactor operation.

From the above results, we can draw the conclusion that, although for *target plates shuffling* method fresh plates are loaded as per schedule, reactivity change on average will be lower than for *target plates in* method. The same can be said about *target plates without shuffles*. Therefore, the schedule plays an important role in target plate irradiation and in reactor operation.

The difference between the *target plates without shuffles* and *target plates shuffling* are negligible. The two hour step does not display any dominant effect on reactivity except for the fact that the fresh target plates introduced in the *target plates shuffling* increases the reactivity slightly.

Comparison in reactivity in terms of multiplication factor (k-effective) plays an important role in this study, because to attain criticality more fuel is needed at BOC and this introduces excess reactivity, which needs to be compensated for by a certain amount of controlled negative reactivity. However, it is still not clear as to which method is preferred when it comes to reactivity effects; thus other parameters identified for this study will be investigated.

4.2.2. Influence on Cycle Length and Fuel Economy

The excess reactivity effects mentioned in Section 4.2.1 play an important role when it comes to long-term reactor operation. How these effects come about, will be clearly shown in this section. The section examines how long the reactor will operate critically and by how much U-235 core mass contents will be burned (i.e. fuel and the control elements) due to the introduction of target plates (i.e. increased core U-235 mass). The period of operation will be determined by evaluating the cycle length for each method accompanied by the mass consumed and remaining in the core at the same time step for all four calculational methods.

To determine the cycle length, MGRAC runs for *The Reference Method*, *target plates in*, *target plates without shuffles* and *target plates shuffling* were executed. Starting with *The Reference Method*, the following settings were

adjusted: firstly, the control rod *searches* were set to *perform critical searches* (i.e. search for k-effective =1) in the MGRAC data input deck and the other conditions left as is from BOC. Then 18.5 days into a cycle, the control rods searches were changed to *no searches* option and the control rods fully extracted, that is, 5937 notches (59.37 cm). Note that when the control rods are at 5937 notches, the active fuel height of the control rods is all in the core and the absorber part (i.e. cadmium) is out of the core. In this way we will ensure that all the fuel left in the core is burned until there is not enough fuel to operate critically (i.e. at k-effective =1).

When the control rods are fully extracted k-effective values of subsequent burnup steps can either rise above one (i.e. k-effective>1) before dropping down below criticality (k-effective=1) or just drop below criticality (k-effective<1) depending on the U-235 mass left in the core at that moment in time. The best linear fit was put along a set of points from when k-effective started dropping below criticality; then from the equation of that straight line graph the cycle length (x-axis, that is, number of days) was determined by setting k-effective =1(on the y-axis). This was set to one because we want to determine when the core will reach its end of life (i.e. end of cycle or cycle length).

The cycle length for *The Reference Method* was determined to be 18.7 days and the cycle length of the other three methods was determined as described relative to *The Reference Method* cycle length. The only difference was that in the three methods the target plates (not included in *The Reference Method*) were removed from the core together with the control rods at 18.5 days; thus this resulted in adding fuel (control rods) to the core and removing some (six target plates irradiation rigs). The graphs for cycle length determination for all four methods are attached in Appendix A.

Full core masses, excluding target plate U-235 mass, were also determined at BOC and at 18.5 days for all the methods. The full core U-235 mass at BOC was 6636.10 grams (excluding target plates U-235 mass).

The results obtained from the four methods are summarized in Table 4-2 below with the fuel "saved" and consumed relative to *The Reference Method* as a result of target plate loading in the three calculational methods discussed.

Table 4-2: Comparison of Cycle Length and Fuel consumed for Different *MGRAC* Runs at 18.5 Days Time Step

MGRAC Inputs (methods)	Cycle Length	Differences (days)	U-235 fuel Masses (g)			U-235 Mass burned (%)
			Full core U-235 mass at 18.5 days	Consumed BOC to 18.5 days	Fuel saved (g)	
Reference Method	18.7	-	6197.54	438.56	-	
Target plates in	19.6	0.9	6210.99	425.11	13.45	3.2
Target plates without shuffles	19.5	0.8	6210.82	425.28	13.28	3.1
Target plates shuffling	19.9	1.2	6217.72	418.38	20.20	4.8

The cycle lengths and masses remaining at 18.5 days are in agreement with what was expected in the sense that we have a longer cycle length for more U-235 mass and a shorter length for less U-235 mass in the core at end of cycle, hence the excess reactivity effects mentioned in Section 4.2.1. It can be noted that the *target plates shuffling* method has more mass remaining in the core at 18.5 days as a result of loading fresh target plates (fuel) in every two hour step when *shuffling* target plates. The contribution of these fresh target plates to the power delivered by the core (MWd) is therefore larger than in the other two cases.

The *target plates without shuffles* method was expected to have a shorter cycle length and less U-235 mass remaining than the *target plates in* method since the target plates are not burned as much as in the *target plates in*

method due to the two hour step in the *target plates without shuffles* method. However, the cycle length is very similar and it has more or less the same U-235 mass. The small difference in cycle length and U-235 mass can perhaps be attributed to mass distribution throughout the core (see Section 4.2.3).

The fact that we are loading and unloading the target plates throughout the cycle, having two competing effects when determining the cycle length, namely, removing six target plate irradiation rigs (removing fuel from the core) and fully extracting the control rods to 5937 notches at 18.5 days can also upset the core burnup rate, hence the mass and power distribution.

The *target plates shuffling* method has an advantage here for longer operation and for predicting the saving of more core U-235 mass than the other two methods as a result of increased excess reactivity (i.e. fresh fuel loading) and more power being produced by the fresher target plates. The two hours step has shown negligible effects in the *target plates in* and *target plates without shuffles* methods unlike in Section 4.2.1 where the reactivity effects differed by –353pcm for the two methods. This again confirms the fact that differences observed in the *target plates shuffling* method is as a result of fresh target plates being loaded and to a lesser extend, by the two hour step.

Xenon poisoning can also have a major influence in our results, that is, the effect in reactivity, mass distribution, etc. The xenon poisoning effects will be investigated in later studies.

Further effects on the cycle length were investigated due to target plates loading, that is, leaving the target plates as per calculational method to just about two days before end of calculation time step (to simulate the schedule). The 20.5 days time step was chosen as the approximate step and MGRAC settings were as for 18.5 days cycle length determination. The results are tabulated in Table 4-3 below.

NWU LIBRARY

Table 4-3: Target Plates influence on Cycle Length and U-235 Mass at 20.5 Days for Different *MGRAC* Runs

MGRAC Inputs (Methods)	Cycle Length		U-235 fuel masses (g) at 20.5 days	
	18.5 Days	20.5 Days	Consumed BOC to 20.5 days	Fuel saved (g)
Reference Method	18.7	-	479.20	-
Target plate in	19.6	21.1	464.82	14.38
Target plates without shuffles	19.5	21.1	465.03	14.17
Target plates shuffling	19.9	21.24	457.39	21.81

From Table 4-3, it can be seen that the cycle length and fuel "saved" has increased as a result of leaving the target plates in for a longer period. The cycle lengths obtained at time steps of 18.5 days and 20.5 days show that EOC will be reached at about these steps, that is, immediately when the target plates are removed k-effective will drop below criticality. Therefore the extra operational days in the methods of loading target plates are mostly as a result of excess reactivity (fuel saved), and as to how long the core remains critical is dependent on the U-235 mass distribution and burnup throughout the core, and the method used.

The *target plates shuffling* method still shows the advantage of loading fresh plates against the burned plates although small when compared to *target plates in* and *target plates without shuffles* method. Xenon poisoning is one of the possible reasons for obtaining results not showing dominant effects when introducing fresh fuel.

4.2.3. Effects on U-235 Core Mass Distribution

In this section, effects introduced by the target plates on core assembly U-235 mass distribution will be examined. Global and local effects on mass distribution will be investigated and also the effect on the target plates (i.e.

target irradiation positions of concern). This might explain the effects observed and discussed in the previous sections.

4.2.3.1. Global effects on U-235 burnup in the core

To examine the effects on core mass distribution as a result of target plates loading, the three methods were compared to *The Reference Method* at 18.5 days, an arbitrary step chosen to examine effects on all three methods relative to *The Reference Method* EOC (i.e. 18.5 days). The core map results are summarised below.

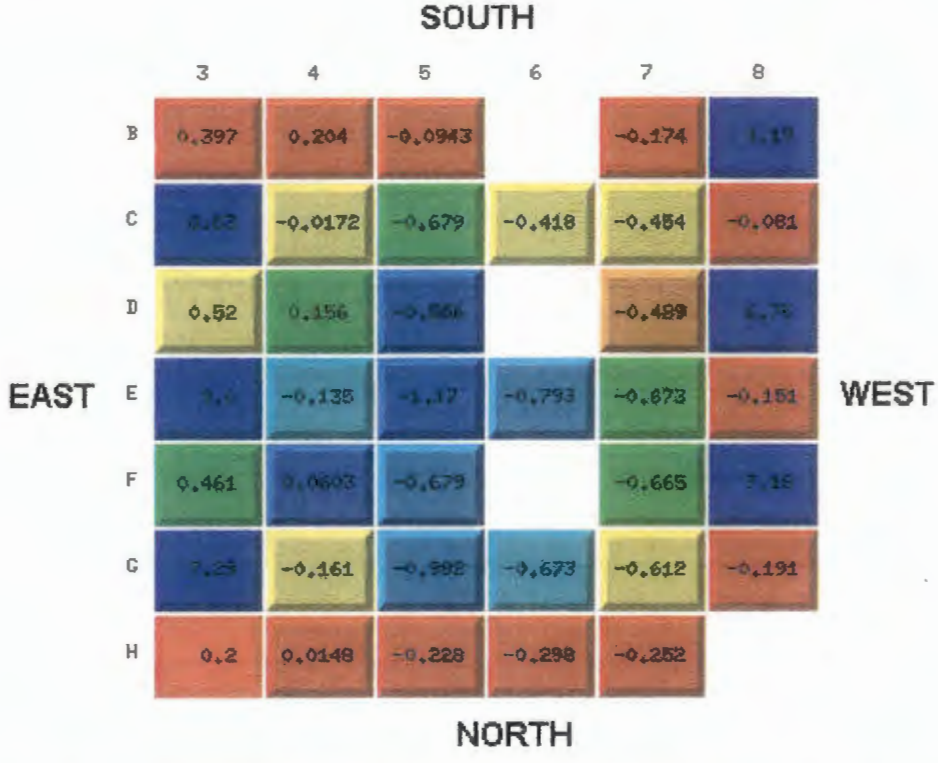

Figure 4-4: Core U-235 Percentage Mass Difference Map between *Target Plates in* and *The Reference Method* at 18.5 Days

The six blue assemblies are the target plate irradiation positions, that is, C3, E3 and G3 on the eastern side and B8, D8 and F8 on the western side of the core. The differences observed in these positions are due to the editing approach implemented in MGRAC, since the control rod model was used for irradiation rigs to do these evaluations. Note that *The Reference Method* has masses (due to the MGRAC edits) in irradiation positions even though they

are not used in the neutronics calculations, where the cross sections are replaced by the "empty rig" off-base values. The differences shown is therefore due to the burnup of the *target plates in* method compared to the no burnup for *The Reference method*.

The effect of target plates loading can clearly be seen in this map, with negative differences indicating that the fuel elements are less burned if the target plates are loaded throughout the cycle.

The *target plates in* method results in higher fuel masses than *The Reference Method* overall. However on the eastern side of the core, positive differences are observed in the irradiation position fuel element neighbours, this implies that *The Reference Method* has higher masses in those positions. Therefore target plate loading has different effects on the western and eastern sides of the core. That is, the neighbouring fuel elements will be less burned for *The Reference Method* on the eastern side of the core than on the western side.

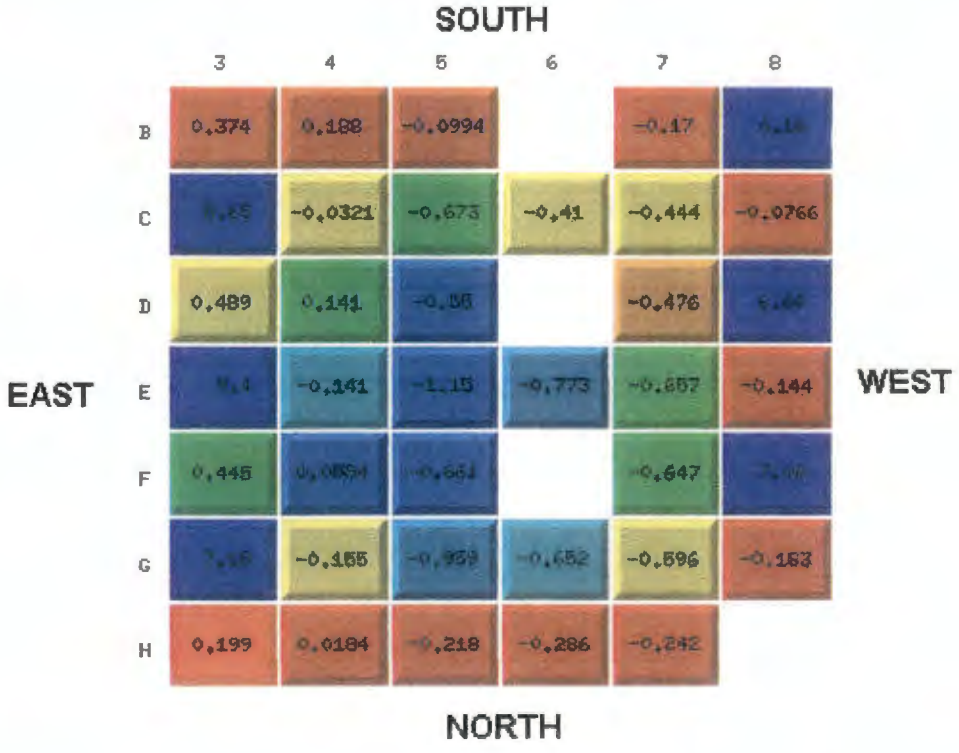

Figure 4-5: Core U-235 Percentage Mass Difference Map between *Target Plates without shuffles* and *The Reference Method* at 18.5 Days

The same trend is observed for the *target plates without shuffles* method (Figure 4-5), as was the case for the *target plates in* method, but the fuel elements are slightly more burned compared to the latter method. The small differences observed in the maps of Figures 4-4 and 4-5 explain differences in the full core masses of Table 4-2 for the *target plates without shuffles* and *target plates in* methods.

These negligible differences are as a result of the two hour step in the *target plates without shuffles* method, and also the control rods U-235 mass burnup. In the *target plates in* method, the control rods are burned slightly less compared to the *target plates without shuffles* method.

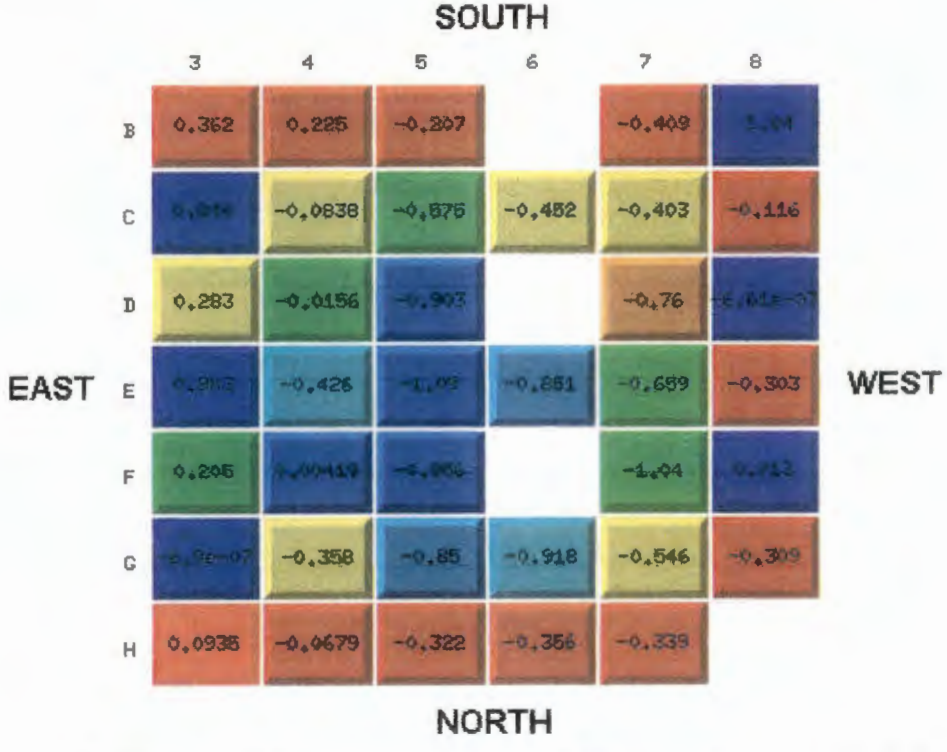

Figure 4-6: Core U-235 Percentage Mass Difference Map between *Target Plates Shuffling* and *The Reference Method* at 18.5 Days

The Core mass distribution trend is still the same in Figure 4-6 as before, but the introduction of fresh fuel at each loading of irradiating target plates is shown by more negative percentage mass differences, hence less burned fuel elements. However, the control rod percentage mass differences are less

negative than for the *target plates in* and the *target plates without shuffles* method; that is, they are more burned.

This behaviour of the control (see Figure 4-4, 4-5 and 4-6) is as a result of the control rod movement due to target plates loading and unloading. The control will be further withdrawn in the case of *target plates without shuffles* and *target plates shuffling* methods every time when plates are removed. The unloading of target plates results in excess reactivity loss, thus the control rods will be further out to compensate for the reactivity loss. This effect is dominant in the *target plates shuffling* method since more reactivity is removed by this method than in the *target plates in* and *target plates without shuffles* methods.

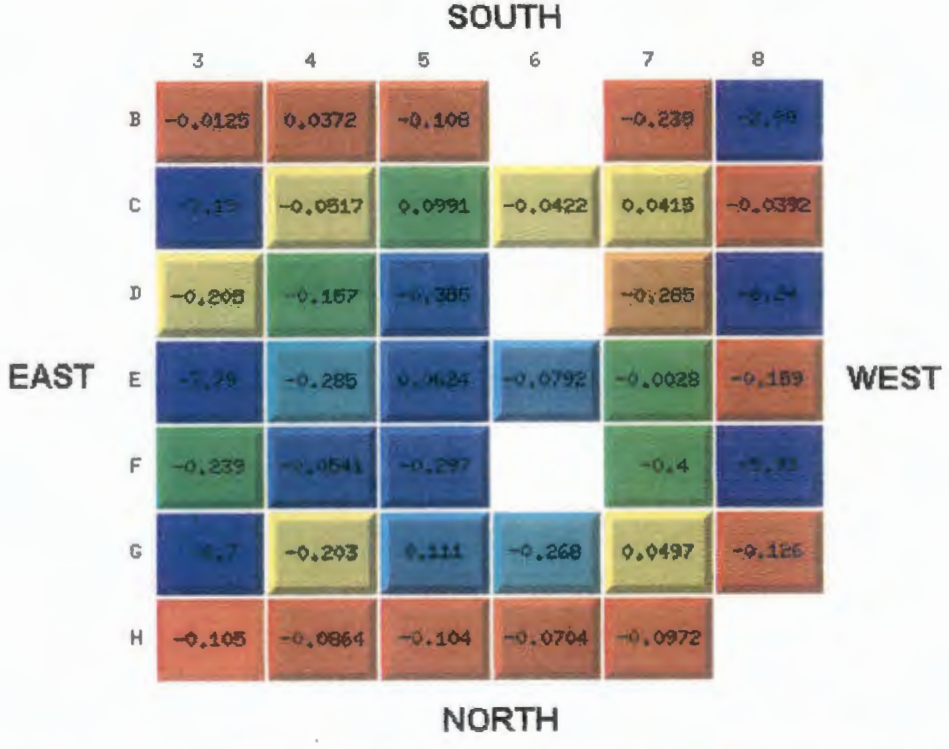

Figure 4-7: Core U-235 Percentage Mass Difference Map between *Target Plates Shuffling* and *Target Plates without Shuffles* at 18.5 Days

Figure 4-7 confirms the fact that fuel elements will be less burned in the cases of *target plates shuffling* calculational method than in the *target plates without shuffles* calculational method. It again shows that fresh target plates loading has more effects than the two hours step, as was the case before.

In summary, target plates loading has shown noticeable and important effects in mass distribution, full core masses, burnup profile and the cycle length. Therefore, the *target plates shuffling method* is an important method, although cumbersome. The *target plates in* and *target plates without shuffles* methods have basically displayed negligible effects thus far, and they can therefore be treated the same in as far as the mass distribution, full core masses, and the cycle length are concerned.

The discussions and core mass maps above are as a result of cycle length determination at 18.5 with a setting as described in the introductory paragraphs of Section 4.2.2. What happens if settings are left as is at 18.5 days, that is, MGRAC settings for the control rods searches are set to *no searches* option from BOC to EOC and the rod positions are fixed. To examine the effects due to this at 18.5 days we look at *target plates shuffling* (worst case scenario) and *The Reference Method*. The percentage difference mass map at 18.5 days for these methods is shown in Figure 4-8 below.

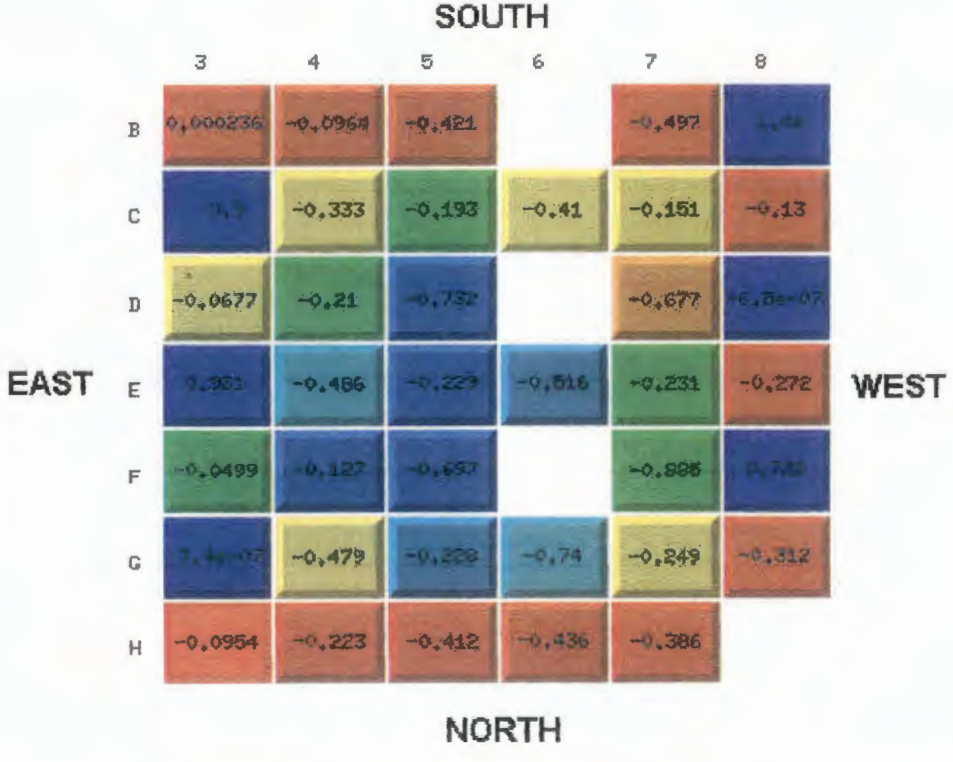

Figure 4-8: Core U-235 Percentage Mass Difference Map between *Target Plates Shuffling* and *The Reference Method* at 18.5 Days

The percentage mass difference of Figure 4-8 suggests that fuel elements are more burned than in the map of Figure 4-6; this is also the case for the other two methods. In the percentage mass maps of Figure 4-4 to Figure 4-7, the control rods are in a position satisfying conditions, k-effective =1 from BOC to 18.5 days (refer to Section 4.2.2) and in Figure 4-8, the rods are in fixed positions (see Appendix G), thus resulting in fuel elements being more burned than in the criticality searches case (i.e. k-effective=1). The control rods are less burned for fixed positions (Figure 4-8) and more burned for criticality searches (Figures 4-4 to 4-7).

The results of Section 4.2.3 have shown and explained the differences observed in Sections 4.2.1 and 4.2.2 and also highlighted the fact that the two hour step is less important in the methods employed. *Shuffling* of target plates, that is, in the *target plates shuffling* method has displayed important effects, while *target plates in* and *target plates without shuffles* displayed similar effects thus far. Therefore, *target plates shuffling,* and *target plates in* or *target plates without shuffles* method still remain important calculational methods.

The following section continues to examine important effects that can assist in choosing the most suitable calculational method or methods of target plate inclusion in core planning and core follow calculations.

4.2.4. Target Plates Effects on Core Power Distribution

Variations in core composition play an important role in reactor design. Of major concern is the local power peaking that occurs at the boundaries between fuel and moderator regions. We might expect that the fuel element adjacent to such water channels or moderator (an effective source of thermal neutrons) will see a larger thermal flux and hence experience a higher power density. Since the local flux near the channel may be considerably higher than the average flux in the region, one must take care that constraints on core power densities are not exceeded.

In this section absolute power density effects were examined globally to see how much power the loading of target plates introduces in the entire core and then determine locally which assembly powers are perturbed.

Effects on power is very important for reactor safety as indicated in the first paragraph of this section; therefore it has to be ensured that introducing the target plates will result in the reactor and assembly power within safety limits.

We first examine the global and then the local effects to quantify power density effects introduced by target plates loading.

4.2.4.1. Global effects on core average power distribution

The effects on absolute power density for the three methods were analysed at BOC. At this stage, the U-235 content of assemblies are at their maximum and high local assembly powers peaks are expected here, so it is a very good case to start with, when investigating core power distribution and peaking.

Since the condition for all three methods are the same at BOC, only the *target plates shuffling* method will be investigated for core power distribution. The important information that can be derived from this investigation is, by how much does the average core power peak change due to loading of the target plates. A comparative relative power map with percentage differences, for *The Reference Method* and *target plates shuffling* method is given in Figure 4-9.

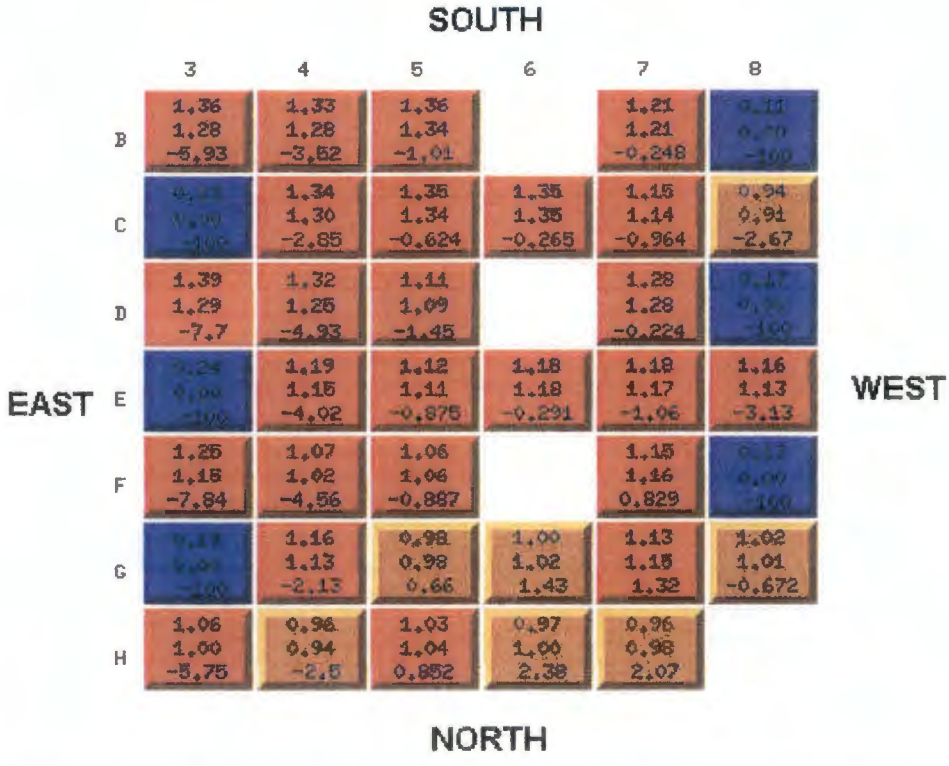

Figure 4-9: Core Relative Power Distribution for *Target Plates Shuffling* and *The Reference Method* at BOC

The ***first values*** on the map are for the *target plates shuffling* method, the ***second values*** for *The Reference Method* and the ***third values*** are the percentage differences.

Larger effects are observed in the irradiation position neighbours on the eastern side of the map, with a power tilt towards the eastern side of the core (i.e. left side). The core-wide relative power peaking has increased with the maximum relative power increase from 1.34 to 1.39 and with assembly increases of up to 8%. The increase is brought about by the fact that the power tilt introduced by the presence of the target plates further increases the power delivered, by the assembly delivering the most power, for example, assembly D3 and B5 in Figure 4-9.

Since the reactor total power remained unchanged (i.e. 20MW) and the power tilt observed in Figure 4-9 only increase the maximum relative power by 4% (1.34 to 1.39) the core-wide effect can be considered to be relatively small.

NWU LIBRARY

However, this may be essential for assembly nodal power peaking and reconstructed powers or plate powers. This plays an important part in safety margin assessment (i.e. plate powers for onset of nucleate boiling–hotspot, etc.) and will be revisited when examining the local effects on relative nodal power density.

Still on a global level, core power density effects as a result of loading a different number of target plates at BOC, 2.417, 4.417 and 6.417 days were also examined for *target plates shuffling* and *The Reference Method*. The results are summarised in Table 4-4 below.

Table 4-4: Target Plate Loading Effects on Core Average Power Density

Target Plate Movement in Irradiation Positions	**Time (Days)**	**Core Ave. Power Density (W/cc)**	
		Target Plates Shuffling	**Reference Method**
All in/all out	BOC	148.7262	156.5172
3 out/all out	2.417 days	155.8449	159.9792
2 out/all out	4.417 days	154.5139	159.9792
1 out/all out	6.417 days	153.2054	159.9792

The average core power density is increased for a smaller active or fuel total volume and decreased for a larger active volume as in Table 4-4. Although the loading of target plates increases the power peaking, on average, we will have a lower core average power density (also per assembly) and this may even result in a lower power per assembly than when the irradiation positions are not loaded. That is, certain assemblies will have to compensate for the ones without fuel (e.g. irradiation positions). Therefore, they will deliver more power, unlike when the irradiation positions are loaded.

4.2.4.2. Local effects on average power distribution

Power peaking in assemblies was examined at BOC (worst case scenario) as was the case for global effects; however, effects were also examined at Mid-cycle and EOC to see the overall effects throughout the cycle.

NWU LIBRARY

The axially averaged or assembly power peaking was observed in assemblies B5 and C6 for *The Reference Method* and for the other three methods the peak occurs in assemblies B3, B5, C6 and D3.

Peaking in assembly B5 and C6 can be attributed to the fact that they are near the inner-core irradiation positions (highly thermalised position, i.e. peaking of thermal neutron flux) and that the power tilt of the neighbouring assemblies is towards assembly B5 and C6. The same reason as for *The Reference Method* applies for assemblies B5 and C6 peaking in the three methods discussed; however the peaks are more pronounced than in *The Reference Method* due to target plate loading (see Figure 4-9).

Assembly D3 has a higher peak than all the assemblies, only when target plates are loaded at BOC, but C6 has one of its plates peaking more than all the plates of all the assemblies irrespective of having less axially averaged relative assembly power (peaking) than D3 at BOC.

From this discussion, it can be noted that, peaking for all the methods including *The Reference Method,* is dependent on the surrounding environment, as briefly explained in the introductory paragraph of this section (i.e. Section 4.2.4).

The effects of loading a certain number of target plates as per schedule on absolute assembly power density were also examined for *target plates shuffling* and *target plates without shuffles* methods. These were done by setting MGRAC inputs with cases from BOC to the case just after the two hour step. Effects were examined for a case just before two hours and a case just after two hours. The power peaking is summarized in Table 4-5 below.

Table 4-5: Effects of *Shuffling* and Not *Shuffling* Target Plates after Two Hours on Assembly Average Power Peaking for Peaking Assemblies (with Plates Irradiated Per Schedule)

		Target plate before the two hours step			**Burned target plates at the end of two hours step**			**Fresh target plates in at the end of the two hours step**		
Cases	**BOC**	**Before two hour step**			**After two hour step**			**After two hour step**		
Peaking Assembly	All plates in	3 out	2 out	1 out	3 in	2 in	1 in	3 in	2 in	1 in
	Absolute Assembly Power Density (W/cc)									
B3	202.6	200.2	**222.9**	**217.2**	217.7	217.7	217.7	**218.8**	**218.3**	**218.5**
B5	201.8	204.2	212.5	206.8	208.6	208.7	208.7	209.2	209.0	209.2
C5	200.3	**216.0**	**221.6**	216.3	218.3	**218.5**	**218.5**	218.3	218.2	218.3
C6	200.6	201.4	200.7	196.7	199.8	199.9	199.9	199.5	199.5	199.5
D3	**207.1**	201.3	219.7	**217.2**	**218.3**	218.3	218.3	218.5	218.0	218.2

Assembly D3 peaks at BOC as mentioned before; this has much to do with the loading of C3, E3 and G3 as per schedule with E3 having dominant influence on this assembly. On average, assembly B3 is more influenced due to target plate loading and unloading. After the two hour step, C5 peaks most for burned target plates with B3 peaking for fresh target plates. The fuel assembly C6 is more influenced by the removal of the target plates and this influence has more to do with the control rod positions, which are neighbours to this assembly, and also the water filled irradiation positions.

Towards the EOC, peaking in assemblies B5, and C6 is also due to the control rod position (i.e. fully extracted).

The power tilt (peaking) in the assemblies specified in Table 4-5 above and throughout the cycle is dependent on how far or to which side of the core changes are made as far as the target plate loading and unloading are concerned. Therefore one must carefully note the effects on the core as a result of variation in core composition.

Table 4-5 also shows how the schedule can influence peaking. Peaking will be more pronounced in one of the assemblies likely to peak (i.e. B3, B5, C5, C6 or D3) as a result of target plate loading, and might be higher than peaking at BOC depending on the specific assembly's surrounding environment.

The importance of employing a schedule when loading target plates is also shown here by the fact that only certain assemblies will peak while the others remain unaffected, thus still ensuring constant power and operation within safety limits. Should the schedule not be used and all the target plates were loaded and unloaded at the same time, it can immediately be noted from Table 4-5 that more assemblies would peak at the same time and this is not favourable for safety, hence an advantage of the schedule.

From this discussion, assemblies that peak regardless of the method employed, either with plates in or out have been identified. This is very important because when changes are made in the core configuration one will immediately know which assemblies are likely to peak. Peaking in assemblies examined due to *target plates shuffling* and *target plates without shuffles* shows negligible differences as indicated in Table 4-5 regardless of the method used.

Safety cannot only be judged by assembly power densities studies. This is because on average, the most peaking assembly can have lower nodal peaks and the less peaking assembly can have high nodal peaks. The axial power shape along a specific assembly is also important and is mostly influenced by the nodal power peaking. Even though assembly D3 peaked at BOC with plates in, as indicated above, this might be different when it comes to nodal power or plate powers. The effects are shown at BOC, Mid-cycle and at the end of the cycle calculation to examine the net effects on maximum nodal power density, with the control rods in the same position for all the methods. The results are summarised in Table 4-6 below.

Table 4-6: Maximum Nodal Power Density for Assemblies at BOC, Mid-cycle and at the End of Calculation Step (i.e. 23.59 Days)

Methods	**BOC**	**Mid-cycle (12.59 Days)**	**End of Calculation Step (23.59 Days)**
	Maximum Nodal Power Density (W/cc)		
Reference	300.8 (**C6**)	226.8 (**C6**)	209.9 (**C6**)
Target plates in	285.6 (**C6**)	219.0 (**B5**)	203.8 (**C6**)
Target plates without shuffles	285.6 (**C6**)	219.1 (**B5**)	203.6 (**C6**)
Target plates shuffling	285.6 (**C6**)	220.5 (**B5**)	209.7 (**B5**)

From Table 4-6 it is clear that assembly C6 peaks most when the maximum nodal power density is considered. This is the case for *The Reference Method* and all three methods at BOC, and also on average throughout the cycle. It also shows a small difference in the nodal power due to target plate loading in the three methods. The nodal peaking of assembly C6 for *The Reference Method* can be found in axial layer 6, which is a 5.975 cm layer from bottom to top, and in layer 7, a 5.95 cm layer from bottom to top for the three other methods. Note that the layers are numbered from bottom to top in OSCAR-3 calculations. Assembly B5 starts peaking towards and at Mid-cycle for the other three methods. The peaks at the mid layers below the centre line has to do with the control rod position, that is, neutrons "seeing" more fuel lower and the absorber (Cadmium) material higher in the core.

To summarise, these results confirm that one cannot judge power peaking (i.e. guarantee its position and value safely) on assembly power density alone. Assembly D3 was identified as the peaking assembly (i.e. average assembly peaking), while assembly C6 was identified to be the nodal peaking assembly.

The plate power map for layer 7 of assembly C6 is shown in Figure 4-10 at BOC for the *target plates shuffling* method.

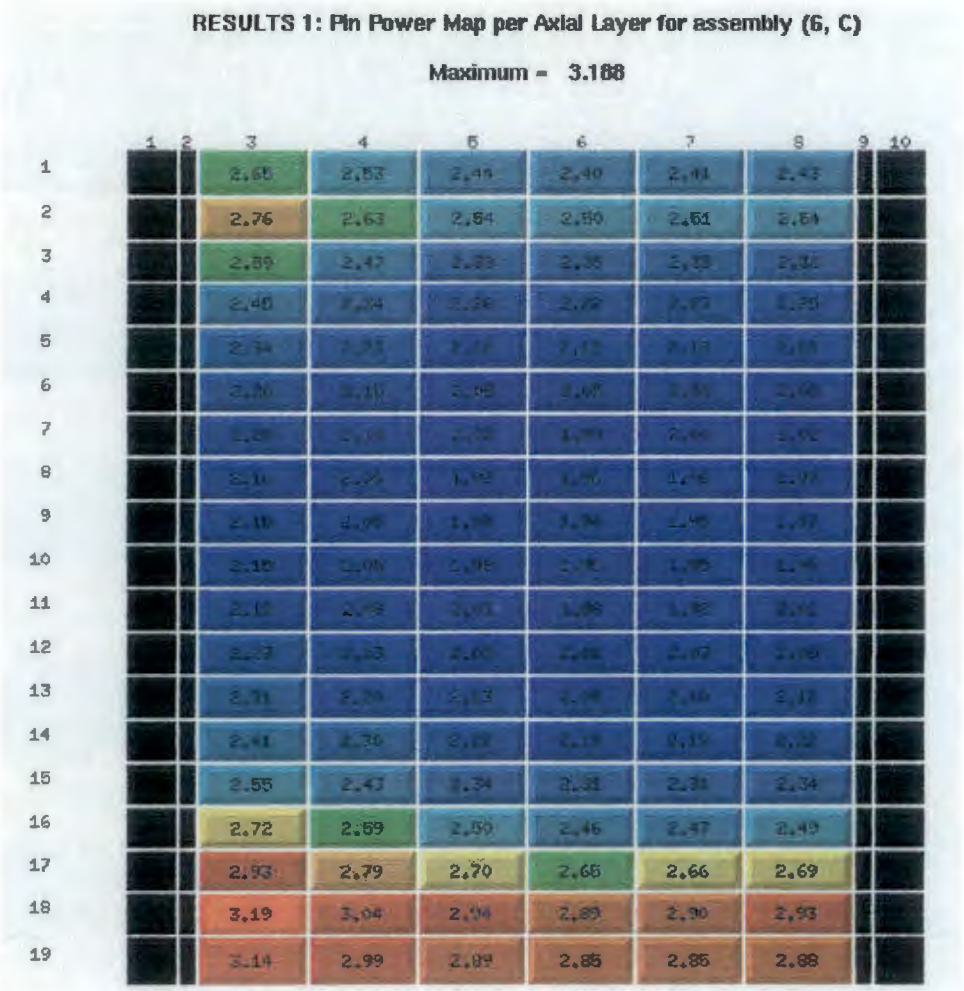

Figure 4-10: Plate Power Map for Axial Layer 7 of Assembly C6 at BOC

The figure shows 19 fuel plates with the maximum peaking in the 18th plate at the bottom left corner (i.e. assembly sub-division in Figure 3-2). The peaking of this assembly (plate power) can be attributed to high fluxes in irradiation position D6 and B6 (Section 4.2.6.3). The effects are the same for all the methods at BOC. *The Reference Method* has the maximum of about 3.168 in layer 7, which shows an increase of about 0.6% for the methods with target plate loading. Nodal and plate power peaks in assemblies D5, D7, E6 and control C5 are towards or to the side of adjacent irradiation position D6 and this is for the same reasons given before.

It has been observed that target plate loading has almost the same effect on the same assemblies for different methods and also nodal power density peaks in the same layer for the three methods except for *The Reference*

Method where peaking is observed in layer 6 for assembly C6. The *target plates shuffling* method shows slightly larger effects, although small, when compared to the reference and the other methods.

In summary, the methods, except for *The Reference Method* have the same nodal and assembly power density effects. Safety margins as far as target plates loading are concerned, are guaranteed by the fact that the differences observed in power peaking for the three methods against *The Reference Method* are negligible. The *target plates without shuffles* and *target plates in* method still display the same effects irrespective of the two hour step differences and the *target plates shuffling* method shows slightly larger differences as before, due to plate shuffling.

Although the core power distribution is different (very small) throughout the cycle, for all the methods discussed due to changes employed in each method, it has been shown that all the methods play an important role when it comes to the evaluation of safety. The fact that the two hour step is not important provided that one load fresh fuel is again evident as in the previous sections. Therefore, ease of use suggests the adoption of the *target plates in* since the two hour step effects are negligible. The only exceptions to this recommendation are possible peaking that may occur during the 2 hour periods when the target plates are unloaded.

Thus the *target plates shuffling* method still remains as an important method, since it shows the advantage of the schedule (i.e. loading fresh fuel) and the more marked effects as a result of target plates *shuffling*.

4.2.4.3. **Effects on the control rod fuel follower power density due to the target plate and control rods movement**: *Target plates shuffling* and *The Reference Method*

To see the effects of the control rods movement on the control rod fuel follower power density, the power densities were examined at BOC, Mid-cycle

(12.59 days) and EOC (23.59 days, i.e. end of calculation). The control rods are at the same position for each case and for both methods. The result for regulating rod C5 was also examined and summarised in the tables below.

Table 4-7: Effects on Control Rod Axially Averaged Power Density at BOC for *Target Plates Shuffling* and *The Reference Method*

Cases At BOC	**Axially Averaged Rod Power Density (W/cc)**					
	Rod1 C5	Rod2 E5	Rod3 G5	Rod4 C7	Rod5 E7	Rod6 G7
Target Plates shuffling	**200**	166	145	171	176	169
Reference Method	**209**	174	154	179	183	180
% Difference	4.3	4.6	5.8	4.5	3.8	6.1

Table 4-8: Effects on Control Rod Axially Averaged Power Density Mid-Cycle for *Plates Shuffling* and *The Reference Method*

Cases At Mid-Cycle	**Axially Averaged Rod Power Density (W/cc)**					
	Rod1 C5	Rod2 E5	Rod3 G5	Rod4 C7	Rod5 E7	Rod6 G7
Target Plates shuffling	**167**	136.68	122	136	148.32	138
Reference Method	**170**	136.75	124	137	148.09	142
% Difference	1.8	0.05	1.6	0.72	-0.155	2.82

Table 4-9: Effects on Control Rod Axially Averaged Power Density at EOC for *Target Plates Shuffling* and *The Reference Method*

Cases At EOC	**Axially Averaged Rod Power Density (W/cc)**					
	Rod1 C5	Rod2 E5	Rod3 G5	Rod4 C7	Rod5 E7	Rod6 G7
Target plates shuffling	**153**	127	112	127	139	129
Reference Method	**157**	131	120	129	142	136
% Difference	2.5	3.05	6.7	1.55	2.11	5.15

The power density for control rods decreases from BOC to EOC for both methods. This is expected since at BOC only a small volume of the fuel follower will be within the active core height, but the volume will increase throughout the cycle calculation as a result of rod extraction. Therefore, these

suggest that the control rod will deliver more power at EOC than at BOC and Mid-cycle, the core burnup history is also important when examining the control rod burnup and power profile.

Higher power densities for *The Reference Method* are a result of the irradiation rigs not delivering power, which tends to be compensated by the fuel assemblies, hence more power delivered by the fuel assemblies. Regulating rod C5 has higher power density throughout the cycle for both cases. This was also observed in the previous sub-section 4.2.4.2 and effects are for the same reason as before.

The target plates loading introduces a change of about 5 % at BOC, 1 % at Mid-cycle and 4% at EOC for the same reasons stated in the previous paragraph. The differences in control rod power density between the various methods as discussed can be very important when examining the control rod worth (not discussed in this study) which plays a vital role when it comes to safety.

4.2.4.4. Effects on the target plate irradiation rig axial power shapes

In the previous sections (and in literature) it was noted that more power will be delivered at the bottom of the core for BOC and at the top for EOC as a result of control rod movement throughout the cycle calculation [3]. This trend is shown for the *target plates shuffling* method for irradiation position E3 in the figures below.

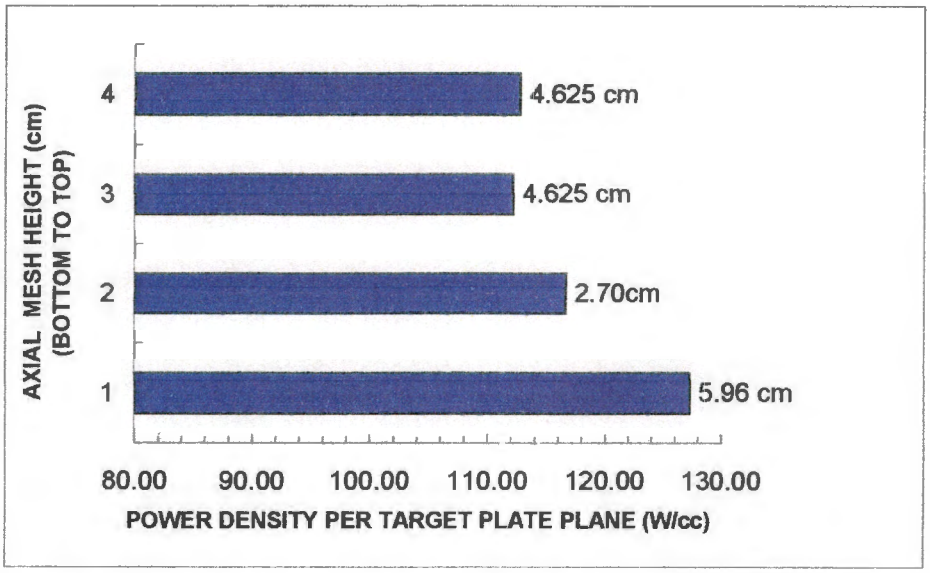

Figure 4-11: Power Density for Axial Planes at BOC

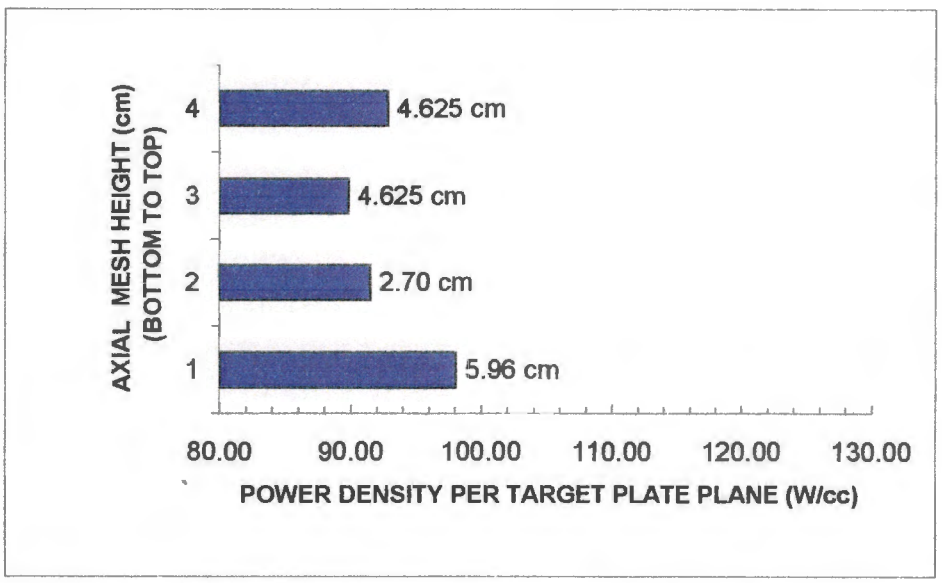

Figure 4-12: Power Density for Axial Planes at Mid-Cycle

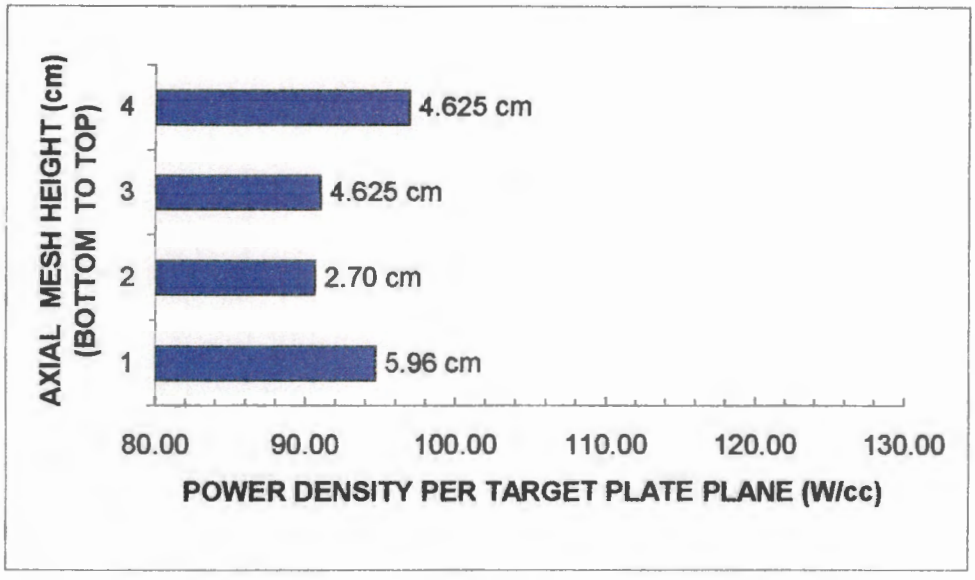

Figure 4-13: Power Density for Axial Planes at EOC

At BOC, rods must be inserted to compensate for large excess reactivity of the fresh core loading. The region of the core in which the rods have been inserted will experience decreased multiplication and hence relatively lower fluxes. This is depicted in Figure 4-11, where large burnup and power is observed towards the bottom meshes of the target plate irradiation rig E3. The power density at Mid-cycle is decreased indicating that the control rod has been withdrawn and the axial power profile is flatter.

As the control rods are withdrawn to compensate for the reduced reactivity, the increase in flux and power peaking will tend towards the top of the core as depicted in Figure 4-13. The graph also shows that during the early stages of the core life, the fuel near the bottom of the core would have been exposed to relatively higher fluxes and hence experience larger burnups.

The control rod effects on axial power or power density will be more pronounced in the case of fuel assemblies because of the larger active height, unlike for the four target plate meshes at the core centreline. This result agrees well with related literature.

NWU LIBRARY

Throughout the discussion on core power distribution it has been noted that effects due to target plate loading and unloading are very small for various methods employed. That is, *target plates without shuffles* and *target plates in* methods displayed negligible differences, as was the case in previous sections. The *target plates shuffling* method showed more dominant effects than the other two methods, although small. Important effects in as far as safety is concerned have been identified, for example, peaking assemblies, nodal peaking in assemblies or assembly, etc. The two hour step has also displayed negligible effects for the *target plates in* and *target plates without shuffles* method, except during the time that they are removed of course.

4.2.5. Yield of Mo-99 Fission Product from Irradiation of U-235 Target Plates

All reactors are a source of neutrons but not all are suitable for Mo-99 production. The factors that determine suitability are power level, neutron flux available for target irradiation and the volume into which targets can be placed [9], [10], [18]. SAFARI-1 satisfies these conditions; therefore to add value to our calculational methods, Mo-99 yield was calculated.

The yields were calculated at the last step of target plate irradiation (i.e. 20.590–23.417 days) using equation (2.3.3) in Section 2.3.3 and plate powers calculated using the **RDBF** tool. The OSCAR-3 calculations give yields at production, that is, before decay; therefore to compare with actual yields (measure and predicted), an appropriate irradiation and decay period was used. An assumption that all fissions resulted from U-235 fuel only, was made. This assumption should not be too bad since 45% enriched target plates are used and the target plates burnup are small (i.e. no time to build Pu).

Note that in all plate holders for six irradiation positions, seven plates were loaded, and compared to experimental values obtained from seven plate irradiations.

In Table 4-10, Mo-99 yields calculated for the three methods of including target plates for core position E3 are tabulated. Note that the purpose of this comparisons are not to validate the model or code but rather illustrate that OSCAR-3 can be used to predict these yields using the different approaches. A more extensive study would be required with a larger number of measured yields to do validation. This falls out of the scope of the current work.

Table 4-10: Mo-99 Measured and Calculated Yield for Irradiation Position E3

Methods	**Mo-99 Yield (Ci/gU)**		**% Difference Between OSCAR-3 and Measured Yield values**
	OSCAR-3	**Measured**	
Target plates in	16.1 (12.9)	10.9	48% (18.3%)
Target plates without Shuffles	16.1 (12.9)		48% (18.3%)
Target plates Shuffling	16.9 (13.5)		55% (24%)

An average chemical extraction efficiency of 80% to be applied to OSCAR-3 yield calculations is assumed (values are in brackets). The *target plates in* and *target plates without shuffles* methods produce yields of about 48% (18.3%) more than the measured yield, while the *target plates shuffling* method produces about 55% (24%).

Since the Mo-99 production project includes a number of processes, for example, target fabrication, irradiation in reactor, cooling for radioactive decay, chemical processing and waste disposal, there can be large uncertainties associated with the experimental yield of Table 4-10. These uncertainties may only be quantified by repeated comparisons over a number of cycles (whereas the present calculations are for a single cycle), thus determining average quantification of efficiencies. Using the values in Table 4-

10, OSCAR-3 predicts that for this production run, the Mo-99 extraction process was around 55% efficient.

Consistency with the results from previous sections is still maintained, that is, the two hour step is still not important and the *target plates shuffling* method still shows larger effects than the other methods employed.

It can therefore be noted that *target plates shuffling* method will play an important role when it comes to the demand and irradiation planning of the Mo-99 fission product.

Target plates are not left in the reactor indefinitely but are removed within about 3 to 10 days after insertion. Mo-99 decays while in the reactor and a balance must be struck between processing costs, specific activity and reactor operation costs. Figure 4-14 shows the saturation activity (activity) as a function of time for the three methods.

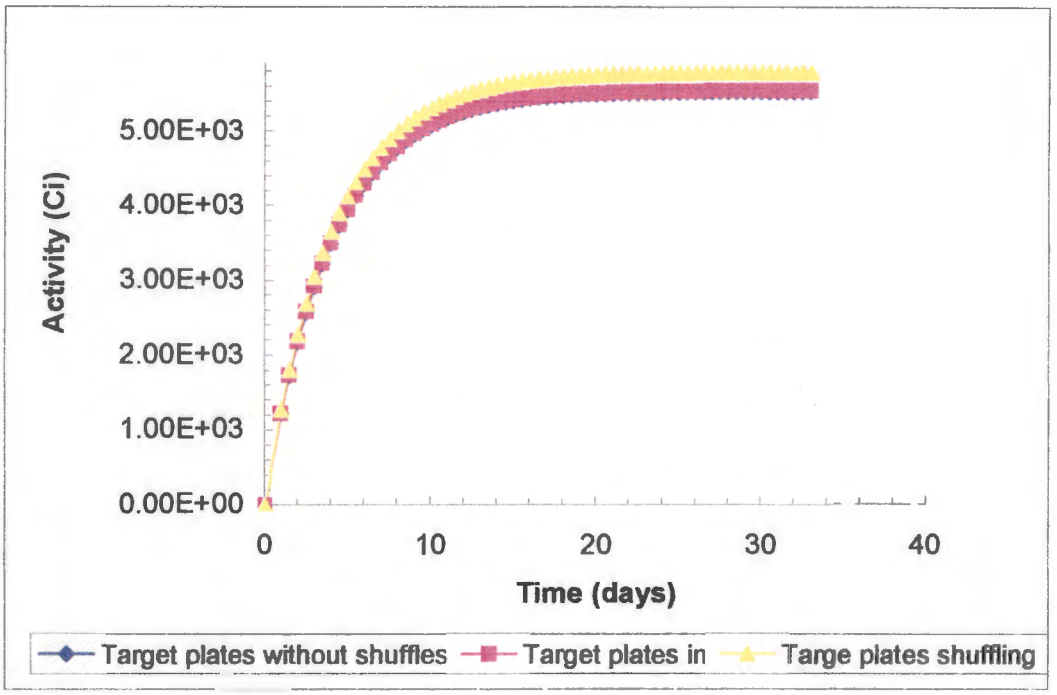

Figure 4-14: Saturation Activity for *Target Plates Shuffling*, *Target Plates In* and *Target Plates without Shuffles*

It can be seen that saturation for *target plates shuffling* will be reached after about 10 days and for the other two methods will be reached a bit earlier.

For yield purposes it is advisable to employ the *target plates shuffling* method, as it is the more realistic approach and also for the reason that the schedule is important as indicated before.

4.2.6. Effects on Core Thermal Neutron Flux Distribution

The neutron flux plays an important part in reactor utilization and it is very important that stable neutron fluxes be maintained at all irradiation sites irrespective of changes made in the core [16], [19]. In this section flux, perturbation as a result of target plate introduction based on the three proposed methods will be investigated. Irradiation position fluxes will also be determined and can be used to calculate Mo-99 yield with the knowledge of the macroscopic fission cross section.

4.2.6.1. Global effects on thermal neutron flux

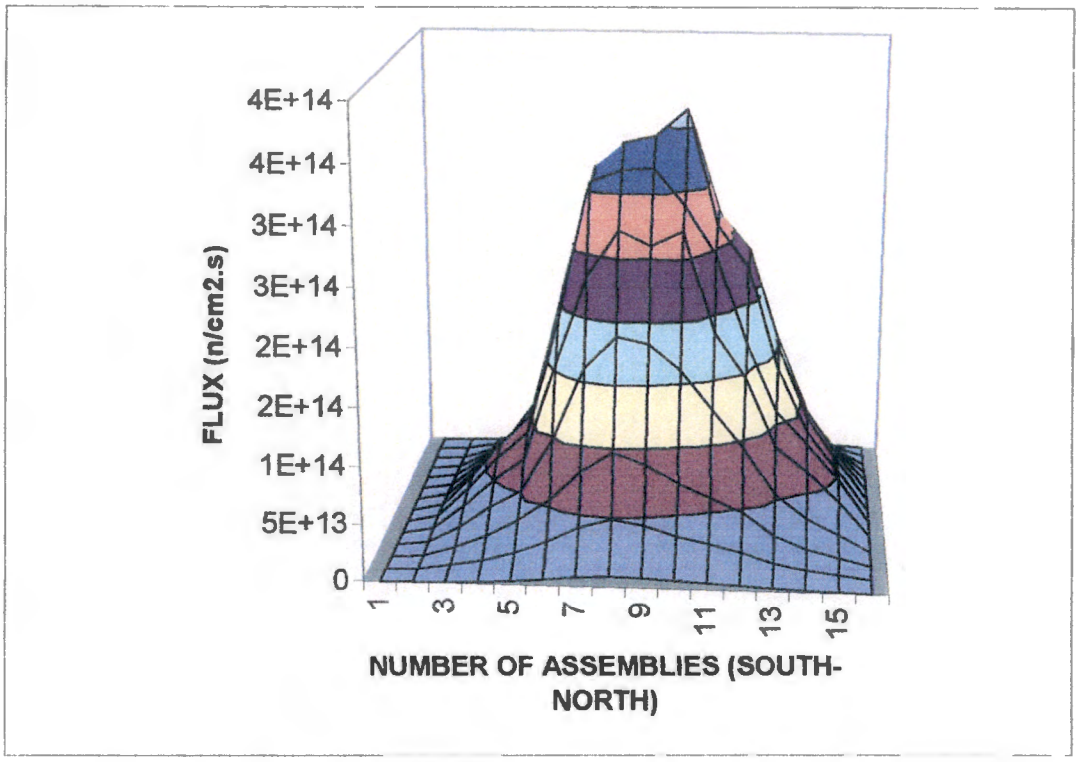

Figure 4-15: Thermal Flux Distribution in the Core

The fluxes, unlike power, will be distributed throughout the core even in non-active assemblies and from the graph it is evident that the flux peaks towards the centre of the core. This distribution is attributed to more leakage experienced towards the outer assemblies and it will be to a lesser extent towards the centre of the core. This shape of core flux distribution is observed for all methods.

The flux shape agrees with what is expected from the plant and the literature, thus adding value to the OSCAR-3 calculational system; that is, the code yields the correct qualitative behaviour for the SAFARI-1 reactor.

4.2.6.2. Local effects on fluxes in target plate irradiation positions

Thermal flux distribution in the irradiation positions was examined relative to *The Reference Method* thermal neutron flux and effects quantified as a result of target plates loading. This was done for BOC, Mid-cycle and EOC for all the methods. The results are summarised in Table 4-11.

Table 4-11: Relative Thermal Flux Distribution in Irradiation Position on the Eastern Side of the Core

Target Plate Positions	Methods	Relative Thermal Neutron Fluxes		
		BOC	Mid-cycle	EOC
C3	Plates Shuffling	0.841	0.839	0.855
	Plates in	0.841	0.832	0.840
	Plates without shuffles	0.841	0.832	0.840
E3	Plates shuffling	0.864	0.851	0.860
	Plates in	0.864	0.851	0.853
	Plates without shuffles	0.864	0.851	0.853
G3	Plates shuffling	0.846	0.827	0.816
	Plates in	0.846	0.827	0.831
	Plates without shuffles	0.846	0.826	0.831

The Reference Method has higher fluxes in the irradiation positions. This effect is due to the fact that neutrons will be more thermalised in the irradiation position, because of more moderation.

The differences in the relative thermal neutron flux for the three methods in Table 4-11 are small. The two hour step effects, *shuffling* plates and no *shuffling* plates effects are very small. The lower fluxes in assembly G3 are as a result of more leakage experienced by the assembly and the overall core flux profile.

It can also be noted that the fluxes in position C3, E3, and G3 are in agreement with the results from the previous sections, that is, high fluxes for a position that displayed higher power density.

In support of this discussion, effects in the western irradiation positions were examined for the same cases and the results are summarised in Table 4-12 below.

Table 4-12: Relative Thermal Flux Distribution in the Irradiation Position on the Western Side of the Core

Target Plate Positions	Methods	Relative Thermal Neutron Fluxes		
		BOC	Mid-cycle	EOC
B8	Plates Shuffles	0.819	0.821	0.827
	Plates in	0.819	0.819	0.827
	No shuffles	0.819	0.819	0.827
D8	Plates shuffles	0.811	0.808	0.815
	Plates in	0.811	0.807	0.816
	No shuffles	0.811	0.806	0.816
F8	Plates shuffles	0.798	0.796	0.803
	Plates in	0.798	0.798	0.805
	No shuffles	0.798	0.796	0.804

Irradiation position F8 has higher fluxes, followed by D8 and the lowest fluxes are in B8 as expected, although the relative flux appears not to follow the trend.

Irradiation position F8 shows that the position and the neighbours to that specific assembly position, play an important role when it comes to flux and power distributions. To elaborate on this, lets look at assembly G3 and F8, both close to the northern boundary of the core. Irradiation position F8 has higher fluxes than the rest of the assemblies or irradiation positions on the western side, unlike in the case of the eastern side were G3 has the lower fluxes. The assembly position and its neighbours come into play here. Position G3 is closer to the boundary at the poolside than F8. Despite this, it experiences larger thermal fluxes due to its environment.

The effect of the control rods on the irradiation positions, B8, D8 and F8 will also be dominant unlike in the eastern irradiation positions which are not as close to the rods as the western irradiation positions.

To examine these effects in more detail, the relative fluxes per layer of irradiation positions, E3 and F8 were plotted per axial layer (i.e. 17 layers in an assembly). This was done for *target plates shuffling*, *target plates without shuffles* and *The Reference Method.* The effects are summarised in Figure 4-16. The relative flux was obtained by dividing the case's flux by *The Reference Method* flux, i.e. a value of 1.0 implies no difference. Also shown is the flux ratio of position F8 and E3 for *The Reference Method.*

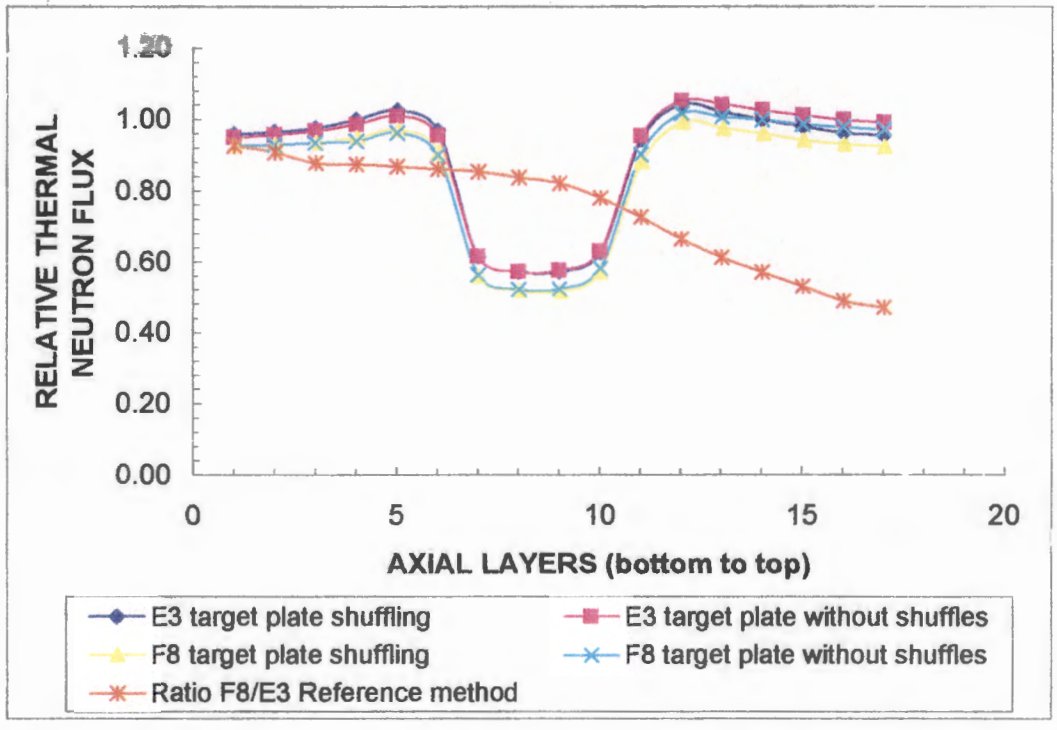

Figure 4-16: Relative Fluxes Per Layer for Assemblies E3 and F8 for *Target Plates Shuffling*, *Target Plates Without Shuffles* and F8/E3 *Reference Method* Flux Ratios at BOC

Clearly, the differences in fluxes are negligible for *target plates shuffling* and *target plates without shuffles*; the same applies to *target plates in* method. Larger differences are however seen compared to *The Reference Method* case. The dip in flux of axial layer 7 to 10 for these methods is as a result of target plates depressing fluxes upon loading; otherwise the flux takes the shape of *The Reference Method* fluxes, as depicted in Figure 4-16.

4.2.6.3. Perturbation effects on the other irradiation sites

Due to many utilization activities at Necsa (SAFARI-1 reactor) and the fact that these activities are expected to increase continuously [19], it is very important to maintain a stable neutron flux at the irradiation sites including the beam tubes. Thus, the neutron fluxes at the irradiation sites should not be perturbed much due to the fission of 45% enriched U-235 target plates. The perturbation effects on the neutron flux at the irradiation sites are tabulated in Table 4-13 below.

Table 4-13: Thermal Neutron Flux Perturbation at Irradiation Sites Due to Target Plates Loading

Irradiation Positions	Thermal Neutron Flux x 10^{14} (n/cm^2.s)				Difference Of Thermal Neutron Flux (%)	
	Reference Method		Target Plates Shuffling			
	BOC	EOC	BOC	EOC	BOC	EOC
A9	0.365	0.300	0.376	0.313	3.0	4.3
B6	1.530	1.260	1.460	1.230	-4.6	-2.4
D6	1.990	1.700	1.900	1.640	-4.5	-3.5
E9	0.880	0.761	0.892	0.780	1.4	2.5
F6	1.940	1.690	1.830	1.600	-5.7	-5.3
G9	0.681	0.596	0.666	0.585	-2.2	-1.9

On average the fluxes in irradiation positions summarised in Table 4-13 drop as a result of target plate loading. The thermal fluxes are perturbed within 6% at BOC and EOC.

From the above results, it is concluded that target plate loading does not perturb the thermal neutron flux at the other irradiation sites (negligible flux perturbation). It means that target plates can be loaded regardless of the other irradiation activities; however, it is important to confirm the effects in detail before the actual irradiation of the target plates.

5. SUMMARY OF RESULTS AND CONCLUSIONS

This study has explored different ways of target plate loading in the present OSCAR-3 core calculation module, with a newly regenerated cross section library. In addition, the correlation of the OSCAR-3 results to the SAFARI-1 plant data has proven to be within reasonable expectations.

Important aspects for safety and utilisation such as reactivity, fuel saving, cycle length, power peaking, plate powers, fluxes and Mo-99 yield have been investigated due to the effects caused by the loading of target plates.

Different methods have shown negligible effects when compared, that is, *target plates in* and *target plates without shuffles*. *Target plates shuffling* and *target plates without shuffles* have also shown the need to use the irradiation schedule. In most instances, marked effects were observed for the *target plates shuffling* method, although small. To finally decide on a method or methods to adopt for core calculations with target plates loaded we summarise the different effects per method in Table 5-1. Note that only some of the most important effects in safety and planning are considered.

Table 5-1: Overall Summary of the Results for Different Methods of Loading Target Plates in OSCAR-3 Core Calculational Module

Methods	Safety		Planning			Ease Of Use
	Reactivity	Peaking Assembly (Nodal) at BOC	Cycle Length (Days)	Fuel Saving (grams)	Yield (Ci/gU) for (E3)	
Reference Method	-	C6	18.7		-	Very Easy
Target plates in	2000	C6	19.6	13.45	16.1 (12.9)	Easy
Target plates without shuffles	1653	C6	19.5	13.28	16.1 (12.9)	Easy
Target plates shuffling	1694	C6	19.9	20.20	16.9 (13.5)	Not Easy

From Table 5-1 we can draw some conclusions in as far as the loading of the target plates in an irradiation position is concerned. Throughout the result discussion sections, different effects have been observed, although with slight differences in some methods.

In safety studies, at BOC, reactivity is increased for the three methods relative to *The Reference Method*. The average reactivity effect over the entire cycle calculation is higher for the *target plates in* method. Peaking at BOC is observed in assembly C6 (nodal peaking), and D3 (assembly peaking) for *target plates shuffling*, *target plates without shuffles* and *target plates in* methods.

In general, for safety studies all methods are important, however, the *target plates in* and *target plates shuffling* methods will be adopted for quantifying reactivity effects for the cycle calculation. The reactivity effects have also shown the importance of the target plate irradiation schedule. That is, higher average reactivity is observed without the schedule than when the schedule is used.

Planning is very important in reactor utilisation. One needs to know how long the reactor will operate under certain conditions, how much fuel will be left at the end of operation (i.e. can be used in subsequent cycles), the flux levels during utilisation, whether domestic demands of the reactor product will be met, etc.

Some of the important effects discussed in these studies, as far as planning is concerned, are listed in Table 5-1. The *target plates shuffling* method showed more important effects when it comes to planning than the other two methods of target plate loading. Thus, this method will be used together with *target plates in,* to study relative effects in planning.

When it comes to ease of use, *target plates in* and *target plates without shuffles* are easier methods to use than the *target plates shuffling* method. Therefore the *target plates in* method will be the method of choice.

The inclusion of target plate irradiation rigs has shown meaningful improvement in planning and utilization, also in the improvement of cycle k-effective relative to the plant data. The study has also shown that detailed modelling of irradiation rigs and the core material in general are essential if realistic core follow and reload studies are to be performed, thus ensuring that safety limits are met.

In conclusion, the results of these calculations have shown that OSCAR-3 is indeed able to model the on-power loading of target plates, provided care is taken in several aspects. The *target plates in* and *target plates shuffling* methods will be adopted in this study as the appropriate methods for target plate irradiation rigs modelling in OSCAR-3 core calculations for reasons already discussed in this study.

In general, OSCAR-3 has provided reasonable and consistent theoretical results, some acceptable in comparison with plant data and experimental results. The inability to handle *shuffling* of target plates in a single MGRAC run for the entire cycle calculations, to have different mixtures in an

assembly's height (e.g. target plates at the four centre-line meshes and the remaining meshes filled with water) does however limit the ease of use in modelling with OSCAR-3 for the SAFARI-1 reactor. CROGEN, an OSCAR-3 sub-code system, has proven to be highly effective in few group homogenised cross section generation, since the cross section library generated displayed consistent results for different methods employed.

Work on improving the cross section library and the OSCAR-3 models employed, is planned to continue in future for improved correspondence with plant data.

6. RECOMMENDATIONS FOR FUTURE WORK

The use of OSCAR-3 to model the target plate irradiation rigs with an improved cross section library has proved to be possible and useful for the SAFARI-1 reactor. Future improvement may include the use of codes or a code (e.g. OSCAR-4) which have the capabilities of handling target plate loading as per irradiation schedule with ease, thus reducing the code limits and approximations. Improvement on the cross section library generated has to be continued, and equilibrium studies (i.e. with an equilibrium cycle) have to be quantified for long-term effects.

Since the ex-core elements like beam tubes, stainless steel hold-down arms, bottom grid plate, adaptors, etc. are within a reasonable distance to influence the neutronics of the core, it might also be an important study to include and quantify them for past and future core calculations for SAFARI-1.

Proposing a new axial mesh definition for use in core diffusion calculations, based on rig type constraints within the reactor will also be an important future study.

Work on the calculational support provided for the SAFARI-1 reactor will continue and the improvement of the current calculational methods will be implemented. This will ensure improved and safe SAFARI-1 reactor operation, yielding an environment for flexible development and commercial programs.

7. REFERENCES

[1]. **Reitsma F., Naidoo D.** and **Prinsloo R.**, *"OSCAR-3 Workshop Manual"*, OSCAR-3 Workshop, Pelindaba, Pretoria, South Africa, 24-28 February 2003.

[2]. **Glasstone S.** and **Sesonske A.**, *"Nuclear Reactor Engineering", Reactor Design Basics*, 4th edition (vol. 1), CBS Publishers & Distributors, 1994.

[3]. **Duderstadt J. J.** and **Hamilton L. J.**, *"Nuclear Reactor Analysis,"* John Wiley & Sons, Inc., 1976.

[4]. **Krane K.S.**, *"Introductory Nuclear Physics,"* John Wiley & Sons, Inc., 1988.

[5]. **Glasstone S.** and **Edlund M. C.**, *"The Elements of Nuclear Reactor Theory"*, D. Van Norstrand Company Inc, 1952.

[6]. **Lamarsh J. R.**, *"Introduction to Nuclear Engineering", 2nd edition,* Addison-Wesley Publishing Company Inc, 1983.

[7]. ***SAFARI-1*** *Material Engineering Drawings.*

[8]. Document **EA-TG-1601**, Material specification*: "Uranium-Aluminium Alloy Billets"*, 29 May 1997 and private communication.

[9]. **IAEA-TECDOC-1065**, *"Production Technologies for Molybdenum-99 and Technetium-99m"*, IAEA, Vienna, 1999.

NWU LIBRARY

[10]. **Calabrese R., Grant C., Marajofsky A.,** and **Parkansky D. G.**, *"Analysis of Mo-99 Production Irradiating 20%U Targets"*, Reduced Enrichment for Research and Tested Reactors, Sao Paulo, Brazil, October 18-23, 1998.

[11]. **Reitsma F., Prinsloo R., Thugwane S., Kierkegaard J.,** and **Eliasson J.**, *"Importance of Including Irradiation Rig Loading in Research Reactors Cycle Planning and Core Follow Calculations"*, The 14th Pacific Basin Nuclear Conference "New Technologies for a New Era", Honolulu, Hawaii, 21-25 March 2004.

[12]. **Stoker C. C.,** and **Ball G.**, *"Calculation of the Isotope Concentrations, Source Terms and Radiation Shielding of the SAFARI-1 Irradiation Products"*, The 9th International Conference on Radiation Shielding, Tsukuba Convention Center, Tsukuba, Japan, October 17-22, 1999.

[13]. **De Leege P. F. A.** and **Gibcus H. P .M.**, *"Reactivity Effects of a Research Reactor (HOR) during the Transition of a HEU to LEU Core"*, PHYSOR 2002, Seoul, Korea, October 7-10, 2002.

[14]. **Reitsma F.** and **Joubert W. R.**, " *A Calculational System to Aid Economic use of MTRs,*" Trans. Intl. Conf. Research Reactor Fuel Management (RRFM'99), Bruges, Belgium, March 29-31, 1999.

[15]. **Müller E. Z., Ball G., Joubert W. R., Schutte H. C., Stoker C. C.** and **Reitsma F.**, *"Development of a Core Follow Calculational System for Research Reactors"*, The 9th Pacific Basin Nuclear Conference, Sydney, Australia, 1-6 May 1994.

[16]. **Ball G.**, *"Efficient use of Neutrons at SAFARI-1"*, Trans. Intl. Conf. Research Reactor Fuel Management (RRFM'99), Bruges, Belgium, March 29-31, 1999.

[17]. **Ball G.**, *"Calculational Support Provided to SAFARI-1"*, AFRA Regional Conference on Research Reactor Operation, Utilisation and Safety, Algiers, April 10-11, 1999.

[18]. **Lee B. C. and Kim H.**, "*Neutronic Analysis for the Fission Mo Production using LEU Target at HANARO"*, The 2002 International Meeting on Reduced Enrichment for Research and Test Reactors", San Carlos de Bariloche, Argentina, November 3-8, 2002.

[19]. **Ball G.**, *"Research Reactor Utilization: An Overview"*, AFRA Regional Conference on Research Reactor Operation, Utilization and Safety, Algiers, April 10-11, 1999.

[20]. **Stumpf W. E., Vermaak A. P.** and **Ball G.**, *" Key Considerations in the Conversion To LEU of A Mo-99 Commercially Producing Reactor," SAFARI-1 of South Africa*, Presented at the 2000 international Meeting on Reduced Enrichment for Research and Tested Reactors, Las Vegas, Nevada, 1-6 October 2000.

8. GLOSSARY

i. **Control Banks-** a group of control rods moving together, i.e. in SAFARI-1 there are 5 such rods.

ii. **Core-follow calculations-** these are calculations performed at the end of each SAFARI-1 reactor cycle for the new cycle with a known history of the previous cycle.

iii. **Cross-section-** description of the interaction of neutrons with the atomic nuclei.

iv. **Cross-section library-** all the cross-section material used are stored here after being generated.

v. **Delayed neutrons-** neutrons born with an appreciable time delay from subsequent decay of radioactive fission products (<1% neutron emitted).

vi. **Depletion-** reduction of the concentration of one or more specified isotopes in a material or one of its constituents.

vii. **Dummy element, plate-** an element or plate without nuclear fuel intended to replace or to represent a fuel element or plate.

viii. **Energy groups-** division of neutron energy range into a number of groups.

ix. **Finite difference method-** A computational approximation to the gradient term requiring a fine mesh discretization for sufficient accuracy.

x. **Group condensation/group collapsing-** refers to the reduction in number of energy groups in which the cross-sections are specified.

xi. **Homogenization-** used to obtain a single set of cross-section data for an assembly to be used in the core calculation.

xii. **Isotopes-** nuclides having the same atomic number but different mass number.

xiii. **k-infinity-** the k-eff multiplication factor of an infinite uniform medium.

xiv. **k-effective-** that eigenvalue number which, when divided into actual mean number of neutrons emitted per fission in an assembly of materials, would make the calculated result for the nuclear chain reaction of that assembly artificially critical.

xv. **Multi-group calculations-** calculation within certain neutron population, which is divided into a finite number of neutron energy groups.

xvi. **Number density-** the number of atoms or nuclei per unit volume.

xvii. **Nodal method-** spatial region is divided into relatively large regions called nodes.

xviii. **Off-base cases/calculations-** calculations performed by HEADE to take the state parameters into account, that is fuel temperature, moderator temperature, moderator density, etc.

xix. **Power density-** the power generated per unit volume of a reactor core.

xx. **Precursors, delayed neutron-** a nuclide whose nuclei undergo beta decay followed by neutron emission (i.e. delayed neutrons).

xxi. **Prompt neutrons-** neutrons born essentially instantaneously upon fission.

xxii. **Reactivity-** a parameter giving the deviation from criticality of a nuclear chain-reacting medium such that positive values correspond to a supercritical state and negative values to a subcritical state.

xxiii. **Reactor cycle-** is a period of operation in which a reactor will remain critical.

xxiv. **Shutdown margin-** the negative reactivity of the core present when all the control banks have been fully inserted to achieve minimum core multiplication.

xxv. **Thermally fissile materials-** nuclides that undergo fission with neutrons of any energy, e.g. U-235, U-233, Pu-239, etc.

9. APPENDICES

APPENDIX A

CYCLE LENGTH DETERMINATION

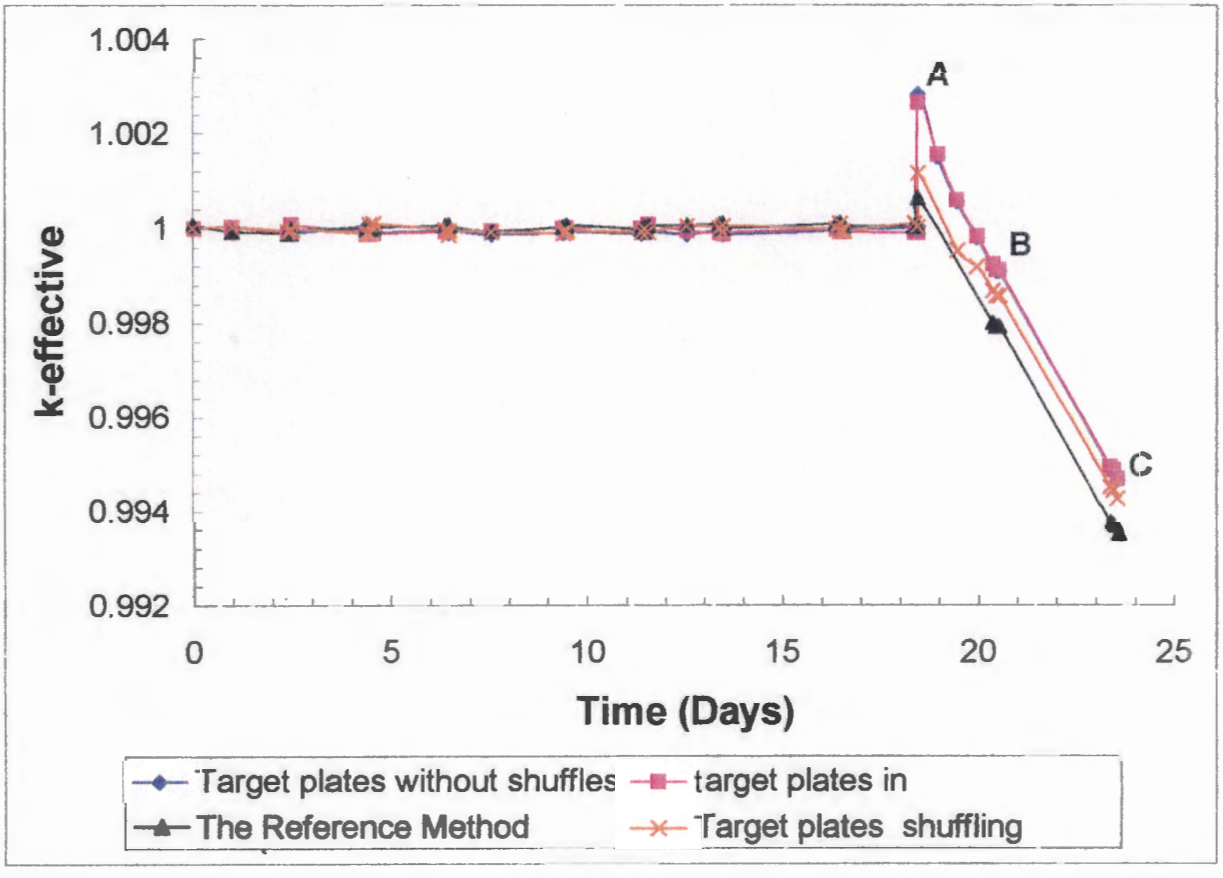

Figure A: Example of Cycle Length Calculation for all Methods: 18.5 Days into a Cycle

Point **A**, **B** and **C**, represent straight-line equations for each method given as,

i. *The Reference: Method*: y = -0.0015x + 1.028
ii. *Target plates in*: y = -0.0015x + 1.0294
iii. *Target plates shuffling*: y = -0.0014x + 1.0279
iv. *Target plates without shuffling*: y = -0.0015x + 1.0293

With requirements that y = 1.000 (i.e. k-eff.=1) and solve for x (i.e. the cycle length in days).

APPENDIX B

HEADE INPUT EXAMPLE FOR THE 300g FUEL ASSEMBLY

```
SFOI
'HEADE-INP V01.08'
> 94  ../output/NEW-SAFH3E1.PRT                  * Printout
* 91  MONITOR                                    * Monitor File
  92  ../../LOGFILE     SFUB                     * Logging File
  93  ERROR                                      * Logging File
   2  /u/oscar3/data/HEADE20.LIB       SUOI  100000  * Library
  80  ../output/NEW-SAFH3E1.HED        SFUB   50000  * HEADE file
  81  SCRATCH                    SFSB   50000  * HEADE interface
  82  SCRATCH                    SUSB   50000  * Geometry scratch
  83  SCRATCH                    SUSB   50000  * Burnup scratch
  84  SCRATCH                    SUSB   50000  * Flux scratch
  85  SCRATCH                    SUSB   50000  * Flux scratch
  86  danc172.SAF                SFOI
'ENDFCD'
*IPATH
  0
'SSFE9029---- FUEL ASSEMBLY MODEL  Library: SLIBH220  '
*  ISYM,IRTYPE,NX,NY,MMAX,IXEDIT,IPRINT,ICTYPE IOPXE
  0    2    10 19 5   1     0     0       0
*  ISCAT NTHER
  3    2
*  MAXO NUP1 NUP2 MAXI MINI NUMF,NUMSK
  100  6    6    100  1    3    5
*  EPSE     EPST     EPSI     EPSS     OMEGA  OMS  OMF
  1.0E-6   1.0E-6   1.0E-5   1.0E-5   1.3    1.3  1.0
*  POWER (WATTS)  INITIAL PPM  ENRICHMENT
  689655.0       0.0         90.0
*  ACTIVE HEIGHT  TOTAL HEIGHT  WATER PRESSURE (BAR)
  59.37          59.37         1.8
*  NMICRO
  38
*  MICROSCOPIC MATERIALS
  'U234'   'U235'   'U236'   'U237'   'U238'   'Np237'   'Np239'
```

```
  'Pu238'  'Pu239'  'Pu240'  'Pu241'  'Pu242'  'Am241'   'Am242m'
  'Am243'  'Cm242'  'Cm243'  'Cm244'  'Cm245'  'I135fp'  'Xe135'
  'Ce141fp' 'Ce142fp' 'Ce144fp' 'Pr143fp' 'Nd143fp' 'Nd144fp'  'Nd145fp'
  'Nd146fp' 'Nd147fp' 'Nd148fp' 'Pm147fp' 'Pm148fp' 'Pm148mfp' 'Pm149fp'
  'Sm147fp' 'Sm148fp' 'Sm149fp'
* NGRB
  6
* BROAD GROUP BOUNDARIES
* 172 group boundaries
  22 47 92 135 152 172
* 69 group bounaries
* 5 15 27 45 55 69
* NSAT
  0
* BURNUP STEPS
  33
* OFFBASE STEPS, IBP,ICR
  6         0  0
* BISECT
  0 0 0 0
* MAP
   0 -1 -1 -1 -1 -1 -1 -1 -1 -1 -1  0
  -1  7  6  5  5  5  5  5  5  6  8 -1
  -1  3  2  1  1  1  1  1  1  2  4 -1
  -1  3  2  1  1  1  1  1  1  2  4 -1
  -1  3  2  1  1  1  1  1  1  2  4 -1
  -1  3  2  1  1  1  1  1  1  2  4 -1
  -1  3  2  1  1  1  1  1  1  2  4 -1
  -1  3  2  1  1  1  1  1  1  2  4 -1
  -1  3  2  1  1  1  1  1  1  2  4 -1
  -1  3  2  1  1  1  1  1  1  2  4 -1
  -1  3  2  1  1  1  1  1  1  2  4 -1
  -1  3  2  1  1  1  1  1  1  2  4 -1
  -1  3  2  1  1  1  1  1  1  2  4 -1
  -1  3  2  1  1  1  1  1  1  2  4 -1
  -1  3  2  1  1  1  1  1  1  2  4 -1
  -1  3  2  1  1  1  1  1  1  2  4 -1
  -1  3  2  1  1  1  1  1  1  2  4 -1
  -1  3  2  1  1  1  1  1  1  2  4 -1
  -1  3  2  1  1  1  1  1  1  2  4 -1
```

```
-1  7 10  9  9  9  9  9  9 10  8  -1
 0 -1 -1 -1 -1 -1 -1 -1 -1 -1 -1   0


*  Node Specifications

*  Cell Type 1: Plate With Fuel
   'SLAB'
   1 5  1.0500 1                    CELLTYPE NR SLHGT ORIENT
   0.1466  0.0384  0.0507  0.0384  0.1466  3 2 1 2 3

*  Cell Type 2: Plate Without Fuel
   'SLAB'
   6 3  0.190  1                    CELLTYPE NR SLHGT ORIENT
   0.1466  0.1275  0.1466             3 2 3

*  Cell Type 3: Side Plate WEST
   'SLAB'
   6 2  0.4207  0                   CELLTYPE NR SLHGT ORIENT
   0.0600  0.4550                    3 2

*  Cell Type 4: Side Plate EAST
   'SLAB'
   6 2  0.4207  0                   CELLTYPE NR SLHGT ORIENT
   0.4550  0.0600                    2 3

*  ---------------------------------------------------------------------

*  Cell Type 5: Plate With Fuel TOP
   'SLAB'
   1 5  1.0500 1                    CELLTYPE NR SLHGT ORIENT
   0.19995 0.0384  0.0507  0.0384  0.1466  3 2 1 2 3

*  Cell Type 6: Plate Without Fuel TOP
   'SLAB'
   6 3  0.190  1                    CELLTYPE NR SLHGT ORIENT
   0.19995 0.1275  0.1466             3 2 3

*  Cell Type 7: Side Plate WEST TOP
   'SLAB'
```

```
  6 2  0.47405  0                    CELLTYPE NR SLHGT ORIENT
  0.0600  0.4550                      3 2

*  Cell Type 8: Side Plate EAST TOP
  'SLAB'
  6 2  0.47405  0                    CELLTYPE NR SLHGT ORIENT
  0.4550  0.0600                      2 3

*  Cell Type 9: Plate With Fuel BOTTOM
  'SLAB'
  1 5  1.0500 1                      CELLTYPE NR SLHGT ORIENT
  0.1466  0.0384  0.0507  0.0384  0.19995 3 2 1 2 3

*  Cell Type 10: Plate Without Fuel BOTTOM
  'SLAB'
  6 3  0.190  1                     CELLTYPE NR SLHGT ORIENT
  0.1466  0.1275  0.19995             3 2 3


* Material Definitions

* Material 1: U-AL
  'U-AL'
  333.0  29.0    0.83266   0.0
  0.0  90.0     0.0 0.0 10.0

* Material 2: AL
  'USER DEFINITION CLAD'
  4 331.0    1  0.0 0.0               Material type, Temp, # of isotopes
  Al  0.06022

* Material 3: Water
  'USER DEFINITION WATER CHANNEL'
  5 318.0    2  0.0 1.0               Material type, Temp, # of isotopes
  H 6.6393E-02   O  3.3197E-02


* Boundary Conditions

* Boundary Condition -1: White
```

```
'WHITE B CONDITION'

* ----------------------------------------------------------------------------

*IEC,IES
 0  0
*POWER EDIT REGIONS
 0
*XSEC  EDITS
 0  0  2
*DETECTOR PRESENCE
 0
*BURNUP DATA
*  RQ         DAYS       PPM     NUMFR
   689655.0   -0.1        0.0     3
   689655.0   -0.25       0.0     3
   689655.0   -0.5        0.0     3
   689655.0   -0.75       0.0     3
   689655.0   -1.0        0.0     3
   689655.0   -2.0        0.0     3
   689655.0   -3.0        0.0     3
   689655.0   -4.0        0.0     3
   689655.0   -6.0        0.0     3
   689655.0   -8.0        0.0     3
   689655.0   -10.0       0.0     3
   689655.0   -15.0       0.0     3
   689655.0   -20.0       0.0     3
   689655.0   -30.0       0.0     3
   689655.0   -40.0       0.0     3
   689655.0   -50.0       0.0     3
   689655.0   -70.0       0.0     3
   689655.0   -90.0       0.0     3
   689655.0   -110.0      0.0     3
   689655.0   -130.0      0.0     3
   689655.0   -150.0      0.0     3
   689655.0   -162.2      0.0     3
   689655.0   -175.2      0.0     3
   689655.0   -187.8      0.0     3
   689655.0   -200.4      0.0     3
   689655.0   -213.0      0.0     3
```

```
  689655.0  -225.6     0.0    3
  689655.0  -238.2     0.0    3
  689655.0  -250.8     0.0    3
  689655.0  -263.4     0.0    3
  689655.0  -276.0     0.0    3
  689655.0  -288.6     0.0    3
  689655.0  -301.2     0.0    3
*OFFBASE DATA
*  FTEMP   BCONC   WTEMP   WDENS   IWFLG   AXEND
   0.0     0.0     60.0    0.0     0       1.0
   0.0     0.0     -20.0   0.0     0       1.0
   0.0     0.0     0.0     0.007   0       1.0
   0.0     0.0     0.0     -0.193  0       1.0
  60.0     0.0     0.0     0.0     0       1.0
 -40.0     0.0     0.0     0.0     0       1.0
```

APPENDIX C

HEADE DATA FLOW IN CROSS-SECTION GENERATION (CROGEN)

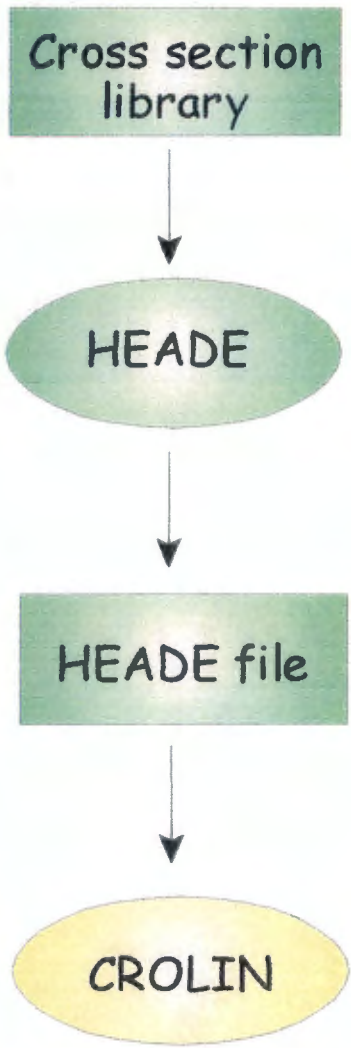

Figure C: HEADE Data Flow In Cross-Section Generation (CROGEN)

NWU LIBRARY

APPENDIX D

STYX DATA FLOW IN CROSS-SECTION GENERATION (CROGEN)

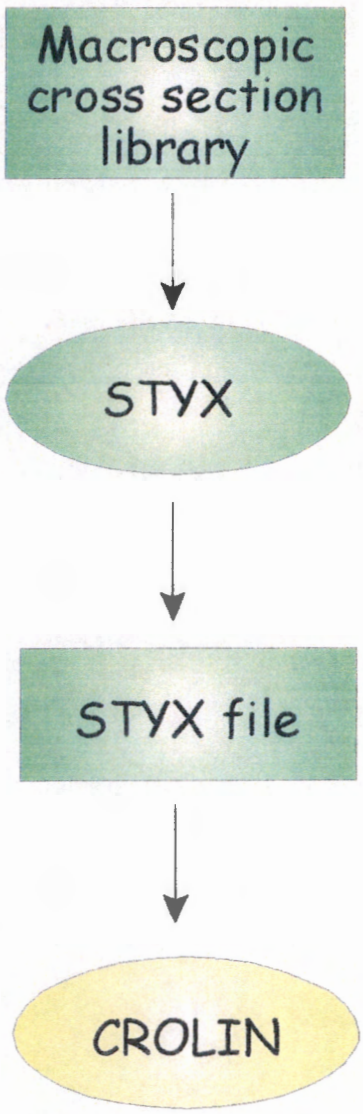

Figure D: Styx Data Flow in Cross Section Generation (CROGEN)

APPENDIX E

CROSS-SECTION DATA MANAGEMENT (CROLIN)

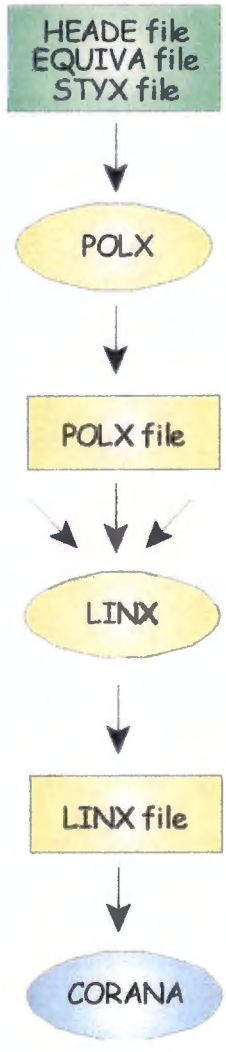

Figure E: Cross-Section Data Management (CROLIN)

NWU LIBRARY

APPENDIX F

CORE FOLLOW CALCULATION DATA FLOW

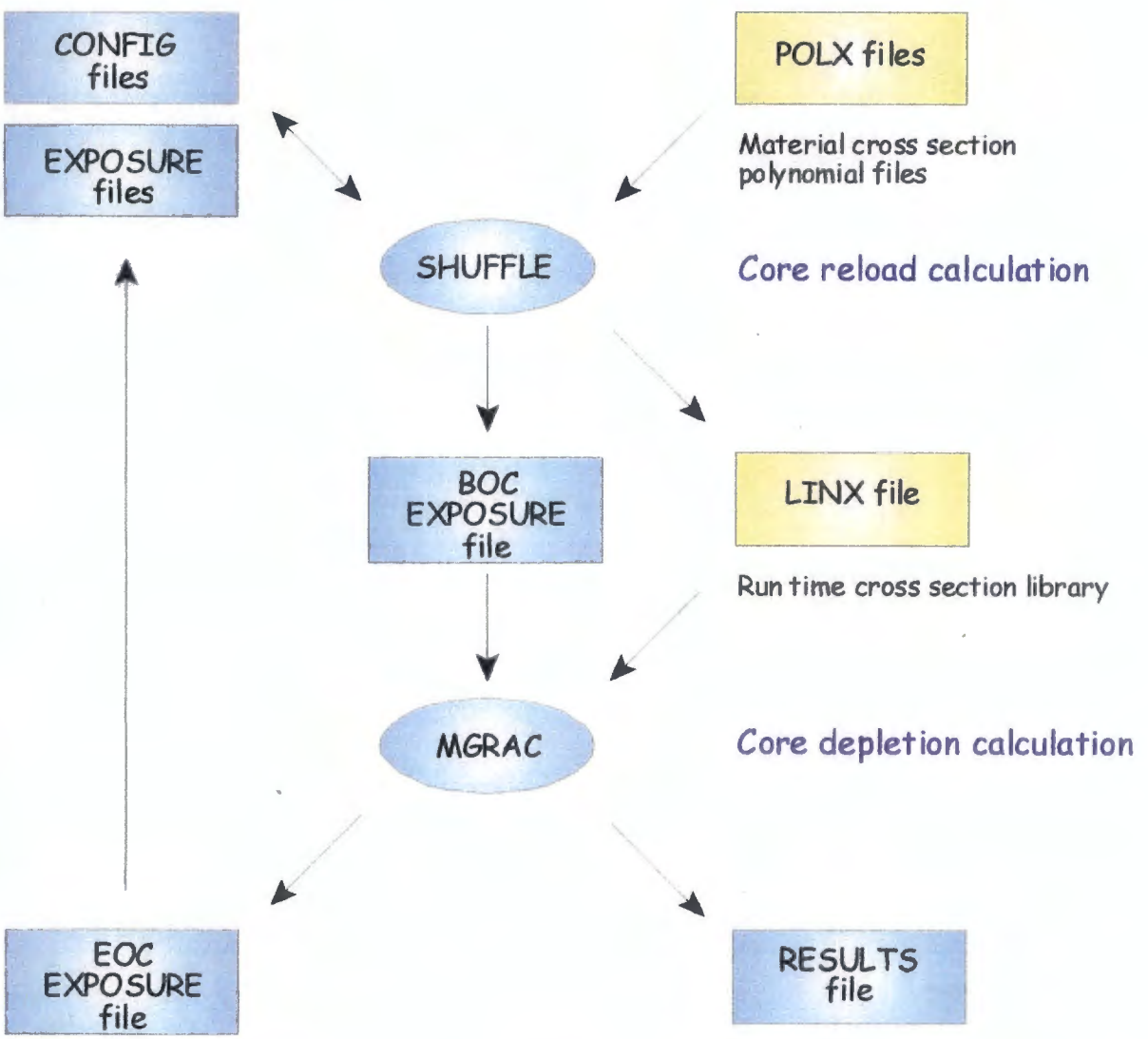

Figure F: Core Follow Calculation Data Flow

APPENDICE G

MGRAC INPUT FOR TARGET PLATES WITHOUT SHUFFLES METHOD

```
SFOI
'MGRAC-INP V01.06'
 91 MONITOR  * monitor file
 92 LOG  * log file
 93 ERROR  * error file
>94 $MAESTROWD/inout/MGRAC.C0405-1.FOLL.PRT  * printout file
 81  $MAESTROWD/inout/SAFARI-LIB-JUNE-2004.LNX    *  input  polynomial  cross-section
library
 82 $MAESTROWD/exposure/C0405-1BOC-ref.X0  * input exposure file
 83 $MAESTROWD/exposure/C0405-1FOLL.X1  * output exposure filename
 84 $MAESTROWD/dbf/FOLL.dbf  * database file
'ENDFCD'
*
* Generic data follows
*
'C0405-1: 16h50 on 2004-04-21'
* REACTR, CYCLE, ICDATE, ICTIME
'SAFARI-1'  'C0405-1 '  20040421  165000

*
NGT,NDELAY,NCHANT,NMIXT,IOPXSC,ISYM,NX,NY,NZ,IRTYPE,THPOW,AHIGHT,TKEFF
  6  0  16  60  1  0  15  14  17  2  20.000000  59.370000  1.000000

* IDYN,ISTAT,IKINE,ITRACE,IRECPF,IBFEED,IPFEED,ISBURN, IREHOM, IBUCKL
   0   1   0   0   1   1   1   1   1   0

* IUTYPE,IOPRNT,IED0,IED1,IED2,IED3,IED4,IED5,IED6,IED7,IED8,IED9,IED10
   1   0   0  3   3   1   0   3   0   0   0   0   3

* Channel subdivisions
 1 1 1 1 1 1 1 1 1 1 1 1 1 1 1 1 1    * NDX(I)
 1 1 1 1 1 1 1 1 1 1 1 1 1 1 1 1      * NDY(I)
 1 1 1 1 1 1 1 1 1 1 1 1 1 1 1 1 1 1  * NDZ(I)
```

```
* Channel sizes
 9.000000 6.000000 2.500000 7.710000 7.710000 7.710000 7.710000 7.710000 7.710000
7.710000 7.710000 7.710000 2.500000 6.000000 9.000000    * HX(I)
 9.000000 6.000000 2.500000 8.100000 8.100000 8.100000 8.100000 8.100000 8.100000
8.100000 8.100000 3.500000 4.600000 15.000000    * HY(I)
 9.000000 6.000000 4.392500 4.392500 5.975000 5.975000 5.950000 2.700000 4.625000
4.625000 4.325000 4.325000 3.085000 4.000000 5.000000 6.000000 9.000000    * HZ(I)

* Channel type allocation map
  0 -1 -1 -1 -1 -1 -1 -1 -1 -1 -1 -1 -1 -1 -1 -1 -1  0
 -1  1  1  1  1  1  1  1  1  1  1  1  1  1  1  1 -1
 -1  1  1  1  1  1  1  1  1  1  1  1  1  1  1  1 -1
 -1  1  1  2  2  2  2  2  2  2  2  2  2  2  1  1 -1
 -1  1  1  2  3  4  5  6  7  7  7  4  8  2  1  1 -1
 -1  1  1  2  3  4  9  9  9 10  9 11  3  2  1  1 -1
 -1  1  1  2  3  4 11  9 12  9 12  9  3  2  1  1 -1
 -1  1  1  2  3  4  9  9  9 10  9 11  4  2  1  1 -1
 -1  1  1  2 13  4 11  9 12  9 12  9 14  2  1  1 -1
 -1  1  1  2 13  7  9 15  9 16  9 11  4  2  1  1 -1
 -1  1  1  2 13  4 11  9 12  9 12  9 14  2  1  1 -1
 -1  1  1  2 13  4  9  9  9  9  9  4  3  2  1  1 -1
 -1  1  1  2  2  2  2  2  2  2  2  2  2  2  1  1 -1
 -1  1  1  1  1  1  1  1  1  1  1  1  1  1  1  1 -1
 -1  1  1  1  1  1  1  1  1  1  1  1  1  1  1  1 -1
  0 -1 -1 -1 -1 -1 -1 -1 -1 -1 -1 -1 -1 -1 -1 -1  0

* Channel type descriptions
1 'h3-h2oref---'  0 0
2 'h3-albox----'  0 0
3 'h3-solal----'  0 0
4 'h3-solbe----'  0 0
5 'h3-a3ringas-'  0 0
6 'h3-a4ringas-'  0 0
7 'h3-holbe----'  0 0
8 'h3-holal----'  0 0
9 'ssfe9028----'  0 0
10 'h3-IPR-thmbl'  0 0
11 'h3-mo-thmbl-'  1 0
12 'scra9028----'  0 0
```

13 'h3-solpb----' 0 0

14 'h3-hydrb----' 0 0

15 'ssfe9019----' 0 0

16 'h3-IPR-F6h2o' 0 0

*Axial mixture allocation per channel type

1 1 1 1 1 1 1 1 1 1 1 1 1 1 1 1 1

2 2 2 2 2 2 2 2 2 2 2 2 2 2 2 2 2

3 3 4 5 5 5 5 5 5 5 5 5 5 5 5 6 7

4 8 9 10 10 10 10 10 10 10 10 10 10 10 10 11 12

5 13 14 10 10 10 10 15 15 15 15 15 15 15 15 16 17

6 8 9 10 10 10 10 10 10 10 10 10 10 10 10 11 12

7 18 19 20 20 20 20 20 20 20 20 20 20 20 20 21 22

8 23 24 25 25 25 25 25 25 25 25 25 25 25 25 26 27

9 28 29 30 30 30 30 30 30 30 30 30 30 30 30 31 32

10 33 34 35 35 35 35 35 35 35 35 35 35 35 35 36 37

11 58 58 59 59 59 59 60 60 60 60 59 59 59 59 58 58

12 38 39 40 40 40 40 40 40 40 40 40 40 40 40 41 42

13 43 44 45 45 45 45 45 45 45 45 45 45 45 45 46 47

14 48 49 50 50 50 50 50 50 50 50 50 50 50 50 51 52

15 53 54 55 55 55 55 55 55 55 55 55 55 55 55 56 57

16 33 34 35 35 35 35 35 35 35 35 35 35 35 35 36 37

* Mixture type description

1 'H3-H2O-REF-_' -1

2 'H3-ALBOX____' -1

3 'H3-SOL-AL-BO' -1

4 'H3-SOL-AL-BI' -1

5 'H3-SOL-AL___' -1

6 'H3-SOL-AL-TI' -1

7 'H3-SOL-AL-TO' -1

8 'H3-SOL-BE-BO' -1

9 'H3-SOL-BE-BI' -1

10 'H3-SOL-BE___' -1

11 'H3-SOL-BE-TI' -1

12 'H3-SOL-BE-TO' -1

13 'H3-A3RNGA-BO' -1

14 'H3-A3RNGA-BI' -1

15 'H3-A3RINGAS ' -1

16 'H3-A3RNGA-TI' -1

17 'H3-A3RNGA-TO' -1
18 'H3-HOL-BE-BO' -1
19 'H3-HOL-BE-BI' -1
20 'H3-HOL-BE___' -1
21 'H3-HOL-BE-TI' -1
22 'H3-HOL-BE-TO' -1
23 'H3-HOL-AL-BO' -1
24 'H3-HOL-AL-BI' -1
25 'H3-HOL-AL___' -1
26 'H3-HOL-AL-TI' -1
27 'H3-HOL-AL-TO' -1
28 'H3-SSFE---BO' -1
29 'H3-SSFE---BI' -1
30 'SSFE9028----' 0
31 'H3-SSFE---TI' -1
32 'H3-SSFE---TO' -1
33 'H3-MOTHMB-BO' -1
34 'H3-MOTHMB-BI' -1
35 'H3-MOL-THIM_' -1
36 'H3-MOTHMB-TI' -1
37 'H3-MOTHMB-TO' -1
38 'H3-SCRA---BO' -1
39 'H3-SCRA---BI' -1
40 'SCRA9028----' 0
41 'H3-SCRA---TI' -1
42 'H3-SCRA---TO' -1
43 'H3-SOL-PB-BO' -1
44 'H3-SOL-PB-BI' -1
45 'H3-SOL-PB___' -1
46 'H3-SOL-PB-TI' -1
47 'H3-SOL-PB-TO' -1
48 'H3-HYDRBT-BO' -1
49 'H3-HYDRBT-BI' -1
50 'H3-HYDRB----' -1
51 'H3-HYDRBT-TI' -1
52 'H3-HYDRBT-TO' -1
53 'H2-SSFE---BO' -1
54 'H2-SSFE---BI' -1
55 'SSFE9019----' 0
56 'H2-SSFE---TI' -1

57 'H2-SSFE---TO' -1
58 'notrace-offb' -1
59 'MOL-trace---' 0
60 'SMFP4537EROD' 0

* Channel physical rotation map
0 0 0 0 0 0 0 0 0 0 0 0 0 0 0 0 0
0 0 0 0 0 0 0 0 0 0 0 0 0 0 0 0 0
0 0 0 0 0 0 0 0 0 0 0 0 0 0 0 0 0
0 0 0 0 0 0 0 0 0 0 0 0 0 0 0 0 0
0 0 0 0 0 0 0 0 0 0 0 0 0 0 0 0 0
0 0 0 0 0 0 0 0 0 0 0 0 0 0 0 0 0
0 0 0 0 0 0 0 0 0 0 0 0 0 0 0 0 0
0 0 0 0 0 0 0 0 0 0 0 0 0 0 0 0 0
0 0 0 0 0 0 0 0 0 0 0 0 0 0 0 0 0
0 0 0 0 0 0 0 0 0 0 0 0 0 0 0 0 0
0 0 0 0 0 0 0 0 0 0 0 0 0 0 0 0 0
0 0 0 0 0 0 0 0 0 0 0 0 0 0 0 0 0
0 0 0 0 0 0 0 0 0 0 0 0 0 0 0 0 0
0 0 0 0 0 0 0 0 0 0 0 0 0 0 0 0 0
0 0 0 0 0 0 0 0 0 0 0 0 0 0 0 0 0

* Channel status map
0 0 0 0 0 0 0 0 0 0 0 0 0 0 0 0 0
0 0 0 0 0 0 0 0 0 0 0 0 0 0 0 0 0
0 0 0 0 0 0 0 0 0 0 0 0 0 0 0 0 0
0 0 0 0 0 0 0 0 0 0 0 0 0 0 0 0 0
0 0 0 0 0 0 0 0 0 0 0 0 0 0 0 0 0
0 0 0 0 0 0 0 0 0 0 6 0 0 0 0 0 0
0 0 0 0 0 3 0 1 0 1 0 0 0 0 0 0 0
0 0 0 0 0 0 0 0 0 0 7 0 0 0 0 0 0
0 0 0 0 0 4 0 2 0 1 0 0 0 0 0 0 0
0 0 0 0 0 0 0 0 0 0 8 0 0 0 0 0 0
0 0 0 0 0 5 0 1 0 1 0 0 0 0 0 0 0
0 0 0 0 0 0 0 0 0 0 0 0 0 0 0 0 0
0 0 0 0 0 0 0 0 0 0 0 0 0 0 0 0 0
0 0 0 0 0 0 0 0 0 0 0 0 0 0 0 0 0
0 0 0 0 0 0 0 0 0 0 0 0 0 0 0 0 0

* Control rod generic data
* NTRAV,HNOTCH,HBOTTM,NVRLAP,NCBANK,CWORTH,IFOLOW
5937 0.010000 15.000000 5937 2 4.000000 0

```
* Hydraulic data
* TINLET,PEXIT,CFLOW
40.000000  1.800000  18.000000

* Library read and initialization data
* PPM,RHOM,FUELT,COOLT,INITBU,INITND
 0.000000  0.998000  60.000000  40.000000  1   0

* Boundary conditions
'BLACK'
'BLACK'   * bottom
'BLACK'   * top

'ENDINP'
*** end of generic data


* CASE data follows:


'BOC'
'FLUX'
'FEEDBK'
0  0  -1  0  0  0  0  0  * IOPPM,IOPROD,IOPPOW,IOPTIN,IOPDOP,IOPMOD,IOPXE,IOPSM
0.000000  1.002000  0.000000 0.000000   * PPM,REL.POW,POFMIN,POFMAX
'ITERAT'
3  5  250  0.0001  1e+20  0.000000   * KITER,NFMAX,NOMAX,EPSO,SHIFT,XRAD
'CONTRO'
4053 4053 5937 5937 5937 5937 5937 5937
'EDITOP'
3 3 1 0 3 0 0 2 0 3
'REC-ON'
'ENDCAS'

'1 day'
'DEPLET'
'TIME'
0       1       0.000000          1.000000       3       0       *   ITXESM,LEVELB,BURNMW,
BURNDS,NUMFLN,IEOC
```

'FEEDBK'
0 0 -1 0 0 0 0 0 * IOPPM,IOPROD,IOPPOW,IOPTIN,IOPDOP,IOPMOD,IOPXE,IOPSM
0.000000 1.011200 0.000000 0.000000 * PPM,RELPOW,POFMIN,POFMAX
'CONTRO'
3763 3763 5937 5937 5937 5937 5937 5937
'EDITOP'
3 3 1 0 3 0 0 2 0 3
'REC-ON'
'ENDCAS'

'1 day-2.417 day '
'DEPLET'
'TIME'
0 1 0.000000 1.417000 3 0 * ITXESM,LEVELB,BURNMW,
BURNDS,NUMFLN,IEOC
'CONTRO'
3763 3763 0 0 5937 5937 5937 0
'EDITOP'
3 3 1 0 3 0 0 2 0 3
'REC-ON'
'ENDCAS'

'2.417 day-2.5 day '
'DEPLET'
'TIME'
0 1 0.000000 0.083000 3 0 * ITXESM,LEVELB,BURNMW,
BURNDS,NUMFLN,IEOC
'CONTRO'
3763 3763 0 0 5937 5937 5937 0
'EDITOP'
3 3 1 0 3 0 0 2 0 3
'REC-ON'
'ENDCAS'

'2.5 day '
'FLUX'
'CONTRO'
3763 3763 5937 5937 5937 5937 5937 5937
'EDITOP'
3 3 1 0 3 0 0 2 0 3

NWU LIBRARY

'REC-ON'
'ENDCAS'

'2.5 day-4.417 day'
'DEPLET'
'TIME'
0 1 0.000000 1.917000 3 0 * ITXESM,LEVELB,BURNMW,
BURNDS,NUMFLN,IEOC
'CONTRO'
3763 3763 5937 5937 0 5937 0 5937
'EDITOP'
3 3 1 0 3 0 0 2 0 3
'REC-ON'
'ENDCAS'

'4.417 day-4.5 day'
'DEPLET'
'TIME'
0 1 0.000000 0.083000 3 0 * ITXESM,LEVELB,BURNMW,
BURNDS,NUMFLN,IEOC
'CONTRO'
3763 3763 5937 5937 0 5937 0 5937
'EDITOP'
3 3 1 0 3 0 0 2 0 3
'REC-ON'
'ENDCAS'

'4.5 day '
'FLUX'
'CONTRO'
3763 3763 5937 5937 5937 5937 5937 5937
'EDITOP'
3 3 1 0 3 0 0 2 0 3
'REC-ON'
'ENDCAS'

'4.5 day-4.590 day'
'DEPLET'
'TIME'

```
0       1       0.000000        0.090000        3       0       *   ITXESM,LEVELB,BURNMW,
BURNDS,NUMFLN,IEOC
'CONTRO'
3763 3763 5937 5937 5937 5937 5937 5937
'EDITOP'
3 3 1 0 3 0 0 2 0 3
'REC-ON'
'ENDCAS'

'4.590 day-6.417 day'
'DEPLET'
'TIME'
0       1       0.000000        1.827000        3       0       *   ITXESM,LEVELB,BURNMW,
BURNDS,NUMFLN,IEOC
'CONTRO'
3763 3763 5937 5937 5937 0 5937 5937
'EDITOP'
3 3 1 0 3 0 0 2 0 3
'REC-ON'
'ENDCAS'

'6.417 day-6.5 day'
'DEPLET'
'TIME'
0       1       0.000000        0.083000        3       0       *   ITXESM,LEVELB,BURNMW,
BURNDS,NUMFLN,IEOC
'CONTRO'
3763 3763 5937 5937 5937 0 5937 5937
'EDITOP'
3 3 1 0 3 0 0 2 0 3
'REC-ON'
'ENDCAS'

'6.5 day'
'FLUX'
'FEEDBK'
0 0 -1 0 0 0 0 0 * IOPPM,IOPROD,IOPPOW,IOPTIN,IOPDOP,IOPMOD,IOPXE,IOPSM
0.000000  1.014300  0.000000  0.000000   * PPM,RELPOW,POFMIN,POFMAX
'CONTRO'
4019 4019 5937 5937 5937 5937 5937 5937
```

'EDITOP'
3 3 1 0 3 0 0 2 0 3
'REC-ON'
'ENDCAS'

'6.5 day-7.590 day'
'DEPLET'
'TIME'
0 1 0.000000 1.090000 3 0 * ITXESM,LEVELB,BURNMW,
BURNDS,NUMFLN,IEOC
'CONTRO'
4019 4019 5937 5937 5937 5937 5937 5937
'EDITOP'
3 3 1 0 3 0 0 2 0 3
'REC-ON'
'ENDCAS'

'7.590 day-9.417 day'
'DEPLET'
'TIME'
0 1 0.000000 1.827000 3 0 * ITXESM,LEVELB,BURNMW,
BURNDS,NUMFLN,IEOC
'CONTRO'
4019 4019 0 0 5937 5937 5937 0
'EDITOP'
3 3 1 0 3 0 0 2 0 3
'REC-ON'
'ENDCAS'

'9.417 day-9.5 day'
'DEPLET'
'TIME'
0 1 0.000000 0.083000 3 0 * ITXESM,LEVELB,BURNMW,
BURNDS,NUMFLN,IEOC
'CONTRO'
4019 4019 0 0 5937 5937 5937 0
'EDITOP'
3 3 1 0 3 0 0 2 0 3
'REC-ON'
'ENDCAS'

'9.5 day'
'FLUX'
'CONTRO'
4019 4019 5937 5937 5937 5937 5937 5937
'EDITOP'
3 3 1 0 3 0 0 2 0 3
'REC-ON'
'ENDCAS'

'9.5 day-11.417 day'
'DEPLET'
'TIME'
0 1 0.000000 1.917000 3 0 * ITXESM,LEVELB,BURNMW,
BURNDS,NUMFLN,IEOC
'CONTRO'
4019 4019 5937 5937 0 5937 0 5937
'EDITOP'
3 3 1 0 3 0 0 2 0 3
'REC-ON'
'ENDCAS'

'11.417 day-11.5 day'
'DEPLET'
'TIME'
0 1 0.000000 0.083000 3 0 * ITXESM,LEVELB,BURNMW,
BURNDS,NUMFLN,IEOC
'CONTRO'
4019 4019 5937 5937 0 5937 0 5937
'EDITOP'
3 3 1 0 3 0 0 2 0 3
'REC-ON'
'ENDCAS'

'11.5 day '
'FLUX'
'FEEDBK'
0 0 -1 0 0 0 0 0 * IOPPM,IOPROD,IOPPOW,IOPTIN,IOPDOP,IOPMOD,IOPXE,IOPSM
0.000000 1.024500 0.000000 0.000000 * PPM,RELPOW,POFMIN,POFMAX
'CONTRO'

```
4235 4235 5937 5937 5937 5937 5937 5937
'EDITOP'
3 3 1 0 3 0 0 2 0 3
'REC-ON'
'ENDCAS'

'11.5 day-11.590 day'
'DEPLET'
'TIME'
0       1       0.000000        0.090000        3       0       *   ITXESM,LEVELB,BURNMW,
BURNDS,NUMFLN,IEOC
'FEEDBK'
0 0 -1 0 0 0 0 0 * IOPPM,IOPROD,IOPPOW,IOPTIN,IOPDOP,IOPMOD,IOPXE,IOPSM
0.000000 0.826200 0.000000 0.000000  * PPM,RELPOW,POFMIN,POFMAX
'CONTRO'
4467 4467 5937 5937 5937 5937 5937 5937
'EDITOP'
3 3 1 0 3 0 0 2 0 3
'REC-ON'
'ENDCAS'

'11.590 day-12.590 day'
'DEPLET'
'TIME'
0       1       0.000000        1.000000        3       0       *   ITXESM,LEVELB,BURNMW,
BURNDS,NUMFLN,IEOC
'CONTRO'
4467 4467 5937 5937 5937 5937 5937 5937
'EDITOP'
3 3 1 0 3 0 0 2 0 3
'REC-ON'
'ENDCAS'

'12.590 day-13.417 day'
'DEPLET'
'TIME'
0       1       0.000000        0.827000        3       0       *   ITXESM,LEVELB,BURNMW,
BURNDS,NUMFLN,IEOC
'CONTRO'
4467 4467 5937 5937 5937 0 5937 5937
```

'EDITOP'
3 3 1 0 3 0 0 2 0 3
'REC-ON'
'ENDCAS'

'13.417 day-13.5 day'
'DEPLET'
'TIME'
0 1 0.000000 0.083000 3 0 * ITXESM,LEVELB,BURNMW,
BURNDS,NUMFLN,IEOC
'CONTRO'
4467 4467 5937 5937 5937 0 5937 5937
'EDITOP'
3 3 1 0 3 0 0 2 0 3
'REC-ON'
'ENDCAS'

'13.5 day'
'FLUX'
'CONTRO'
4467 4467 5937 5937 5937 5937 5937 5937
'EDITOP'
3 3 1 0 3 0 0 2 0 3
'REC-ON'
'ENDCAS'

'13.5 day-16.417 day'
'DEPLET'
'TIME'
0 1 0.000000 2.917000 3 0 * ITXESM,LEVELB,BURNMW,
BURNDS,NUMFLN,IEOC
'CONTRO'
4467 4467 0 0 5937 5937 5937 0
'EDITOP'
3 3 1 0 3 0 0 2 0 3
'REC-ON'
'ENDCAS'

'16.417 day-16.5 day'
'DEPLET'

'TIME'
0 1 0.000000 0.083000 3 0 * ITXESM,LEVELB,BURNMW,
BURNDS,NUMFLN,IEOC
'CONTRO'
4467 4467 0 0 5937 5937 5937 0
'EDITOP'
3 3 1 0 3 0 0 2 0 3
'REC-ON'
'ENDCAS'

'16.5 day'
'FLUX'
'FEEDBK'
0 0 -1 0 0 0 0 0 * IOPPM,IOPROD,IOPPOW,IOPTIN,IOPDOP,IOPMOD,IOPXE,IOPSM
0.000000 0.812700 0.000000 0.000000 * PPM,RELPOW,POFMIN,POFMAX
'CONTRO'
4549 4549 5937 5937 5937 5937 5937 5937
'EDITOP'
3 3 1 0 3 0 0 2 0 3
'REC-ON'
'ENDCAS'

'16.5 day-16.590 day'
'DEPLET'
'TIME'
0 1 0.000000 0.090000 3 0 * ITXESM,LEVELB,BURNMW,
BURNDS,NUMFLN,IEOC
'CONTRO'
4549 4549 5937 5937 5937 5937 5937 5937
'EDITOP'
3 3 1 0 3 0 0 2 0 3
'REC-ON'
'ENDCAS'

'16.590 day-18.417 day'
'DEPLET'
'TIME'
0 1 0.000000 1.827000 3 0 * ITXESM,LEVELB,BURNMW,
BURNDS,NUMFLN,IEOC
'CONTRO'

4549 4549 5937 5937 0 5937 0 5937
'EDITOP'
3 3 1 0 3 0 0 2 0 3
'REC-ON'
'ENDCAS'

'18.417 day-18.5 day'
'DEPLET'
'TIME'
0 1 0.000000 0.083000 3 0 * ITXESM,LEVELB,BURNMW,
BURNDS,NUMFLN,IEOC
'CONTRO'
4549 4549 5937 5937 0 5937 0 5937
'EDITOP'
3 3 1 0 3 0 0 2 0 3
'REC-ON'
'ENDCAS'

'18.5 day'
'FLUX'
'CONTRO'
4549 4549 5937 5937 5937 5937 5937 5937
'EDITOP'
3 3 1 0 3 0 0 2 0 3
'REC-ON'
'ENDCAS'

'18.5 day-20.417 day'
'DEPLET'
'TIME'
0 1 0.000000 1.917000 3 0 * ITXESM,LEVELB,BURNMW,
BURNDS,NUMFLN,IEOC
'CONTRO'
4549 4549 5937 5937 5937 0 5937 5937
'EDITOP'
3 3 1 0 3 0 0 2 0 3
'REC-ON'
'ENDCAS'

'20.417 day-20.5 day'

'DEPLET'
'TIME'
0 1 0.000000 0.083000 3 0 * ITXESM,LEVELB,BURNMW,
BURNDS,NUMFLN,IEOC
'CONTRO'
4549 4549 5937 5937 5937 0 5937 5937
'EDITOP'
3 3 1 0 3 0 0 2 0 3
'REC-ON'
'ENDCAS'

'20.5 day'
'FLUX'
'FEEDBK'
0 0 -1 0 0 0 0 0 * IOPPM,IOPROD,IOPPOW,IOPTIN,IOPDOP,IOPMOD,IOPXE,IOPSM
0.000000 0.817300 0.000000 0.000000 * PPM,RELPOW,POFMIN,POFMAX
'CONTRO'
4715 4715 5937 5937 5937 5937 5937 5937
'EDITOP'
3 3 1 0 3 0 0 2 0 3
'REC-ON'
'ENDCAS'

'20.5 day-20.590 day'
'DEPLET'
'TIME'
0 1 0.000000 0.090000 3 0 * ITXESM,LEVELB,BURNMW,
BURNDS,NUMFLN,IEOC
'CONTRO'
4715 4715 5937 5937 5937 5937 5937 5937
'EDITOP'
3 3 1 0 3 0 0 2 0 3
'REC-ON'
'ENDCAS'

'20.590 day-23.417 day'
'DEPLET'
'TIME'
0 1 0.000000 2.827000 3 0 * ITXESM,LEVELB,BURNMW,
BURNDS,NUMFLN,IEOC

'CONTRO'
4715 4715 0 0 5937 5937 5937 0
'EDITOP'
3 3 1 0 3 0 0 2 0 3
'REC-ON'
'ENDCAS'

'23.417 day-23.5 day'
'DEPLET'
'TIME'
0 1 0.000000 0.083000 3 0 * ITXESM,LEVELB,BURNMW,
BURNDS,NUMFLN,IEOC
'CONTRO'
4715 4715 0 0 5937 5937 5937 0
'EDITOP'
3 3 1 0 3 0 0 2 0 3
'REC-ON'
'ENDCAS'

'23.5 day'
'FLUX'
'FEEDBK'
0 0 -1 0 0 0 0 0 * IOPPM,IOPROD,IOPPOW,IOPTIN,IOPDOP,IOPMOD,IOPXE,IOPSM
0.000000 0.814600 0.000000 0.000000 * PPM,RELPOW,POFMIN,POFMAX
'CONTRO'
4973 4973 5937 5937 5937 5937 5937 5937
'EDITOP'
3 3 1 0 3 0 0 2 0 3
'REC-ON'
'ENDCAS'

'23.5 day-23.590 day'
'DEPLET'
'TIME'
0 1 0.000000 0.090000 3 0 * ITXESM,LEVELB,BURNMW,
BURNDS,NUMFLN,IEOC
'CONTRO'
4973 4973 5937 5937 5937 5937 5937 5937
'EDITOP'
3 3 1 0 3 0 0 2 0 3

'REC-ON'
'ENDCAS'

'ENDRUN'

* MAESTRO SPECIFIC DATA